Ecological Indicators 139 (2022) 108899

Contents lists available at ScienceDirect

Ecological Indicators

journal homepage: www.elsevier.com/locate/ecolind

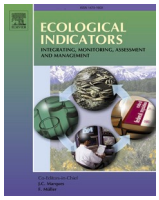

Original Articles

Coastal ecosystem services in South Africa's largest natural bay: The role of marine benthic filter feeders in mitigating pollution

Eleonora Puccinelli [a,b,*], Francesca Porri [c,d], Katye Altieri [a], Raquel Flynn [a], Hazel Little [a], Tayla Louw [a], Paula Pattrick [e,f], Conrad Sparks [g], Mutshutshu Tsanwani [a,h], Sonya de Waardt [g], David Walker [g], Sarah Fawcett [a,i]

[a] Department of Oceanography, University of Cape Town, Rondebosch 7701, Cape Town, South Africa
[b] University of Brest – UMR 6539 CNRS / UBO / IRD / Ifremer, LEMAR – IUEM – Rue Dumont d' Urville, 29280 Plouzané, France
[c] South African Institute for Aquatic Biodiversity (SAIAB), Somerset Street, 6139 Makhanda, South Africa
[d] Ichthyology and Fisheries Sciences Department, Rhodes University, Makhanda 6139, South Africa
[e] South African Environmental Observation Network (SAEON), Elwandle Coastal Node, Gqeberha 6001, South Africa
[f] ABALOBI, NPO, 1 Westlake Dr, Cape Town 7945, South Africa
[g] Department of Conservation and Marine Sciences, Cape Peninsula University of Technology, Cape Town 8000, South Africa
[h] Oceans and Coasts Research, Department of Environment, Forestry and Fisheries, Cape Town 8001, South Africa
[i] MARIS, University of Cape Town, Rondebosch 7701, Cape Town, South Africa

ARTICLE INFO

Keywords:
Water quality
Filter feeders
Coastal circulation
Nutrient loading
Atmospheric deposition
Metal contamination

ABSTRACT

Nearshore water quality can be highly impacted by anthropogenic activities ongoing along the coast, the effects of which on natural environments can be permanent and irreversible, with consequences for ecosystem biodiversity and functioning, as well as for associated services. Benthic filter feeders (e.g., mussels) provide several services for coastal regions, including improving water quality by reducing eutrophication, being a major source of food for humans, and as a habitat-forming species. Here, we seek to understand the role of benthic filter feeders in enhancing water quality in an urban coastal system in order to assess their role as ecosystem service providers and how they should be included in ecosystem-based evaluations. Using as a model False Bay, South Africa's largest natural bay and a socio-economic hotspot, this multidisciplinary study was designed to identify possible pollution sources to a highly-urbanised coastal region, assess their effects on several biological and biogeochemical parameters, and evaluate the role of mussels in mitigating these anthropogenic inputs. We consider several sources of pollution, including nutrient loading from wastewater and river outflows, heavy metals, and aerosol deposition. We find that pollutant inputs are largely attenuated by the circulation of the bay and by the presence of filter feeders that bioaccumulate contaminants, thereby removing them from coastal waters. Our work thus emphasizes the potential for mussels and natural abiotic processes to ameliorate anthropogenic impacts, although these mitigation strategies are not without environmental risk. We recommend that such information should be included in national assessments used to develop appropriate strategies and policies for coastal environmental management and conservation.

1. Introduction

Coastal waters are among the most productive systems on Earth, providing a wide variety of services to humans including food, as well as ensuring water quality through filtration and detoxification facilitated by suspension feeders, submerged vegetation, and wetlands (Worm et al., 2006; Barbier, 2019). Over the last few centuries, significant human population growth has disproportionately affected coastal regions globally (Halpern et al., 2008; Balk et al., 2009; Smith, 2011; Merkens et al., 2016), with the recent exponential increase in coastal urbanisation further impacting natural marine systems through the construction of artificial infrastructures, habitat damage or loss, and degradation of water quality (MAE, 2005; Bulleri and Chapman, 2010; Lai et al., 2015; Marzinelli et al., 2018; Aguilera et al., 2020). Poor water quality results from land- and ocean-based human activities that cause chemical and biological pollution, increased sediment loads, and

* Corresponding author at: Department of Oceanography, University of Cape Town, Rondebosch 7701, Cape Town, South Africa.
E-mail address: eleonorapuccinelli@gmail.com (E. Puccinelli).

https://doi.org/10.1016/j.ecolind.2022.108899
Received 14 February 2022; Received in revised form 19 April 2022; Accepted 20 April 2022
Available online 5 May 2022

eutrophication (Halpern et al., 2008; Huijbers et al., 2013; Johnston et al., 2016; Ali and Khairy, 2016; Lu et al., 2018).

Shifts in climate can also alter natural ecological processes across a range of spatial and temporal scales. With climate change, extreme events such as floods, droughts, and storms are increasing in frequency and magnitude (Benedetti-Cecchi et al., 2006; Neumann et al., 2015) and ocean currents are changing in response to alterations in temperature, rainfall, and wind patterns (Winton et al., 2012; Holliday et al., 2020). Such changes will alter the land–ocean freshwater flux, with a higher flux potentially enhancing upper water column stratification, thus decreasing the vertical nutrient supply and coastal productivity (MacKenzie and Adamson, 2004; Arellano and Rivas, 2019; Janout et al., 2020). A large freshwater flux may also lead to terrestrial nutrient loading, potentially driving harmful algal blooms and eutrophication in nearshore waters, with an associated decrease in dissolved oxygen (O'Neil et al., 2012; Lapointe et al., 2017; Tsikoti and Genitsaris, 2021). Increased eutrophication can also result from a decline in the freshwater flux as this reduces the dilution effect (Bakun, 1990; Romero et al., 2013). In synergy with natural and/or anthropogenic disturbances, climate change is also driving changes in the geographical range, metabolism, abundance, and diversity of key organisms in coastal ecosystems, with consequences that extend to food-web dynamics and ecosystem functioning (Harley et al., 2006; Nagelkerken and Connell, 2015).

Increasing stress on natural systems, either directly through pollution and/or habitat destruction or indirectly through climate change and related perturbations, is predicted to drive changes in marine biodiversity, with repercussions for ecosystem functioning (Worm et al., 2005; Doney et al., 2012; Tilman et al., 2014; Hautier et al., 2015). High species richness and diversity enhance ecosystem productivity and stability (Stachowicz et al., 2007; Duffy et al., 2017), while a decline in biodiversity narrows ecosystem functioning with a consequent loss of services (Balvanera et al., 2006; Worm et al., 2006). Biodiverse communities are thus more likely to withstand anthropogenic stressors without compromising (or at least, not fully compromising) the functioning and services of the system they inhabit (Worm et al., 2006; Stachowicz et al., 2007; Teixeira et al., 2019). The impact of biodiversity loss at a global scale is not yet fully understood (Hooper et al. 2005), with a lack of information from marine environments identified as a particular gap (Hendriks et al., 2006; Townsend et al., 2018).

Filter feeders such as bivalves (e.g., mussels) have been extensively used as environmental tools for the restoration of heavily anthropogenically-impacted systems (Lorey, 2002; Dumbauld et al., 2009; La Peyre et al., 2014; McAfee et al., 2016; Puccinelli et al., 2016b; Pereira et al., 2019). The utility of mussels as sinks for waste is related to their ability to capture suspended material by filtering water at high rates (Nakamura and Kerciku 2000). As such, mussels can control phytoplankton stocks, rates of primary productivity, water clarity, nutrient cycling, and food web dynamics (Kohata et al., 2003; Higgins et al., 2011; Vanni, 2021). Additionally, mussels are pivotal as bioengineers (Cole and McQuaid, 2010; Lathlean and McQuaid, 2017) and provide a direct ecosystem service as a food source (Drimie and McLachlan, 2013). However, mussels can also accumulate pollutants such as metals (i.e., "bioaccumulation"; Spada et al., 2013), which may compromise their ecological resilience and/or utility as a service provider (Stankovic and Jovic, 2012).

Analyses of carbon (C) and nitrogen (N) stable isotopes (SI) and fatty acids (FA) have been used extensively to study marine food webs. These techniques provide time-integrated information on organism diet and can be used to trace the flux of organic matter from producers to consumers (Peterson and Fry, 1987; Hansson et al., 1997; Dalsgaard et al., 2003; Kelly and Scheibling, 2012). Additionally, the N isotope ratios (i.e., $\delta^{15}N$, in ‰ vs. N_2 in air, $= [(^{15}N/^{14}N)_{sample}/(^{15}N/^{14}N)_{ref} - 1] \times 1000$) of dissolved inorganic N forms such as nitrate can be used to distinguish anthropogenic versus natural nutrient inputs to coastal regions, track pollutant sources through aquatic systems, and evaluate their spatial and temporal persistence (McClelland and Valiela, 1998; Kendall and Aravena, 2000; Mayer et al., 2002; Nestler et al., 2011; Qin et al., 2019). In the case of primary consumers such as bivalves, biomass $\delta^{15}N$ is indicative of organism trophic level, while biomass $\delta^{13}C$ (in ‰ vs. VPDB, $= [(^{13}C/^{12}C)_{sample}/(^{13}C/^{12}C)_{ref} - 1] \times 1000$) is directly related to organism food source (DeNiro and Epstein, 1981, 1978), with an estimated isotopic enrichment between trophic levels of 2.3‰ for $\delta^{15}N$ and 1‰ for $\delta^{13}C$ (McCutchan et al., 2003). FA analyses provide insights into the pathways of FA synthesis, metabolism, and reproduction strategies of organisms (Iverson et al., 1997; Puccinelli et al., 2016a; Puccinelli et al., 2017; Ruess and Müller-Navarra, 2019). The majority of FA in aquatic systems, including the Essential FA (EFA) 20:5n-3 and 22:6n-3, are largely synthesized by primary producers, yet are also critical for the health of consumers (Arts et al., 2001; Parrish, 2013). Because primary consumers and higher trophic organisms must acquire these FA through their diet (Dalsgaard et al., 2003), it is possible to use FA as trophic markers (Kelly and Scheibling, 2012; Puccinelli et al., 2016c).

In urbanized coastal regions, metals (e.g., arsenic, cadmium, chromium, copper, lead, zinc) represent a major threat to mussel communities and compromise the quality and safety of this food resource (Dallinger et al., 1987; Yi et al., 2011; Jaishankar et al., 2014). Natural sources of metals include soil erosion and weathering, while anthropogenic processes such as mining, urban and industrial runoff, sewage, and agricultural discharge can also increase ambient metal concentrations (Bradl, 2005; Morais et al., 2012). Metals do not decompose in the environment and can be assimilated by mussels during filter feeding, bioaccumulating in their tissues (Casas and Bacher, 2006; Boudjema et al., 2022) to levels far in excess of those that are safe for higher organism and/or human ingestion (DOH, 1994; Taljaard, 2006).

Using South Africa's largest natural bay, False Bay, as a model for a rapidly-urbanizing, coastal system, we investigated the role of mussels in controlling water quality in a near-shore environment subject to pollutant inputs in order to evaluate their role as an ecosystem service provider. Our specific objectives included:

Determine the concentration of contaminants – in the form of inorganic N, metals, and anthropogenic aerosols – in coastal waters, evaluate their persistence with distance from the shore, and identify the natural processes that may attenuate them;
Characterize the role of mussels in attenuating inputs of pollution and thus enhancing water quality;
Characterize the biodiversity of the marine community supported by mussel populations to assess the possible anthropogenic effects thereon.

2. Study area

False Bay, located near the City of Cape Town (population of >4 million; Stats SA 2016), is southern Africa's largest natural bay (nearly 1000 km^2) (Fig. 1). The bay is south-facing and open to the sea, and is located in the transition zone between the cold west coast and warm-temperate south coast bioregions of South Africa (Emanuel et al., 1992). As such, its biological diversity is extremely high (Awad et al., 2002; Griffiths et al., 2010) and large portions of the bay are denoted conservation regions, including marine protected areas with restricted and controlled-use zones (Pfaff et al., 2019). False Bay's intertidal rocky shore is colonized by benthic filter feeders, predominantly the mussel *Mytilus galloprovincialis* (Robinson et al., 2005).

Surface water circulation in False Bay, while complex (Dufois and Rouault, 2012), is generally clockwise, with water entering the bay from the west. During summer (November-March), south-easterly winds promote offshore transport and (related) upwelling on the southeast side of the bay, while in winter, north-westerly winds favour onshore transport and enhanced mixing (Grundlingh et al., 1989; Grundlingh and Largier, 1991; Dufois and Rouault, 2012; De Vos, 2014; Jacobson, 2014). False Bay also experiences periodic warm-water intrusions from

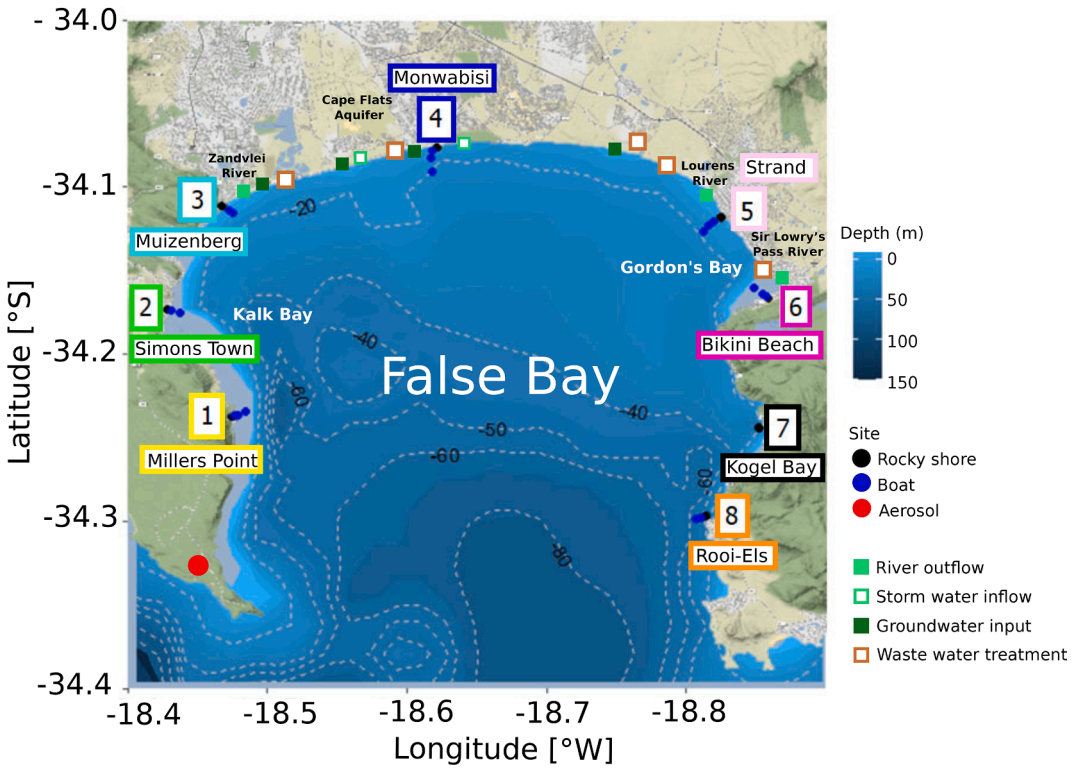

Fig. 1. Map of the study area indicating the colour-coded rocky shore *sites* (black symbols) and onshore-offshore boat *stations* (blue symbols) sampled in False Bay in May 2018. The contour lines and blue shading show the bathymetry of the bay. The red circle indicates the location of the Cape Point Global Atmosphere Watch station, the site used for aerosol collection. Potential anthropogenic outflow sources to False Bay are also shown: river outflow (light green filled squares), storm water inflow (light green open squares), groundwater input (dark green squares), waste water treatment works (brown open squares). (For interpretation of the references to colour in this figure legend, the reader is referred to the web version of this article.)

the Agulhas Current system to the east (Shannon and Chapman, 1983). In contrast to the large-scale bay circulation, Gordon's Bay to the north-east of False Bay (Fig. 1) hosts a semi-permanent anticyclonic eddy that drives a local anticlockwise circulation pattern (Atkins, 1970; Taljaard et al., 2000b) and increases the residence time of waters in this region (Pfaff et al., 2019).

False Bay hosts three small- to medium-sized harbours (Gordon's Bay, Kalk Bay, and Simons Town) that support limited commercial activities and are instead mainly dedicated to small-scale fisheries and recreational activities (Pfaff et al., 2019). The bay is under increasing anthropogenic pressure, largely due to rising urbanisation, as well as riverine inputs of transported pollutants, the latter mainly affecting the northern shoreline of the bay (Fig. 1; O'Callaghan, 1990; Binning and Baird, 2001; Pfaff et al., 2019). The rivers entering False Bay discharge anthropogenic contaminants from residential and industrial sewage and agriculture by-products (pesticides, fertilizers, farm waste; O'Callaghan 1990, Binning and Baird 2001), and there is also the possibility of atmospheric deposition of pollutants that originate inland (Abiodun et al. 2014).

3. Materials and methods

3.1. Sample collection

The sampling was conducted at eight rocky shore *sites* distributed along the False Bay coastline in May 2018 (Fig. 1). Along onshore-offshore *transects* perpendicular to each intertidal site (except site 7 (Kogel Bay)), samples were also collected between the surface and the seafloor. Sampling was conducted aboard the MA-RE 1 7.3 m Gemini inflatable craft, with each transect including two (transects 3- Muizenberg, 8- Rooi-Els) or three (transects 1- Millers Point, 2- Simons Town, 4- Monwabisi, 5- Strand, 6- Bikini Beach) *stations*: inshore A, mid-shore B, and offshore C (Table S.1). At each station, seawater samples were collected from two to four depths using a hand-held 5 L Niskin bottle. Hydrographic data (temperature, salinity, oxygen concentrations) were generated using a Seabird conductivity-temperature-depth (CTD) profiler that was calibrated by the manufacturer a month before our sampling. The depth of the euphotic zone (Z_{eu}) was estimated using a Secchi disk (Idso and Gilbert, 1974; Table S.1).

3.2. Biogeochemical parameters

Seawater samples were collected at the rocky shore sites and boat stations (see Table S.1 for sampling depths) for the analysis of nutrient concentrations (nitrate, nitrite, ammonium, phosphate, silicate), dissolved inorganic C (DIC) and total alkalinity (AT), nitrate isotope ratios, chlorophyll *a* concentrations, phytoplankton taxonomy, SI of particulate organic matter (N and C), and rates of net primary productivity (NPP), N (as nitrate, ammonium, and urea) uptake, and nitrite oxidation (i.e., a measure of nitrification).

3.2.1. Nutrients, carbonate system parameters, and nitrate isotopes

Seawater samples for nutrients and nitrate isotopes were collected in duplicate in 50 mL Falcon tubes and high-density polyethylene bottles, respectively, and frozen at −20 °C until analysis. Nitrate + nitrite ($NO_3^- + NO_2^-$) and silicic acid ($Si(OH)_4$) concentrations were measured using a Lachat QuickChem flow injection analysis platform following published auto-analysis protocols (Grasshoff, 1976; Diamond, 1994). The detection limit for both nutrients was 0.1 μM and the precision was ≤0.2 μM. Phosphate (PO_4^{3-}) and nitrite (NO_2^-) concentrations were measured manually using standard colorimetric methods (Bendschneider and Robinson, 1952; Strickland and Parsons, 1968; Parsons et al., 1984), with a detection limit of 0.05 μM and precision of ≤0.2 μM. NO_3^- concentrations were calculated by subtracting NO_2^- from $NO_3^- + NO_2^-$.

Aliquots of a certified reference material (CRM; JAMSTEC; Lot CG) were analysed during auto-analyser and manual runs to ensure measurement accuracy. The fluorometric method (Holmes et al. 1999) was used to analyse ammonium (NH_4^+) concentrations, with a detection limit of 0.05 μM and precision of ≤0.2 μM. All NH_4^+ measurements were corrected for the matrix effect (ME) that results from calibrating seawater samples with Milli-Q water standards (Saxberg and Kowalski, 1979); the ME was always <10%. Urea-N (hereafter, urea) concentrations were measured following the colorimetric method of Revilla et al. (2005) using a Thermo Scientific Genesys 30 Visible spectrophotometer with 5 cm path-length cell. The detection limit was 0.05 μM and the precision was ≤0.5 μM.

Samples for DIC and AT were collected by repeatedly overflowing 1 L glass bottles with seawater, injecting saturated $HgCl_2$ (1% final concentration), and immediately sealing with gas-tight crimp seals. Samples were analysed using a VINDTA 3C system (Marianda, Inc.) equipped with a CM-5011 carbon coulometer and calibrated using CRMs for oceanic CO_2 (provided by A.G. Dickson from Scripps Institution of Oceanography). The uncertainty associated with DIC and AT was ±6 μM and ±4 μM, respectively. For each sample, using CO2Sys_v2.1. (Lewis and Wallace, 1998) and our measurements of temperature, salinity, DIC, AT, PO_4^{3-}, and $Si(OH)_4$, we computed pH, carbonate ion concentration ($[CO_3^{2-}]_{computed}$), and, because mussel shells are composed of both calcite (outer layer) and aragonite (inner layer), the calcite and aragonite saturation state (Ω_{Ca} and Ω_{Ar}, respectively, where $\Omega = [CO_3^{2-}]_{computed}/[CO_3^{2-}]_{saturation}$). When Ω_{Ca} or $\Omega_{Ar} = 1$, seawater is in equilibrium with respect to the mineral phase, while Ω_{Ca} or $\Omega_{Ar} > 1$ indicates supersaturation and Ω_{Ca} or $\Omega_{Ar} < 1$ indicates undersaturation (Riebesell, et al., 2010). We used the stoichiometric equilibrium constants for carbonic acid of Lueker et al. (2000), for potassium bisulfate of Dickson (1990), and for boron of Lee et al. (2010).

The $\delta^{15}N$ and $\delta^{18}O$ ($\delta^{18}O$, in ‰ vs. VSMOW, $=[(^{18}O/^{16}O)_{sample}/(^{18}O/^{16}O)_{ref} -1] \times 1000$) of seawater nitrate ($\delta^{15}N_{NO3}$ and $\delta^{18}O_{NO3}$) were measured using the denitrifier method (Sigman et al., 2001; Casciotti et al., 2002; Weigand et al., 2016). Prior to isotopic analysis, samples were treated with sulfamic acid to remove NO_2^- since the denitrifier method converts both NO_2^- and NO_3^- to nitrous oxide gas (N_2O) (Granger and Sigman, 2009). The NO_3^- was then quantitatively converted to N_2O by the denitrifying bacteria, *Pseudomonas aureofaciens*, which lacks an N_2O reductase enzyme. The N and O isotope ratios of the resultant N_2O were measured using a Delta V Advantage isotope ratio mass spectrometer (IRMS) with purpose-built online N_2O extraction and purification system. Results were referenced to atmospheric N_2 and VSMOW using the CRMs IAEA-NO-3 ($\delta^{15}N = 4.7 \pm 0.2$‰; Gonfiantini et al., 1995 and $\delta^{18}O = 25.6 \pm 0.4$‰; Böhlke et al., 2003) and USGS-34 ($\delta^{15}N = -1.8 \pm 0.1$‰ and $\delta^{18}O = -27.9 \pm 0.3$‰; Böhlke et al., 2003). The analytical precision for repeat $\delta^{15}N_{NO3}$ and $\delta^{18}O_{NO3}$ measurements was ≤0.1‰ and ≤0.3‰, respectively.

3.2.2. Chlorophyll *a* and phytoplankton taxonomy

At each site and station, seawater (300 mL) was filtered through a 0.3 μm glass fibre filter (GF-75; Sterlitech) for the determination of chlorophyll *a* concentrations. In the laboratory, chlorophyll *a* was extracted in 90% acetone for 24 hr at −20 °C in the dark, after which fluorescence was determined using the non-acidified protocol of Welschmeyer (1994).

For phytoplankton community composition, samples (250 mL) were collected at the rocky shore sites and surface boat stations in amber glass bottles and immediately fixed with Lugol's solution (1% final concentration). Samples were settled overnight in 20 mL Utermöhl chambers (Utermöhl, 1958), then settled phytoplankton were enumerated using an Olympus CKX41 inverted microscope at 200x magnification, with identification to the highest taxonomic level possible. For each sample, minimum of 300 cells was counted.

3.2.3. Particulate organic matter

Seawater samples (300 mL) were filtered on-site through ashed (450 °C for 5 hr) GF-75 filters to capture particulate organic N (PON) and C (POC) and stored in ashed foil envelopes at −80 °C pending analysis. Filters were oven-dried at 40 °C for 24 hr, trimmed to remove unused perimeter filter, and pelletised in tin capsules. Samples were analysed for PON and POC content and $\delta^{13}C$ and $\delta^{15}N$ using a Flash Elemental Analyzer 1112 Series coupled to a Delta V Plus IRMS. A protocol blank (unused pre-combusted filter + tin capsule) was run after every 10–20 samples, and laboratory standards calibrated to IAEA reference materials were run after every five samples. The detection limit was 2 μg C and 1 μg N, and analytical precision was < 0.1‰ for $\delta^{13}C$ and $\delta^{15}N$.

3.2.4. Rates of NPP, N uptake, and nitrite oxidation

Simulated *in situ* experiments were conducted to determine the rates of NPP and N (as NO_3^-, NH_4^+, and urea) uptake at the boat stations only. Seawater was collected at the surface at each inshore (A) and offshore station (C), pre-filtered (200 μm) to remove large grazers, and transferred to six 1 L clear polycarbonate bottles. Duplicate bottles were amended with ^{15}urea-N, $^{15}NH_4Cl$, or $K^{15}NO_3$ (final ^{15}N concentration of 0.1 μM, 0.05 μM, or 0.5 μM) and $NaH^{13}CO_3$ was added to four bottles (final ^{13}C concentration of 100 μM). Bottles were incubated onboard for 4–6 hr in a custom-built incubator that was cooled via a continuous supply of running seawater and equipped with a neutral density filter to simulate light at ~1 m. Experiments were terminated via filtration onto ashed 0.3 μm GF-75 filters that were stored in cryovials at −80 °C until analysis. Incubation filters were analysed for C and N isotope ratios as described in section 2.3.3 above.

Rates of NPP and NO_3^-, NH_4^+, and urea uptake (ρNO_3^-, ρNH_4^+, ρurea; μM hr^{-1}) were calculated using the measured DIC and N-nutrient concentrations following Dugdale and Wilkerson (1986) as:

$$\rho_x = \left(\frac{(R_{xs})}{((R_{enr}) - (F))\,xT}\right) \times \text{PON or POC} \quad (1)$$

where *x* is NPP, NO_3^-, NH_4^+ or urea; R_{xs} is the measured sample ^{15}N or ^{13}C atom % minus the natural abundance atom % (*F*, = 0.366% for ^{15}N and 1.07% for ^{13}C), R_{enr} is the atom % ^{15}N or ^{13}C in the incubation seawater following tracer addition, and *T* is the incubation length (hr).

For NO_2^- oxidation, seawater was collected at stations A and C, from the surface and halfway to seafloor, and transferred to four 250 mL opaque polycarbonate bottles (two per depth). Experiments were initiated via the addition of $Na^{15}NO_2$ (final ^{15}N concentration of 0.4 μM), after which bottles were placed in the incubator for 24 hr. A 50 mL subsample was taken from each incubation bottle at 0 and 24 hr (i.e., T_0 immediately following $^{15}NO_2^-$ addition and T_f upon termination of the experiment) and frozen at −20 °C pending analysis. In the laboratory, samples were treated with sulfamic acid to remove residual $^{15}NO_2^-$ (Peng et al., 2015), then analysed using the denitrifier method as described in section 2.3.1 above, with an additional CRM, USGS-32 ($\delta^{15}N = 180 \pm 0.3$‰; Böhlke et al., 1993), included in each run. The rate of NO_2^- oxidation ($V_{NO_2^-}$; μM/hr) was calculated following Peng et al. (2015) as:

$$V_{NO_2^-} = \frac{\Delta[\ ^{15}NO_3^-]}{f^{15}_{NO_2^-} \times T} \quad (2)$$

where $\Delta[\ ^{15}NO_3^-]$ is the difference in the concentration of $^{15}NO_3^-$ between the T_{final} and $T_{initial}$ samples due to $^{15}NO_2^-$ oxidation, $f^{15}_{NO_2^-}$ is the fraction of $^{15}NO_2^-$ at the start of the incubation, and T is the incubation length (hr). The detection limit for $V_{NO_2^-}$, calculated following Santoro et al. (2013), ranged from 0.11 to 0.36 nM/day.

3.3. Mussel biology

At each rocky shore site except site 5 (Strand) where mussels were absent, *M. galloprovincialis* samples were collected for condition index,

tissue $\delta^{13}C$ and $\delta^{15}N$, and FA composition. Sampling was also conducted to assess the biodiversity associated with the mussel beds and to quantify benthic invertebrate settlement and recruitment.

3.3.1. Condition index and biodiversity

Twenty-five mussels from each site were collected for assessment of condition index (CI). The shell and soft body tissue of each mussel were separated and dried at 60 °C for 48 hr, after which the CI was calculated following Davenport and Chen (1987):

$$CI = dry\ soft\ tissue\ weight / dry\ shell\ weight \times 100 \quad (3)$$

The biodiversity of the community associated with the mussel beds was determined through destructive sampling. At each site, six replicate quadrats (15 × 15 cm) with 100% primary mussel cover were collected and stored in 100% ethanol. All organisms >0.5 mm were counted and identified to the highest taxonomic level possible using an Olympus SZX16 stereomicroscope.

3.3.2. Stable isotopes

Six mussel replicates of the same size (approximately 5 cm length) were haphazardly collected at each site for samples of adductor muscle. This tissue was chosen because of its long turnover rate (approximately nine months; Hill and McQuaid, 2009), which makes it the preferred indicator of integrated conditions. Mussels were dissected in the laboratory, rinsed with Milli-Q water to remove sediment, shell pieces, and other debris, then placed in 2 mL cryotubes and stored at −20 °C. Samples were subsequently dried at 60 °C for 48 hr, after which 0.5 mg of ground tissue was transferred to a tin capsule and analysed for $\delta^{13}C$ and $\delta^{15}N$ as described in section 2.3.3.

3.3.3. Fatty acids

Mussels were collected in triplicate at each site for samples of adductor muscle that were stored at −80 °C until analysis. Total lipids were extracted and trans-esterified using a modification of the Folch et al. (1957) procedure. Samples were lyophilised for 24 hr, then homogenised in 6 mL of a fresh solution of methanol and chloroform (2/1; v/v) and closed under an N_2 atmosphere. The FA methyl esters (FAME) were obtained after acidic transesterification of the sample by the addition of a H_2SO_4/methanol solution (3.4%; v/v) and heating at 100 °C for 10 min. FAME composition was determined using a Varian CP8400 Gas Chromatograph equipped with a ZBWAX column (30 m × 0.25 190 mm ID × 0.2 μm), with hydrogen as the carrier gas. Peaks were identified by comparison with retention times of external standards (Supelco 37 Component FAME Mix, PUFA No.1 and No.3, and Bacterial Acid Methyl Ester Mix; Sigma). FA are reported using the notation A:Bn-*x*, where A is the number of carbon atoms, B is the number of double bonds, and *x* indicates the position of the first double bond relative to the terminal methyl group (Puccinelli et al., 2016c).

3.3.4. Distribution of benthic invertebrate larvae

To determine the abundance and distribution of early-stage mussels in the water column, duplicate 60–100 L aliquots of seawater were collected adjacent to the rocky shore sites and from the surface boat stations using a submersible pump and filtered through a 75 μm sieve. The sieve contents were then stored in 500 mL bottles in 100% ethanol. Samples were processed for larval identification using a stereoscopic microscope (Leica MZ75, 2.0x magnification).

3.4. Potential pollutants

Along with measurements of nutrient concentrations and nitrate isotope ratios, which can provide information on anthropogenic N inputs and background nutrient cycling, samples were collected for the analysis of heavy metals and aerosols, the latter indicative of atmospheric deposition to surface waters (Altieri et al., 2021a).

3.4.1. Metals

Mussels and sediment samples were collected at each rocky shore site for metal concentrations (n = 5 per site). Where possible, sediment samples were also collected from the inshore boat stations using a hand-held Van Veen grab (40 × 10 cm, 0.1 m^2). Samples were stored in clean plastic jars at −20 °C pending analysis. The entire mussel soft body was analysed, with frozen samples freeze-dried for 48 hr, weighed, and homogenised with a mortar and pestle. Subsamples (~0.5 g) were digested in 7 mL of a 6:1 nitric acid:hydrogen peroxide solution using a MARS microwave digestion system. Metal concentrations were measured using Inductively Coupled Plasma Mass Spectrometry (Agilent 7900) with an Octopole Reaction System. The results were compared to the CRM TORT-3 (CNRC; average uncertainty of ± 1.5 μg/g).

3.4.2. Aerosols

Aerosols were collected daily during the sampling period on pre-combusted glass fibre filters using cyclone size-segregated samplers for fine- (<1 μm) and coarse mode (<10 μm) aerosols at the Cape Point Global Atmosphere Watch (GAW) station (34°21′S, 18°29′E). Filters were stored at −20 °C until aqueous extraction and sample analysis following standard procedures (Chen et al., 2010). Aqueous extracts were analysed for NO_3^-, NO_2^-, and NH_4^+, as well as other anions (Cl^- and SO_4^{2-}) and cations (Na^+, K^+, Ca^{2+}, Mg^{2+}), using two Dionex Aquion Ion Chromatography Systems (Thermo Scientific) (Altieri et al., 2021b). Aerosol concentrations were converted to dry deposition fluxes following Duce et al. (1991). Aerosol NO_3^- was also measured for its $\delta^{15}N$ and $\delta^{18}O$ using the denitrifier method (Sigman et al., 2001; Casciotti et al., 2002; Weigand et al., 2016), amended for atmospheric samples (Hastings et al., 2003; Altieri et al., 2013). Air mass back trajectories were computed for all sample days using the NOAA Hybrid Single-Particle Lagrangian Integrated Trajectory (HYSPLIT) model. The South African Weather Service provided ^{222}Rn concentration data for air mass source analysis that was used to further constrain air mass history (Brunke et al., 2004).

3.5. Data analysis

3.5.1. Univariate analyses

We tested the effects of the factor *Site* on the CI, $\delta^{13}C$, and $\delta^{15}N$ of mussels using a one-way analysis of variance (ANOVA; factor *Site*, fixed, n = 7). In the event of significant results, Tukey HSD *post hoc* tests were conducted. Analyses were performed using R version 3.6.3. (R Core Team, 2020).

Variability among sites for metals in mussels and sediment was evaluated using a Kruskal-Wallis test. In the event of significant results, we performed *post hoc* pairwise tests adjusted by a Bonferroni correction for multiple tests. Statistical analyses were conducting using SPSS 2019 v26. The efficiency of metal accumulation in mussels was evaluated using a BioSediment Accumulation Factor (BSAF), corresponding to the ratio of metals in mussels versus sediment (Lau et al., 1998). The degree of metal contamination in sediment was determined from the Contamination Factor (CF) and Pollution Load Index (PLI) (El-Sammak and Aboul-Kassim, 1999). CF is the factor by which the metal concentrations exceed previous measurements at the same sites, computed here relative to data from 2001 (Mdzeke 2004). The PLI measures the contamination load as:

$$PLI = \sqrt[4]{(CF_{Zn})(CF_{Cu})(CF_{Cd})(CF_{Pb})} \quad (4)$$

where CF_{Zn}, CF_{Cu}, CF_{Cd}, and CF_{Pb} are the CFs for zinc, copper, cadmium, and lead, respectively. PLI values > 1.2 imply high sedimentary metal contamination (El-Sammak and Aboul-Kassim, 1999). Metals in mussels and sediment were compared to the permissible legal limits in shellfish for South Africa (DOH, 1994, 2004) and recommended sediment quality guidelines for southern Africa (Taljaard, 2006).

3.5.2. Multivariate analyses

A multivariate permutational analysis (PERMANOVA; Anderson 2001) was performed to test for differences among sites (factor *Site*, fixed, n = 7) in the community associated with the mussel beds and the FA composition of the mussels. Variation in the distribution of larvae among sites was investigated using a PERMANOVA two-factor design (factor *Site*, fixed, n = 8; factor *Transect*, fixed, n = 7). Homogeneity of dispersions was tested using PERMDISP (Anderson et al., 2008a). Each term in the PERMANOVA analysis was tested using > 9999 permutations as the relevant permutable units (Anderson and Braak, 2003). In the event of significant results, PERMANOVA pairwise tests were performed.

Principal component analyses (PCA) were used to explore differences in the community associated with the mussel beds, mussel FA composition, and larval distribution in relation to the factors investigated. The combined results of the PCA and similarity percentage analyses (SIMPER) were used to assess the variables responsible for differences among groups of samples. All analyses were based on Bray-Curtis dissimilarities calculated from percentage data after square root transformation. For the community associated with the mussel beds, Shannon (H') and Pielou's (J') indexes were computed to determine species diversity and evenness among sites. The analyses were conducted using the PERMANOVA+ add-on package of PRIMER v6 (Clarke and Gorley, 2006; Anderson et al., 2008).

4. Results

Samples were collected at eight rocky shore sites and along seven onshore-offshore transects, each consisting of two or three stations (A, B, C). The term *site* is thus used to denote rocky shore sampling locations (1 to 8), *transect* to indicate the entire onshore-offshore sampling (1 to 8, excluding site 7 (Kogel Bay, where boat sampling was not conducted), and *station* to refer to individual sampling locations along the boat transects (A, B, C).

4.1. Physical environment

Vertical profiles of temperature, salinity, and dissolved oxygen concentrations at the boat stations are shown in Fig. 2 and Fig S.1. Generally, the water column was well mixed, with a clear thermocline evident only at the deepest station, 8B (Rooi-Els) (Fig. 2a and Fig S.1 g1). Sea surface temperature ranged between 15.5 and 18.2 °C, and temperature decreased with depth to a minimum of 13.5 °C at station 8B. Salinity was generally higher to the west of the bay and at the offshore stations (except station 5C (Strand) where it reached a minimum), with values ranging between 34.4 and 35.8 (Fig. 2b and Fig S.1e2). Dissolved oxygen was variable, with concentrations of 180 μM to 312 μM (Fig. 2c). Surface oxygen concentrations were roughly in equilibrium with the atmosphere at stations 3A and 3B (Muizenberg, Fig S.1c3), 4B (Monwabisi, Fig S.1d3), and 6B (Bikini Beach, Fig S.1f3), and undersaturated at the other stations. Stations along transect 5 had the lowest oxygen concentrations, with average surface values equivalent to ~50% saturation.

4.2. Biogeochemistry

4.2.1. Nutrients and carbonate system parameters

Nutrient concentrations are summarised in Table 1a, with station averages (i.e., surface to depth at the boat stations) for the N species (NO_3^-, NH_4^+, urea) shown in Fig. 3a, and depth profiles of NO_3^-, NO_2^-, Si$(OH)_4$, and PO_4^{3-} shown in Fig S.2. The average NO_3^- concentration across the study region was 5.1 ± 5.1 μM, excluding transects 5 and 6 (Strand and Bikini Beach) where NO_3^- was 14.7 ± 6.3 μM and 7.4 ± 3.2 μM, respectively. At station 5A, surface NO_3^- reached > 20 μM, decreasing offshore. In general, NO_3^- did not vary with depth, except at station 8B (Rooi-Els) where it showed a typical nutrient-like profile, reaching a concentration of 13.0 ± 1.1 μM at 25 m.

The NO_2^- concentrations were generally low, averaging 0.5 ± 0.4 μM, and as per NO_3^-, were higher at transect 5 (1.5 ± 0.3 μM). NH_4^+ concentrations were higher in shallower waters and at the inshore stations, with the highest concentrations observed at transects 5 and 6 (3.7 ± 0.3 μM versus an average of 1.8 ± 0.4 μM for the other transects). The urea concentrations were generally low, averaging 0.6 ± 0.3 μM for all stations and depths, but reached a maximum of 4.4 μM at 9 m at station 5B.

The Si$(OH)_4$ concentrations averaged 7.0 ± 2.0 μM across the region and increased with depth at site 8B only, reaching 17.0 μM. Rocky shore site 3 (Muizenberg) and station 5B at 6 m were the only other cases where Si$(OH)_4$ exceeded 10 μM. The PO_4^{3-} concentrations were generally low (0.6 ± 0.2 μM) and there was no clear trend among sites or stations, although at stations 4A and B (Monwabisi), PO_4^{3-} exceeded 1 μM.

pH, Ω_{Ca}, and Ω_{Ar} followed a west-east pattern, with significant higher values to the west of False Bay (transects 1 to 4; $p < 0.05$), regardless of depth or distance from the shore (Table S.2). Specifically, pH in the west ranged from 7.6 to 8.1 (average of 8.0 ± 0.1), while values of 7.6 to 7.9 (average of 7.8 ± 0.1) were computed for the eastern stations. Ω_{Ca} ranged from 1.9 to 4.5 (average of 3.5 ± 1.0) in the west and from 1.8 to 3.0 (average of 2.3 ± 0.1) in the east, while Ω_{Ar} ranged from 1.0 to 2.9 (average 2.2 ± 0.6) and from 1.1 to 1.9 (average 1.5 ± 0.2) in the west and east, respectively.

4.2.2. Isotopes of particulate organic matter and nitrate

$\delta^{13}C_{POC}$ did not vary with depth; however, there was a significant

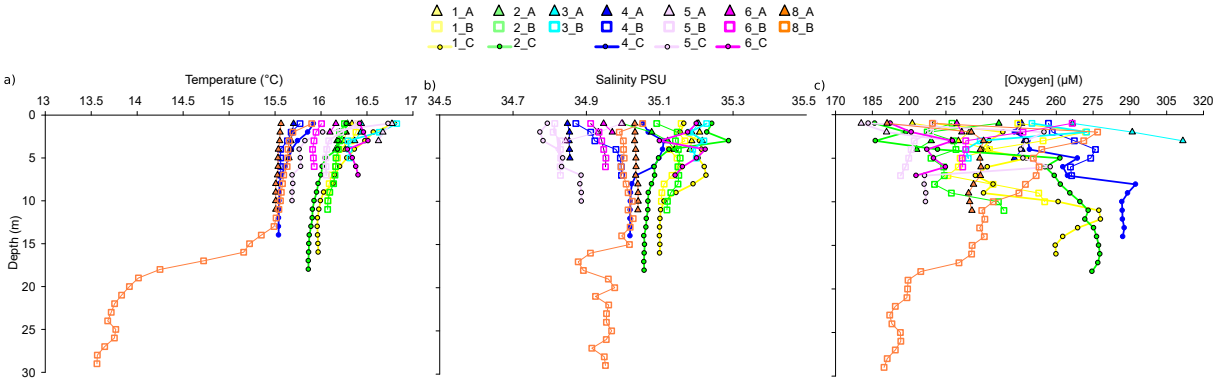

Fig. 2. Vertical profiles of a) temperature, b) salinity, and c) oxygen concentrations from the seven onshore-offshore transects sampled in False Bay in May 2018. The symbol shape indicates the station position (A = triangle (onshore), B = square (mid-shore), C = circle (offshore)) and the colour indicates the transect: 1- Millers Point (yellow), 2- Simons Town (green), 3- Muizenberg (cyan), 4- Monwabisi (blue), 5- Strand (light pink), 6- Bikini Beach (magenta), 8- Rooi-Els (orange). (For interpretation of the references to colour in this figure legend, the reader is referred to the web version of this article.)

Table 1

a) Concentrations of nutrients (NO_3^-, $Si(OH)_4$, PO_4^{3-}, NO_2^-, NH_4^+, urea) and b) stable isotopic composition of seawater nitrate ($\delta^{15}N_{NO3}$ and $\delta^{18}O_{NO3}$), suspended particulate organic nitrogen and carbon ($\delta^{15}N_{PON}$ and $\delta^{13}C_{POC}$), and mussels ($\delta^{15}N_{mussel}$ and $\delta^{13}C_{mussel}$), as well as chlorophyll *a* (Chl-*a*) and suspended PON and POC concentrations for samples collected at select intertidal sites and nearshore stations in False Bay in May 2018. Values are reported as mean ± standard error, except for Chl-*a* where only one sample was collected.

a)

Kind of sampling	Site name & number	Station	Depth (m)	Depth (m)	[NO3] (μM)	± SE	[SiO4] (μM)	± SE	[PO4] (μM)	± SE	[NO2] (μM)	± SE	[NH4] (μM)	± SE	[Urea] (μM)	± SE	[Chla] (μg/L)
Rocky shore	1- Millers Point		surface		3.67	0.02	7.48	0.21	0.50	0.02	0.44	0.17	1.01	0.02	0.57	0.02	2.46
Rocky shore	2- Simons Town		surface		2.74	0.01	8.23	0.10	0.28	0.10	0.18	0.01	2.89	0.05	0.59	0.00	1.66
Rocky shore	3- Muizenberg		surface		4.04	0.07	10.68	0.05	0.36	0.04	0.30	0.00	4.31	0.06	0.89	0.10	1.11
Rocky shore	4- Monwabisi		surface		6.39	0.27	7.67	0.11	0.51	0.02	0.62	0.21	4.19	1.88	0.74	0.20	1.77
Rocky shore	5- Strand		surface		15.49	1.03	6.94	0.32	0.94	0.11	1.24	0.06	2.33	0.11			0.44
Rocky shore	6- Bikini Beach		surface		7.77		9.32		0.76	0.30	0.53	0.15	4.23	0.11	0.78	0.04	0.62
Rocky shore	7- Kogel Bay		surface		7.71	0.07	8.17	0.05	0.46	0.05	0.50	0.09	4.48	2.14	1.11	0.02	1.43
Rocky shore	8- Rooi-Els		surface		7.02	0.71	7.90	0.01	0.66	0.31	1.10	0.69	2.61	0.07			0.54
Boat	1- Millers Point	A	surface	4	3.49	0.39	5.85	1.11	0.84	0.44	0.33	0.02	2.37	1.04	0.54	0.00	0.30
Boat	1- Millers Point	A	4	4	6.51	0.02	4.71	0.07	0.86	0.01	1.07	0.10	1.24	0.15	0.61	0.21	0.34
Boat	1- Millers Point	B	surface	8	2.45	0.03	8.33	0.07	0.51	0.03	0.22	0.01	2.50	0.11	0.66		0.31
Boat	1- Millers Point	B	4	8	1.49	0.06	6.50	0.01	0.24	0.02	0.36	0.06	1.61	0.99	0.76	0.22	0.29
Boat	1- Millers Point	B	8	8	1.69	0.14	4.66	0.44	0.46	0.02	0.23	0.02	0.14	0.01	0.28	0.04	0.41
Boat	1- Millers Point	C	surface	20	0.79	0.04	5.10	0.18	0.27	0.01	0.09	0.01	2.34	1.93	0.44		2.15
Boat	1- Millers Point	C	6	20	0.91	0.02	6.49	0.19	0.20	0.03	0.14	0.02	2.87	1.50	0.52	0.07	3.79
Boat	1- Millers Point	C	13	20	0.96	0.02	6.84	0.48	0.69	0.14	0.03	0.02	1.34	0.82	0.37	0.01	4.34
Boat	1- Millers Point	C	20	20	0.80	0.12	5.36	0.18	0.31	0.03	0.07	0.02	1.19	1.07	0.14	0.08	3.56
Boat	2- Simons Town	A	surface	4	1.91	0.02	6.95	0.07	0.50	0.01	0.16	0.01	1.78	0.65	0.51	0.01	0.86
Boat	2- Simons Town	A	4	4	1.18	0.05	5.34	0.16	0.35	0.02	0.10	0.02	1.39	0.01	0.63	0.15	0.93
Boat	2- Simons Town	B	surface	9	1.71	0.02	7.12	0.07	0.50	0.02	0.15	0.01	1.02	0.32	0.63	0.03	0.95
Boat	2- Simons Town	B	5	9	1.61	0.04	8.53	0.07	0.74	0.14	0.26	0.24	2.41	1.08	0.45	0.05	0.98
Boat	2- Simons Town	B	9	9	1.56	0.18	7.15	0.26	0.43	0.04	0.10	0.00	1.99	0.45	0.39	0.07	1.17
Boat	2- Simons Town	C	surface	18	1.61	0.24	7.20	0.73	0.68	0.04	0.11	0.05	2.44	0.05	0.32	0.08	0.88
Boat	2- Simons Town	C	6	18	1.77	0.09	7.28	0.33	0.33	0.02	0.06	0.02	2.73	1.26	0.30	0.06	1.22
Boat	2- Simons Town	C	12	18	1.27	0.16	5.67	0.03	0.25	0.01	0.06	0.00	2.56	2.13	0.51	0.21	1.76
Boat	2- Simons Town	C	18	18	1.16	0.02	8.68	0.04	0.74	0.08	0.06	0.01	0.93	0.35	0.41	0.07	0.76
Boat	3- Muizenberg	A	surface	1	0.89	0.04	4.77	0.07	0.34	0.02	0.10	0.01	2.47	0.07	0.48	0.00	1.65
Boat	3- Muizenberg	B	surface	4	1.20	0.03	7.95	0.13	0.33	0.07	0.15	0.01	0.18	0.02	0.42	0.12	1.05
Boat	3- Muizenberg	B	4	4	1.04	0.07	8.12	0.01	0.32	0.02	0.19	0.02	1.13	0.51	0.49	0.00	1.84
Boat	4- Monwabisi	A	surface	4	2.98	0.25	2.68	0.21	1.00	0.04	0.28	0.05	1.18	0.87	0.41	0.05	3.16
Boat	4- Monwabisi	A	4	4	3.47	0.02	3.09	0.01	1.10	0.01	0.26	0.02	3.45	1.02	0.52	0.02	3.22
Boat	4- Monwabisi	B	surface	7	3.40	0.93	7.35	0.85	1.10	0.05	0.28	0.01	1.90	0.21	0.70	0.01	4.21
Boat	4- Monwabisi	B	4	7	2.05	0.04	5.41	0.05	0.74	0.10	0.14	0.01	0.13	0.04	0.18	0.08	1.34
Boat	4- Monwabisi	B	7	7	1.24	0.10	6.80	0.29	0.69	0.08	0.11	0.04	1.13	1.04	0.29	0.11	7.23
Boat	4- Monwabisi	C	surface	14	3.52	0.83	6.57	0.46	0.32	0.09	0.02	0.02	0.07	0.03	0.69	0.05	1.87
Boat	4- Monwabisi	C	4	14	1.11	0.04	8.16	0.08	0.51	0.03	0.06	0.04	0.23	0.10	0.14		2.19
Boat	4- Monwabisi	C	8	14	1.20	0.02	8.79	0.06	0.26	0.02	0.02	0.01	0.13	0.07	0.41	0.19	21.76
Boat	4- Monwabisi	C	14	14	1.32	0.03	4.99	0.17	0.83	0.10	0.03	0.00	0.85	0.67	0.31	0.09	5.28
Boat	5- Strand	A	surface	1	20.86	1.42	9.84	0.37	0.83	0.06	1.59	0.18	3.95	0.01	0.97	0.19	0.79
Boat	5- Strand	B	surface	6	14.09	0.37	8.08	0.16	0.76	0.07	1.74	0.17	4.87	0.17	0.69	0.00	1.98
Boat	5- Strand	B	6	6	20.00	0.20	10.20	0.02	0.65	0.05	1.59	0.19	4.33	0.07	4.38		4.11
Boat	5- Strand	C	surface	9	12.86	0.34	7.99	0.09	0.89	0.16	1.57	0.10	1.49	0.79	1.80	0.76	1.87
Boat	5- Strand	C	5	9	9.49	0.48	8.26	0.29	0.87	0.17	0.98	0.06	4.24		1.33	0.55	3.52
Boat	5- Strand	C	9	9	8.28	0.77	7.93	0.35	0.54	0.05	1.72	0.30	1.24	0.08			2.26

(*continued on next page*)

Table 1 (*continued*)

a)

Kind of sampling	Site name & number	Station	Depth (m)	Depth (m)	[NO3] (μM)	± SE	[SiO4] (μM)	± SE	[PO4] (μM)	± SE	[NO2] (μM)	± SE	[NH4] (μM)	± SE	[Urea] (μM)	± SE	[Chla] (μg/L)
Boat	6- Bikini Beach	A	surface	1	8.32	0.06	8.28	0.07	0.76	0.03	0.93	0.00	4.77	0.19	0.47	0.31	0.85
Boat	6- Bikini Beach	B	surface	5	6.52	0.24	7.28	0.13	0.54	0.07	0.91	0.11	2.06	0.04	0.58	0.20	3.31
Boat	6- Bikini Beach	B	5	5	9.27	0.42	9.15	0.26	0.79	0.34	0.66	0.10	3.76		0.94	0.10	1.74
Boat	6- Bikini Beach	C	surface	7	11.11	0.02	8.32	0.04	0.90	0.01	0.00	0.04	3.83	1.25	0.30		2.66
Boat	6- Bikini Beach	C	4	7	7.17	1.02	7.14	0.71	0.83	0.14	0.33	0.20	2.37	0.06	0.74	0.04	14.69
Boat	6- Bikini Beach	C	7	7	6.97	0.73	7.40	0.70	0.73	0.18	0.87	0.11	1.72	0.05	0.64	0.24	5.66
Boat	8- Rooi-Els	A	surface	12	5.13	0.01	7.53	0.02	0.53	0.05	0.44	0.00	2.32	0.73	0.99	0.15	2.64
Boat	8- Rooi-Els	A	4	12	4.45	0.30	8.11	0.32	0.49	0.04	0.49	0.06	2.82	0.13			2.39
Boat	8- Rooi-Els	A	8	12	6.09	0.21	7.31	0.25	0.75	0.05	0.39	0.04	2.82	0.30	0.89		1.29
Boat	8- Rooi-Els	A	12	12	5.48	0.10	8.65	0.08	0.65	0.10	0.41	0.10	2.40	0.84	0.79	0.07	1.01
Boat	8- Rooi-Els	B	surface	25	2.08	0.08	7.01	0.01	0.29	0.05	0.33	0.06	0.40	0.04	0.79	0.05	6.65
Boat	8- Rooi-Els	B	4	25	2.85	0.12	6.23	0.22	0.66	0.09	0.31	0.01	1.38	0.08	0.55	0.05	9.97
Boat	8- Rooi-Els	B	12	25	3.57	0.08	8.08	0.05	0.30	0.03	0.53	0.07	1.34	0.10	0.72	0.12	2.67
Boat	8- Rooi-Els	B	25	25	12.99	0.11	17.03	0.12	0.76	0.06	0.49	0.00	2.35	0.20	0.49	0.00	

b)

Kind of sampling	Site name & number	Station	Depth (m)	Bottom depth (m)	NO3 $\delta^{15}N$ ± SE (‰)		NO3 $\delta^{18}O$ ± SE (‰)		PON $\delta^{15}N$ ± SE (‰)		PON ± SE (μM)		POC $\delta^{13}C$ ± SE (‰)		POC ± SE (μM)		Mussel $\delta^{15}N$ ± SE (‰)		Mussel $\delta^{13}C$ ± SE (‰)	
Rocky shore	1- Millers Point		surface						6.24	1.54	2.01	0.27	-12.61	0.80	22.03	4.82	7.87	0.05	-15.73	0.51
Rocky shore	2- Simons Town		surface						4.40	2.24	2.44	0.38	-14.63	0.50	24.29	6.46	8.15	0.04	-15.52	0.17
Rocky shore	3- Muizenberg		surface						6.60		2.02	0.23	-11.61		20.14	0.76	9.14	0.09	-14.52	0.04
Rocky shore	4- Monwabisi		surface		8.79	0.08	4.99	0.15	7.35	0.14	3.56	0.27	-7.82	0.56	62.74	4.85	8.12	0.07	-15.17	0.39
Rocky shore	5- Strand		surface		7.94	0.62	3.76	0.77	7.49	1.49	2.53	0.33	-8.86	1.06	38.25	6.92				
Rocky shore	6- Bikini Beach		surface		6.61	0.32	2.52	0.35	7.79	2.54	1.97	0.00	-9.63	1.10	30.51	1.99	8.74	0.07	-15.39	0.65
Rocky shore	7- Kogel Bay		surface		6.84	0.26	4.36	0.35	6.91	1.14	3.34	0.22	-10.35	0.50	38.34	3.60	8.03	0.08	-13.96	0.09
Rocky shore	8- Rooi-Els		surface		6.82	0.13	2.01	0.15	11.40	5.34	1.56	0.03	-13.30	2.86	17.83	1.64	8.23	0.06	-14.24	0.18
Boat	1- Millers Point	A	surface	4					6.18	0.25	2.16	0.79	-16.49	0.88	22.73	6.87				
Boat	1- Millers Point	A	4	4	5.83	0.00	0.36	0.00												
Boat	1- Millers Point	B	surface	8					6.28		0.72		-20.01		11.08					
Boat	1- Millers Point	B	4	8	5.78	0.00	1.04	0.00	6.78		0.74		-19.67		12.50					
Boat	1- Millers Point	B	8	8	5.38	0.00	1.65	0.00	6.16		0.52		-18.16		7.09					
Boat	1- Millers Point	C	surface	20	7.55	0.00	4.37	0.00	6.62		1.81		-19.01		19.42					
Boat	1- Millers Point	C	6	20					6.87		4.05		-16.35		42.22					
Boat	1- Millers Point	C	13	20					7.06		2.74		-16.51		30.66					
Boat	1- Millers Point	C	20	20					7.61		1.83		-16.80		22.34					
Boat	2- Simons Town	A	surface	4					6.40		1.82	0.59	-19.25		15.57	3.00				
Boat	2- Simons Town	A	4	4					7.35		1.28		-24.56		17.70					
Boat	2- Simons Town	B	surface	9	7.14	0.00	4.64	0.00	6.32		1.27		-18.82		11.73					
Boat	2- Simons Town	B	5	9	6.26	0.00	6.00	0.00	6.21		1.44		-19.42		14.36					
Boat	2- Simons Town	B	9	9	6.92	0.00	5.71	0.00	6.29		1.52		-17.36		15.67					
Boat	2- Simons Town	C	surface	18	7.15	0.24	5.53	3.29	6.26		1.43		-19.58		15.40					
Boat	2- Simons Town	C	6	18	6.45	0.00	5.74	0.00	6.28		1.21		-18.19		11.76					
Boat	2- Simons Town	C	12	18	7.09	0.00	7.81	0.00												
Boat	2- Simons Town	C	18	18					7.26		0.68		-20.63		8.45					
Boat	3- Muizenberg	A	surface	1	6.78	0.00	4.81	0.00	5.71	0.02	1.90	0.14	-15.63	0.17	16.17	0.17				
Boat	3- Muizenberg	B	surface	4					5.66		1.18		-19.12		12.25					

(*continued on next page*)

Table 1 (*continued*)

Kind of sampling	Site name & number	Station	Depth (m)	Bottom depth (m)	NO3 $\delta^{15}N$ ± SE (‰)		NO3 $\delta^{18}O$ ± SE (‰)		PON $\delta^{15}N$ ± SE (‰)		PON ± SE (µM)		POC $\delta^{13}C$ ± SE (‰)		POC ± SE (µM)		Mussel $\delta^{15}N$ ± SE (‰)	Mussel $\delta^{13}C$ ± SE (‰)
Boat	3- Muizenberg	B	4	4					6.43		1.79		-16.77		19.36			
Boat	4- Monwabisi	A	surface	4					4.45	2.25	2.83	0.27	-11.01	1.81	30.78	2.95		
Boat	4- Monwabisi	A	4	4					6.83		2.39		-10.23		33.33			
Boat	4- Monwabisi	B	surface	7					4.59		4.31		-14.41		39.11			
Boat	4- Monwabisi	B	4	7					7.79		6.92		-14.44		67.62			
Boat	4- Monwabisi	B	7	7	11.37	0.00	12.28	0.00	7.46		3.94		-13.06		47.01			
Boat	4- Monwabisi	C	surface	14					7.24		1.54		-18.03		17.43			
Boat	4- Monwabisi	C	4	14							0.00				0.00			
Boat	4- Monwabisi	C	8	14					7.36		11.26		-14.98		134.56			
Boat	4- Monwabisi	C	14	14	10.39	0.00	20.13	0.00	7.40		3.01		-17.17		42.29			
Boat	5- Strand	A	surface	1	8.18	0.17	1.75	0.15	6.55	0.26	2.21	0.44	-9.61	1.21	33.88	7.60		
Boat	5- Strand	B	surface	6	8.01	0.42	3.03	0.12	5.69		1.50		-14.33		19.88			
Boat	5- Strand	B	6	6	8.18	0.18	1.69	0.23	6.02		5.43		-9.02		86.35			
Boat	5- Strand	C	surface	9	7.53	0.28	2.94	0.21	1.91		2.33		-14.00		19.05			
Boat	5- Strand	C	5	9	7.60	0.14	3.03	0.16	5.53		1.53		-15.23		17.25			
Boat	5- Strand	C	9	9	7.61	0.16	2.25	0.76	6.54		1.21		-14.49		16.62			
Boat	6- Bikini Beach	A	surface	1	7.67	0.48	3.44	0.50	6.36	0.22	1.68	0.39	-16.32	0.51	15.63	2.33		
Boat	6- Bikini Beach	B	surface	5	7.96	0.07	2.92	0.14	7.07		2.17		-19.73		20.09			
Boat	6- Bikini Beach	B	5	5					5.61		1.00		-14.68		12.14			
Boat	6- Bikini Beach	C	surface	7					6.16		2.56		-18.17		22.02			
Boat	6- Bikini Beach	C	4	7					7.50		6.26		-16.03		54.72			
Boat	6- Bikini Beach	C	7	7					7.35		2.07		-15.11		19.49			
Boat	8- Rooi-Els	A	surface	12	6.78	0.13	1.79	0.27	7.54	1.07	2.17	0.91	-17.18	3.83	19.24	7.23		
Boat	8- Rooi-Els	A	4	12					6.68		1.14		-18.13		12.19			
Boat	8- Rooi-Els	A	8	12	6.81	0.09	2.36	0.49	7.44		1.06		-18.70		14.99			
Boat	8- Rooi-Els	A	12	12	6.66	0.00	1.45	0.00	7.18		1.30		-19.91		17.59			
Boat	8- Rooi-Els	B	surface	25					7.35		4.10		-16.30		36.54			
Boat	8- Rooi-Els	B	4	25					7.50		5.64		-15.94		50.26			
Boat	8- Rooi-Els	B	12	25					7.24		1.37		-17.51		13.67			
Boat	8- Rooi-Els	B	25	25	8.56	0.29	3.59	0.82	7.21		0.98		-17.92		14.84			

difference among stations ($p < 0.05$; Table 1b). Transects 1 (Millers Point), 2 (Simons Town), 3 (Muizenberg), and 8 (Rooi-Els) had lower average $\delta^{13}C_{POC}$ (-18.3 ± 1.8‰) than transects 4 (Monwabisi), 5 (Strand), and 6 (Bikini Beach) (-13.8 ± 3.3‰) where the inshore sites and stations were characterized by the highest $\delta^{13}C_{POC}$ (rocky shore and station A, −10.5 ± 1.2‰). The $\delta^{13}C_{POC}$ at site 7 (Kogel Bay) was similarly high (-10.4 ± 0.5‰; note that no offshore sampling occurred at this site). We observed a clear onshore-offshore pattern, with $\delta^{13}C_{POC}$ decreasing with distance from the coast (Table 1b). For example, at transect 4, $\delta^{13}C_{POC}$ decreased from −7.8 ± 0.6‰ at the rocky shore to −16.8 ± 1.6‰ at station 4C.

$\delta^{15}N_{PON}$ averaged 6.6 ± 1.0‰ across the study region and varied significantly among stations and with depth ($p < 0.05$), with significant interactions between the two factors (*post-hoc* test, $p < 0.05$). $\delta^{15}N_{PON}$ increased with depth at stations 4A, 4B, 5C, and 6C, with the largest $\delta^{15}N$ change observed between the surface and 5 m samples (increase of 1.3‰ to 3.6‰; Table 1b, Fig S.3). An onshore-offshore decline in surface $\delta^{15}N_{PON}$ occurred at transects 3, 4, and 5, with the rocky shore sites characterized by a higher $\delta^{15}N_{PON}$ (by 0.9‰ to 2.8‰) than the offshore stations. The opposite pattern was observed for transect 2 where the rocky shore site had a lower $\delta^{15}N_{PON}$ (by 1.9‰) than the offshore stations. The lowest $\delta^{15}N_{PON}$ (1.9‰) was measured in the surface at station 5C.

$\delta^{15}N_{NO3}$ ranged between 5.4‰ and 11.4‰, with an average across all sites and stations of 7.4 ± 1.2‰ (7.1 ± 0.8‰ without transect 4), and did not vary significantly with depth. The highest average $\delta^{15}N_{NO3}$ was recorded at transects 4 (average of 10.2 ± 1.3‰) and 5 (average of 7.9 ± 0.3‰), and the lowest at transect 1 (average of 6.1 ± 1.0‰) (Table 1b, Fig S.3). No clear onshore-offshore pattern was evident, except at transect 1 where $\delta^{15}N_{NO3}$ increased by 1.9‰ between stations A/B and C. By contrast, we observed a clear west-east rise in $\delta^{15}N_{NO3}$ from an average of 6.6 ± 0.4‰ at sites and stations 1 through 3 to 7.5 ± 0.4‰ at sites and transects 5 through 8. At each site or station, $\delta^{15}N_{NO3}$ was always similar to or higher than the corresponding $\delta^{15}N_{PON}$, with the exception of rocky shore sites 6 and 8 where $\delta^{15}N_{PON}$ was 1.2‰ and 4.6‰ higher, respectively, than $\delta^{15}N_{NO3}$ (Table 1b).

$\delta^{18}O_{NO3}$ ranged from 0.4‰ to 20.1‰, with an average across all sites and stations of 5.3 ± 1.2‰ (3.7 ± 0.6‰ without transect 4 where $\delta^{18}O_{NO3}$ was extraordinarily high). At transects 5 through 8, $\delta^{18}O_{NO3}$ generally followed $\delta^{15}N_{NO3}$, changing in an approximate ratio of 1:1 (Fig S.4). By contrast, at transects 1 through 3, $\delta^{18}O_{NO3}$ changed by ~4‰ while $\delta^{15}N_{NO3}$ varied by <1‰. As for $\delta^{15}N_{NO3}$, the $\delta^{18}O_{NO3}$ at transect 1 was anomalously low compared to the other stations (1.8 ± 0.8‰).

4.2.3. Rates of NPP, N uptake, and nitrite oxidation

Rates of NPP and N uptake were variable and did not follow a west-east gradient (Fig. 3). NPP varied by three orders of magnitude, with the highest rates at inshore station 4A (Monwabisi, 1.7 ± 0.7 μM/hr) and the lowest at station 1A (Millers Point, 0.0 ± 0.0 μM/hr). Stations 6A and C (Bikini Beach) hosted the second highest rates of 0.9 ± 0.2 μM/hr and 0.7 ± 0.1 μM/hr, respectively, and 0.8 ± 0.1 μM /hr was measured at station 3A (Muizenberg). NPP at the other stations was ≤0.4 μM/hr, with an average for all stations of 0.5 ± 0.1 μM/hr (Fig. 3b, Table 2).

As for NPP, N uptake did not show an inshore-offshore pattern, and there was no clear correlation with N-nutrient concentration (Fig S.5). NH_4^+ was the favoured N substrate, followed by NO_3^- and then urea. ρNH_4^+ ranged from below detection to 0.2 μM/hr (Fig. 3c, pink bars; Table 2), with the highest detectable rates measured at stations 3A (0.2 ± 0.0 μM/hr), 4A (0.1 ± 0.0 μM/hr), and 6C (0.2 ± 0.0 μM/hr), and the lowest at transect 1 (0.5 ± 0.0 μM/hr) where the concentrations of all N species were low. The NO_3^- uptake rates ranged from below detection to 0.1 μM/hr (Fig. 3c, blue bars) and were higher on the east side of the bay, with the highest ρNO_3^- at stations 4C (0.1 ± 0.03 μM/hr) and 6C (0.03 ± 0.0 μM/hr) where the ambient NO_3^- and PON concentrations reached 21 μM and 6.3 μM, respectively (Table 1b). ρurea ranged from below detection to 0.1 μM/hr (Fig. 3c, yellow bars), with the highest rate measured at site 5C (Strand; 0.1 ± 0.0 μM/hr) where the ambient urea concentration reached a maximum (1.8 ± 0.8 μM).

Rates of NO_2^- oxidation could be measured for transects 4, 5, and 6 only, with the rates at or near the methodological detection limit at the other stations (Table 2). The highest NO_2^- oxidation rate occurred at 4 m at station 4A (1.2 μM/hr), followed by 9 m at station 5C (0.9 μM/hr) and the surface at station 5A (0.6 μM/hr). At the stations with measurable NO_2^- oxidation rates, this flux accounted for >100% of the NO_3^- assimilated by phytoplankton.

4.2.4. Phytoplankton biomass and community composition

Chlorophyll *a* concentrations were generally low at the rocky shore sites (1.3 ± 0.7 μg/L) and surface stations (2.0 ± 1.5 μg/L) and increased with depth, with maximum values in the mid-depths (4–10 m; average of 3.9 ± 1.2 μg/L; Table 1b). The highest concentration was measured at station 4C (Monwabisi), 21.8 μg/L at 8 m, and the lowest concentration at station 1B, 0.3 μg/L at 8 m.

The POC concentrations followed a similar pattern, reaching a maximum in the subsurface (4–6 m), with the highest concentrations at 6 m at station 5B (Strand, 86.3 μM), followed by 4 m at 4B (67.6 μM), 6C (Bikini Beach, 54.7 μM), and 8B (Rooi-Els, 50.3 μM). The rocky shore sites were characterized by similar POC concentrations to each other (30.8 ± 14.2 μM), except site 4 where POC was considerably higher (62.7 ± 4.8 μM).

Phytoplankton abundance was highest at transects 1 and 8 (up to 435 and 603 cells/mL, respectively) and lowest at transects 3 and 5 (89 and 40 cells/mL) (Fig. 4). Dinoflagellates were the main phytoplankton group at most of the boat stations, accounting for 70.4 ± 35.6% of the community, followed by diatoms (29.2 ± 35.8%) and a small contribution of silicoflagellates (0.4 ± 1.3%), mostly at station 2C (Simons Town) (Table S.3, Fig S.6). The dinoflagellate community was predominantly composed of *Tripos fusus*, which accounted for 52.5 ± 9.9% of the total cells at the boat stations, reaching 89.3 cells/mL (92% of cells) and 100.5 cells/mL (93% of cells) at stations 1C and 8B. By contrast, diatoms were the dominant group at nearly all the rocky shore sites (average of 89.6 ± 16.2% of the phytoplankton community), with 100% presence at sites 1, 3, 5, and 6. *Grammatophora spp*. and *Melosira spp*. dominated at sites 3 and 6, whereas *Navicula spp*. was most abundant at sites 1 and 2.

4.3. Mussels

4.3.1. Condition index and biodiversity

Mussel CI was significantly higher at sites on the east versus the west side of the bay ($p < 0.01$; Fig. 5a). A west-east pattern was also evident in the number of species associated with the mussel beds, with sites on the west side of the bay characterized by a higher species richness (Fig. 5b). Sites 1 (Millers Point) and 2 (Simons Town) had the highest biodiversity, with 48 and 53 unique species, while sites 4 (Monwabisi) and 7 (Kogel Bay) had the lowest biodiversity, with 24 and 26 unique species, respectively. Among the organisms found in the mussel beds, only four species were present at all sites: the polychaetes, *Glycera tridactyla* and *Pseudonereis variegata*, and the limpets, *Scutellastra granularis* and *Fissurella mutabilis,* which together accounted for 49% and 46% of the total species at sites 1 and 2, 43% at site 4, and ~ 20% at the other sites (Table S.4). Other abundant species included the polychaetes, *Syllidae* spp. (22% at site 1), the anemone, *Corynactis annulata* (24% at site 2), the bivalve, *Lasaea adansoni* (18% at site 3 (Muizenberg), 23% at site 4, 16% at site 8 (Rooi-Els)), and the amphipod *Apohyale grandicornis* (44% at site 8). The Shannon Diversity Index (H') and Pielou's Evenness Index (J') differed among sites ($p < 0.05$), with sites 1 and 8 characterized by the lowest H' and J' (average of 1.3 ± 0.1 and 1.8 ± 0.25 for H' and J', respectively) and site 7 by the highest (2.11 ± 0.1 and 3.1 ± 0.1), while the other four sites were characterized by similar intermediate values (average of 1.8 ± 0.1 and 2.6 ± 0.1, respectively).

The most abundant mussel, *M. galloprovincialis*, was generally longer

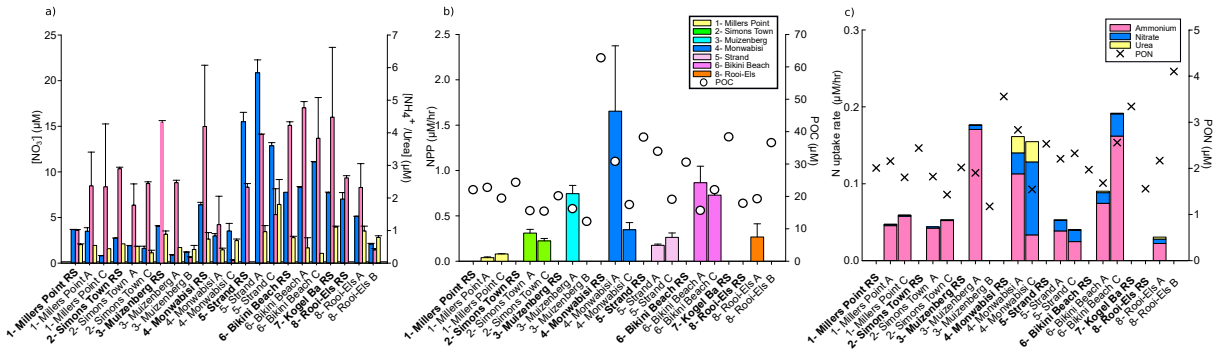

Fig. 3. Bar plots of a) nitrate (NO_3^-, blue bar), ammonium (NH_4^+, pink bar), and urea (yellow bar) concentrations; b) surface rates of net primary production (NPP) along with the particulate organic carbon (POC) concentrations; and rates of c) NO_3^- uptake (ρNO_3^-), NH_4^+ uptake (ρNH_4^+), and urea uptake (ρurea) along with the particulate organic nitrogen (PON) concentration at each site and station. Values are expressed as mean ± standard deviation. Rocky shore sites are highlighted in bold on the x-axes. Uptake experiments were not conducted at the mid-shore stations (B) (although nutrient and POC and PON concentrations were measured; Table 1a and b; Fig S.2). (For interpretation of the references to colour in this figure legend, the reader is referred to the web version of this article.)

Table 2
Rates of net primary production (NPP), nitrate uptake (ρNO_3^-), ammonium uptake (ρNH_4^+), urea uptake (pUrea), and nitrite oxidation ($V_{NO_2^-}$) measured at select stations in nearshore False Bay in May 2018. Values are mean ± standard error. Missing values indicate that samples were not collected, while * indicates that the measured rates were below the calculated detection limit and were thus not significantly higher than zero.

Site number	Site name	Station	Sample depth	NPP (µM/hr)			ρNO_3^- (µM/hr)			ρNH_4^+ (µM/hr)			ρUrea (µM/hr)			$V_{NO_2^-}$ (µM/hr)		
1	Millers Point	A	surface	0.04	±	0.01	0.00	±	0.00	0.05	±	0.00	0.00	±	0.00			
1	Millers Point	A	4 m													*		
1	Millers Point	C	surface	0.08	±	0.00	0.00	±	0.00	0.06	±	0.00	0.01	±	0.00			
2	Simons Town	A	surface	0.31	±	0.04	0.00	±	0.00	0.04	±	0.00	0.00	±	0.00			
2	Simon's Town	A	4 m													*		
2	Simon's Town	C	surface	0.22	±	0.03	0.00	±	0.00	0.05	±	0.00	0.00	±	0.00	*		
2	Simon's Town	C	12 m													*		
3	Muizenberg	A	surface	0.75	±	0.09	0.01	±	0.00	0.17	±	0.00	0.01	±	0.00			
4	Monwabisi	A	surface	1.65	±	0.72	0.03	±	0.02	0.11	±	0.00				*		
4	Monwabisi	A	4 m													1.19	±	1.18
4	Monwabisi	C	surface	0.35	±	0.08	0.09	±	0.03	0.03	±	0.00				*		
5	Strand	A	surface	0.18	±	0.01	0.01	±	0.00	0.04	±	0.00	0.01	±	0.00	0.61	±	0.02
5	Strand	C	surface	0.26	±	0.05	0.01	±	0.00	0.02	±	0.00	0.06	±	0.00	0.13	±	0.03
5	Strand	C	9 m													0.87	±	0.23
6	Bikini Beach	A	surface	0.87	±	0.18	0.01	±	0.00	0.07	±	0.00	0.01	±	0.00	0.28	±	0.26
6	Bikini Beach	C	surface	0.73	±	0.08	0.03	±	0.00	0.16	±	0.00	0.01	±	0.00	0.22		
6	Bikini Beach	C	7 m													0.65	±	0.11
8	Rooi-Els	A	surface	0.27	±	0.15	0.01	±	0.00	0.02	±	0.00	0.01	±	0.00		*	
8	Rooi-Els	A	8 m													0.01		

on the east side of the bay ($p < 0.05$; Fig. 5c), while the lengths of the three other mussel species (*Aulacomya ater*, *Choromytilus meridionalis*, *Perna perna*) varied inconsistently among sites. Mussel recruits (<1 cm) were significantly more abundant on the west side of the bay, with a maximum of over 2000 recruits enumerated at site 2 compared to 180 at site 8 (Fig. 5d).

4.3.2. Stable isotopes

The $\delta^{15}N$ and $\delta^{13}C$ of *M. galloprovincialis* averaged 8.3 ± 0.4‰ and −14.5 ± 0.5‰, respectively (Table 1b). The $\delta^{13}C_{mussel}$ did not vary significantly among rocky shore sites, in contrast to $\delta^{15}N_{mussel}$, which was significantly higher at sites 3 (Muizenberg, 9.1 ± 0.2‰) and 6 (Bikini Beach, 8.7 ± 0.1‰) compared to the other sites (average of 8.1 ± 0.1‰) ($p < 0.05$).

4.3.3. Fatty acids

Mussel FA composition varied significantly among rocky shore sites (PERMANOVA: MS = 102.46, Pseudo-F = 2.55, $p < 0.01$), with the outcome of the PCA and PERMANOVA identifying two separate groups corresponding to the western (sites 1, 2, 3) and eastern sides (sites 4, 6, 7, 8) of the bay. SIMPER analysis indicates that the eastern specimens were characterised by diatom (16:0, 16:1n-7, 20:5n-3) and dinoflagellate (18:4n-3, 22:6n-3) trophic markers, which together accounted for 48.2 ± 3.6% of the total FA, while BAME, 20:2NMI, 20:4n-6, 22:4n-6, and 22:5n-3 characterized the western sites (40.6 ± 2.3% of total FA) (Table 3, Fig S.7).

4.3.4. Benthic invertebrate larvae distribution

Most of the benthic invertebrate larvae collected were *M. galloprovincialis*, followed by barnacle nauplii and D-larvae (the earliest larval phase) from recently fertilised eggs (Fig. 6; Table S.5). The average invertebrate benthic larvae abundance was highest on the east side of the bay, with station 6C (Bikini Beach) characterized by the highest mean values of 10.7 ± 9.3 individual/L. Of these larvae, the majority were *M. galloprovincialis*, which together accounted for 92% of the counts. An onshore-offshore pattern of increasing larvae abundances with distance offshore was evident ($p < 0.001$), with extremely low numbers of larvae at the rocky shore sites (typically below detection) compared to the offshore stations (average of 0.8 ± 2.5 individual/L).

4.4. Potential pollutants

4.4.1. Metal concentrations

The concentrations of metals in the mussel tissue were highest at site 6 (Bikini Beach) and lowest at site 8 (Rooi-Els; Table S.6a, Fig S.8). Similarly, the sedimentary metal concentrations were highest at the

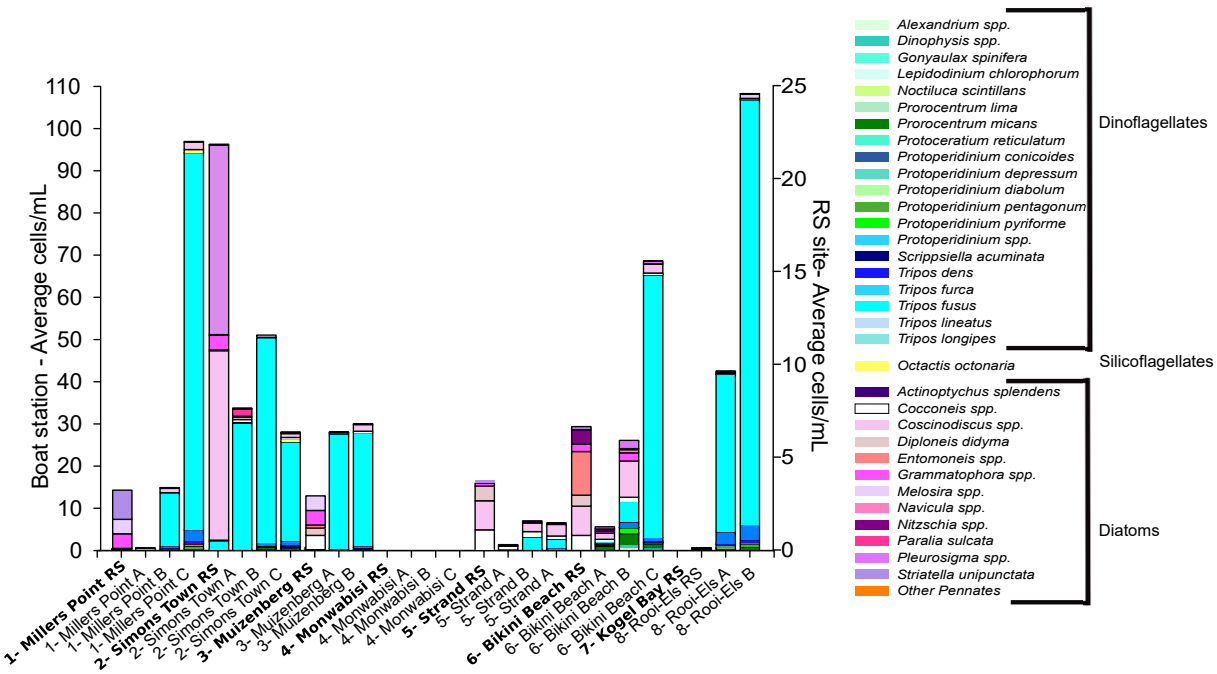

Fig. 4. Cell counts of the various phytoplankton species identified via light microscopy in False Bay in May 2018. Rocky shore (RS) sites are highlighted in bold on the x-axes. The right-hand y-axis refers to the RS data, while the left-hand y-axis refers to the boat transects (stations A, B, C). Samples were not collected at Monwabisi (transect 4) or Kogel Bay (site 7).

rocky shore and inshore station at site 6 (Table S.6b and c). Sediment samples collected from the inshore stations generally had a similar metal content to the rocky shore sediments, except at site 6 where the rocky shore concentrations were more than double the inshore sediments, with particularly high concentrations of aluminium (Al), barium (Ba), iron (Fe), and lead (Pb). The CF and PLI indexes were below the threshold limit for contamination, except for copper (Cu) at site 6 where the PLI was 2.2 (Table S.6d).

Mussels had significantly higher ($p < 0.05$) concentrations of arsenic (As), boron (B), cadmium (Cd), Cu, mercury (Hg), selenium (Se), molybdenum (Mo), tin (Sn), and zinc (Zn) than the sediments, which had higher concentrations of Al, Ba, Fe, manganese (Mn), and strontium (Sr) (Fig S.8). The concentrations of Cu, Cd, Pb, Sn in mussels from site 6 exceeded the permissible legal limits for shellfish, as did Cd at sites 1 (Millers Point), 7 (Kogel Bay), and 8 (Rooi-Els). Regardless of site, the BSAF factor was highest for antimony (Sb; 105), followed by Hg (38.3), Mo (22.1), and Pb (13.3) (Table S.6a).

4.4.2. Aerosols

Three 24-hr size-segregated aerosol samples were collected during the study, on the 14th, 15th, and 16th of May. No rain was recorded during this period, and the atmospheric temperature averaged 16.0 ± 2.9 °C. The ^{222}Rn concentrations were always above the threshold of 500 mBq/m^3 for pure marine air and rose over the three days (Fig. 7, right axis), indicative of an increasing continental influence. The air mass back trajectories were consistent with this interpretation and with the observed increase in total aerosol concentration in both the fine and coarse modes over the three days (Fig. 7, left axis). Aerosol NO_3^- concentrations ranged from 6.2 to 44.1 nmol/m^3 and NO_3^- was predominantly present in the coarse mode whereas NH_4^+ ranged from 0.2 to 11.2 nmol/m^3 and was mainly in the fine mode. The aerosol NO_3^- $\delta^{15}N$ ranged from 3.1 to 7.0‰ and $\delta^{18}O$ ranged from 69 to 74‰ (Table S.7). Averaged over the three sampling days, NO_3^- and NH_4^+ dry deposition to False Bay was 67.4 ± 9.4 μmol/m^2/day and 4.7 ± 4.2 μmol/m^2/day, respectively.

5. Discussion

This multidisciplinary study was designed to evaluate the potential role of benthic filter feeders in mitigating anthropogenic inputs to the coastal waters of a rapidly urbanising area, focusing on False Bay, a socio-economic hotspot in South Africa. Most of the parameters investigated here followed west-east and/or onshore-offshore patterns (Fig. 8), and we detected evidence of nutrient and metal pollution at Strand (site/transect 5) and Bikini Beach (site/transect 6), and atmospheric N deposition in the vicinity of Muizenberg (site/transect 3), in all cases proximate to densely populated stretches of coastline. Below, we discuss potential explanations for the patterns we observed, and consider the socio-economic implications for coastal environments.

5.1. Pollution inputs

5.1.1. N-nutrient loading

The concentrations of nutrients, chlorophyll *a*, and metals were low at most locations across nearshore False Bay, except at transects 5 and 6 (Strand and Bikini Beach) where we recorded elevated values, particularly at the stations nearest the coast. Nutrients derived from urban and agricultural wastewater are a major source of pollution to coastal areas (Paerl, 1997; McClelland and Valiela, 1998; Castro et al., 2007). An excess of these nutrients can enhance primary productivity, especially in shallow environments where light does not limit phytoplankton growth (Howarth, 1988; Cloern et al., 2014), such as nearshore False Bay. A high nutrient load can lead to eutrophication, evidenced by organic matter accumulation and excessive oxygen consumption (leading in extreme cases to hypoxia and/or anoxia) (Richardson and Jørgensen, 1996; Paerl, 2006; Gorman et al., 2009). While the oxygen concentrations in False Bay never reached hypoxic levels (defined as ≤ 60 μM, Vaquer-Sunyer and Duarte, 2008), we did measure the lowest oxygen at transect 5 (Fig. 2) along with elevated N-nutrients (particularly NO_3^- and NH_4^+) and fairly high POC concentrations (Fig. 2c, Fig. 3a and b; Fig S.1e3 and Fig S.2). These observations suggest enhanced phytoplankton activity and thus biomass accumulation in response to nutrient inputs, and the start of eutrophication due to bacterial decomposition of organic

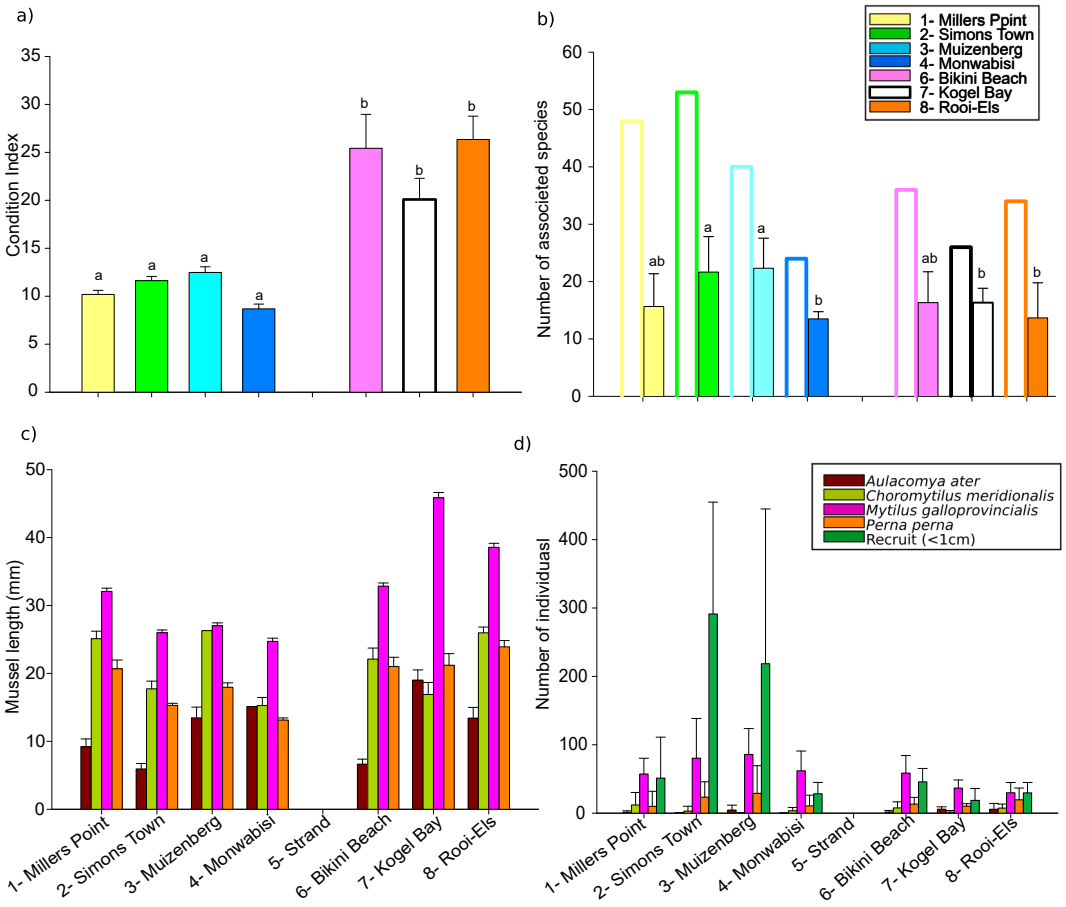

Fig. 5. Mussel data for samples collected at seven rocky shore sites in False Bay in May 2018. a) Mussel condition index (n = 25 per site); b) number of unique species found at each site (open bar) and average number of species (filled bar) associated with the mussel beds; c) mussel length; and d) number of mussels present in the quadrats used to sample for the data shown in panels b and c. Information presented in panels b, c, and d was acquired by destructive sampling (6 replicate quadrats per site). Data are expressed as mean ± standard deviation. The letters in panels a and b indicate significant differences among sites. Mussels were not present at site 5 (Strand).

matter.

Eutrophication can have a negative impact on the coastal benthos, causing shifts in community composition (Blumenshine et al., 1997), mass mortality linked to oxygen starvation (Rosenberg and Loo, 1988), a decline in species richness and diversity (Burkholder et al., 2007), and an increase in the abundance and biomass of fast growing algae (Mangialajo et al., 2008). The diversity associated with the mussel beds was generally low on the east side of False Bay, and mussels were entirely absent at site 5 (Strand) (Fig. 5), consistent with an environmental response to an anthropogenic perturbation. Such anthropogenic effects can be exacerbated in semi-enclosed areas such as bays where water circulation and ventilation is limited compared to the open ocean (Le Pape et al., 1996; Wang et al., 1999; Kemp et al., 2005). The semi-permanent anticyclonic eddy near Gordon's Bay, which retains water and dampens mixing to the north-east (Atkins, 1970; Taljaard et al., 2000), likely drove the accumulation of nutrients and other (in)organic compounds at transects 5 and 6 (Bikini Beach) (Pfaff et al., 2019).

The high N-nutrient concentrations measured proximate to Gordon's Bay could have been discharged by the Gordon's Bay waste water treatment works, the Sir Lowry's Pass and/or Lourens Rivers, and/or urban storm water runoff (Taljaard et al., 2000a, 2000b; Giljam, 2002; Pfaff et al., 2019). We assign an allochthonous provenance to these nutrients rather than an autochthonous mechanism of supply such as upwelling because the NO_3^- and NH_4^+ concentrations were highest inshore (at stations 5A and 6A), decreasing offshore. While a similar trend in NO_3^- could result from upwelling, the coincident $Si(OH)_4$ and PO_4^{3-} concentrations were near-constant across all the transect 5 and 6 stations, inconsistent with upwelling, which would supply NO_3^-, $Si(OH)_4$, and PO_4^{3-} in a near-constant molar ratio. The idea that nutrient loading occurred near Gordon's Bay is also supported by the low salinity measured at transect 5, which implicates freshwater discharge from a river or outflow. Furthermore, NO_3^- concentrations were higher at the surface than at depth at offshore stations 5C and 6C, which can be explained by the mixing of a low-salinity, high-NO_3^- terrestrial input with saltier offshore waters.

The $\delta^{15}N$ data further evince N-nutrient loading near Gordon's Bay. The $\delta^{15}N_{NO3}$ and $\delta^{15}N_{mussel}$ were highest at transects 5 and 6, with $\delta^{15}N_{NO3}$ rapidly decreasing offshore (Table 1). High values of $\delta^{15}N_{NO3}$ can indicate the input of an external N source, such as domestic and/or industrial wastewater (Flipse and Bonner, 1985; McClelland et al., 1997), as might be expected from the outflows at Gordon's Bay. Alternatively, $\delta^{15}N_{NO3}$ can increase due to isotopic fractionation associated with NO_3^- assimilation by phytoplankton, which raises the $\delta^{15}N$ of the NO_3^- pool as its concentration declines (Mariotti et al., 1981). However, $\delta^{15}N_{NO3}$ at transect 5 increased shoreward along with an increase in the NO_3^- concentration. Additionally, the $\delta^{15}N_{NO3}$ at each station was elevated throughout the water column (7.5–8.2‰) relative to the source waters to False Bay (Subantarctic Mode Water (SAMW) and Subtropical Thermocline Water (STW); $\delta^{15}N_{NO3} < 7‰$ (see transect 8; Fig S.3; Flynn et al., 2020)) rather than in the euphotic zone only as would be expected for NO_3^- assimilation.

NO_3^- is not the only possible source of anthropogenic N to False Bay, with high concentrations of NH_4^+ commonly present in land-derived inputs to coastal waters. While we have no measurements of NH_4^+

Table 3
Total fatty acid composition of the mussel *Mytilus galloprovincialis* collected at seven intertidal sites in False Bay in May 2018. The values are percentages expressed as mean ± standard error (n = 3 per site, except for site 1 where only 1 sample was measured). PUFA = Polyunsaturated Fatty Acids, MUFA = Monounsaturated Fatty Acids, SFA = Saturated Fatty Acids, EFA = Essential Fatty Acids (20:4n-6, 20:5n-3, 22:6n-3), BAME = Bacterial Fatty Acids, and NMI = Non Methylated Fatty Acids. Mussels were not present at site 5 (Strand).

Site number	1- Millers Point	2- Simons Town			3- Muizenberg			4- Monwabisi			6- Bikini Beach			7- Kogel Bay			8- Rooi-Els		
14:0	0.69	0.44	±	0.63	0.76	±	0.19	1.08	±	0.34	0.70	±	0.28	0.51	±	0.16	0.79	±	0.06
16:0	15.50	14.50	±	2.38	14.90	±	1.19	16.87	±	0.50	16.39	±	1.40	15.19	±	0.03	18.53	±	0.05
18:0	5.98	6.50	±	1.37	6.65	±	0.10	6.23	±	0.72	5.86	±	0.69	4.38	±	0.40	5.06	±	0.07
20:0	0.84	0.98	±	0.04	0.88	±	0.05	0.56	±	0.52	0.83	±	0.06	0.90	±	0.41	0.63	±	0.06
16:1n-7	1.18	0.90	±	1.28	1.15	±	0.34	1.66	±	0.39	1.03	±	0.65	0.66	±	0.11	1.28	±	0.28
18:1n-7	1.40	1.39	±	0.42	1.46	±	0.07	1.45	±	0.18	1.16	±	0.24	1.28	±	0.56	1.39	±	0.23
18:1n-9	1.53	0.48	±	0.68	0.57	±	0.15	0.86	±	0.11	0.84	±	0.38	1.44	±	1.32	1.47	±	0.17
20:1n-7	0.94	1.16	±	0.23	1.06	±	0.10	0.97	±	0.38	0.96	±	0.11	0.73	±	0.08	0.79	±	0.16
20:1n-9	4.10	3.28	±	0.35	3.22	±	0.35	3.53	±	0.45	3.40	±	0.09	3.96	±	1.13	4.17	±	0.18
20:1n-11	1.00	1.34	±	0.11	1.22	±	0.08	1.32	±	0.44	1.22	±	0.08	0.82	±	0.37	0.73	±	0.12
16:3n-4	0.58	0.25	±	0.36	0.41	±	0.40	0.46	±	0.44	0.88	±	0.25	0.76	±	0.36	0.81	±	0.06
18:2n-6	0.96	1.02	±	0.05	0.96	±	0.09	0.94	±	0.12	0.77	±	0.15	0.97	±	0.40	0.67	±	0.05
18:4n-3	0.70	0.50	±	0.70	0.39	±	0.37	0.79	±	0.14	0.99	±	0.64	0.80	±	0.00	1.20	±	0.14
20:2NMI	11.79	11.96	±	2.48	11.37	±	1.49	9.60	±	1.82	8.93	±	0.90	9.58	±	0.44	7.66	±	0.57
20:4n-6	6.11	3.77	±	0.40	4.78	±	0.45	2.91	±	0.51	3.22	±	0.22	4.66	±	2.80	3.28	±	0.06
20:5n-3	7.92	8.52	±	2.18	9.59	±	1.64	8.36	±	1.82	9.00	±	0.93	7.45	±	0.54	8.72	±	0.03
22:4n-6	1.13	0.73	±	0.32	0.99	±	0.12	0.57	±	0.12	0.52	±	0.02	0.77	±	0.40	0.39	±	0.00
22:5n-3	1.58	2.75	±	1.64	1.94	±	0.15	1.66	±	0.16	1.43	±	0.04	1.37	±	0.04	1.17	±	0.00
22:6n-3	15.97	15.91	±	0.50	15.99	±	2.07	20.12	±	2.05	21.33	±	2.30	19.26	±	4.84	22.94	±	0.57
22:3NMI	0.80	0.84	±	0.10	0.79	±	0.08	0.79	±	0.17	1.01	±	0.23	0.71	±	0.36	0.48	±	0.10
BAME	19.30	22.77	±	3.37	20.92	±	3.58	19.28	±	1.19	19.54	±	2.91	23.80	±	0.08	17.84	±	1.19
SFA	42.31	45.20	±	1.69	44.11	±	2.39	44.00	±	0.48	43.33	±	1.28	44.78	±	0.85	42.85	±	0.95
MUFA	10.15	8.55	±	2.84	8.68	±	0.58	9.80	±	1.01	8.60	±	1.36	8.89	±	2.67	9.83	±	0.92
PUFA	47.54	46.25	±	1.15	47.21	±	1.83	46.20	±	0.79	48.07	±	0.30	46.33	±	1.82	47.32	±	0.03
EFA	30.01	28.20	±	2.28	30.36	±	1.12	31.39	±	1.34	33.54	±	1.97	31.37	±	1.50	34.95	±	0.48

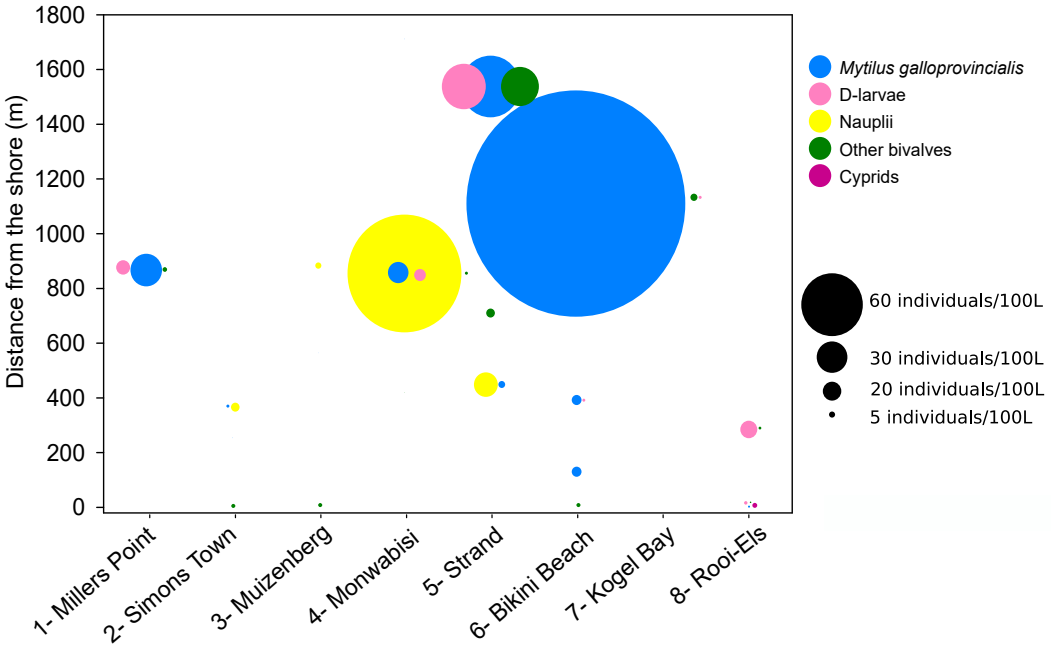

Fig. 6. Abundance and distribution of invertebrate benthic larvae for samples collected from rocky shore sites and inshore-offshore stations in False Bay in May 2018. Offshore larval sampling was not conducted at transect 7 (Kogel Bay).

$\delta^{15}N$, which might allow for a diagnosis of NH_4^+ source(s) (Maeda et al., 2016), $\delta^{15}N_{PON}$ in marine waters is set by the $\delta^{15}N$ of the N sources assimilated by phytoplankton (Altabet, 1988; Wada, 1980; Fawcett et al., 2011) such that we can use this parameter to evaluate the NH_4^+ dynamics in coastal False Bay. The $\delta^{15}N_{PON}$ at the inshore stations of transects 5 and 6 averaged 6.4 ± 0.2‰, ~1‰ lower than the surface $\delta^{15}N_{NO3}$ (7.5 ± 0.3‰; Fig S.3e, f). The isotope effect associated with NO_3^- assimilation by phytoplankton averages ~5‰ (Granger et al., 2004; Fripiat et al., 2019) such that the $\delta^{15}N_{PON}$ recorded here is considerably higher than expected for PON produced from the consumption of NO_3^- alone (i.e., using the Rayleigh model for kinetic isotope fractionation, where $\delta^{15}N_{PON}$ is expected to equal $\delta^{15}N_{NO3}$ minus the isotope effect; Sigman et al., 1999; Altabet and Francois, 2001). This mismatch suggests phytoplankton assimilation of another N source, likely urea or NH_4^+, a notion that is consistent with the observed rates of ρNH_4^+, which were far higher than the coincident rates of ρNO_3^-.

In coastal areas, urea is typically rapidly consumed and its $\delta^{15}N$ is generally low (<1‰; Waser et al., 1998). Urea assimilation would thus

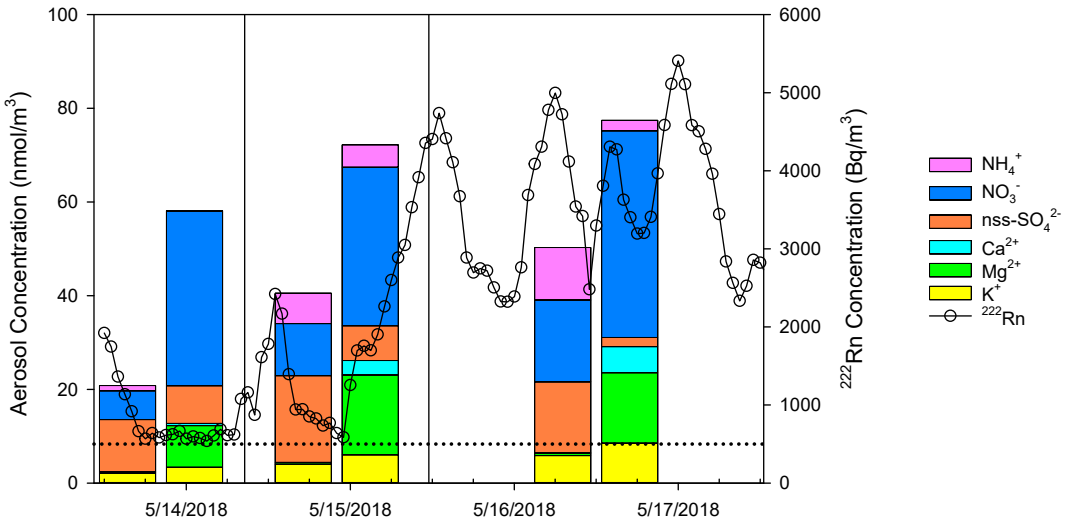

Fig. 7. Three 24-hour size-segregated aerosol samples collected at the Cape Point Global Atmosphere Watch (GAW) station in May 2018, in both the fine (<1 μm, left bar for each date) and coarse modes (>1 μm, right bar for each date). The stacked bar chart indicates the concentration of each major inorganic ion (left axis; nmol m^{-3}): ammonium (NH_4^+, pink), nitrate (NO_3^-, blue), non-sea-salt sulphate (nss-SO_4^{2-}, orange), calcium (Ca^{2+}, cyan), magnesium (Mg^{2+}, green), potassium (K^+, yellow). The connected circle symbols indicate the hourly ^{222}Rn concentrations that were measured continuously over the sampling period (right axis; Bq m^{-3}), while the dotted horizontal line indicates the ^{222}Rn threshold above which air masses are considered to have a continental origin (500 Bq m^{-3}). (For interpretation of the references to colour in this figure legend, the reader is referred to the web version of this article.)

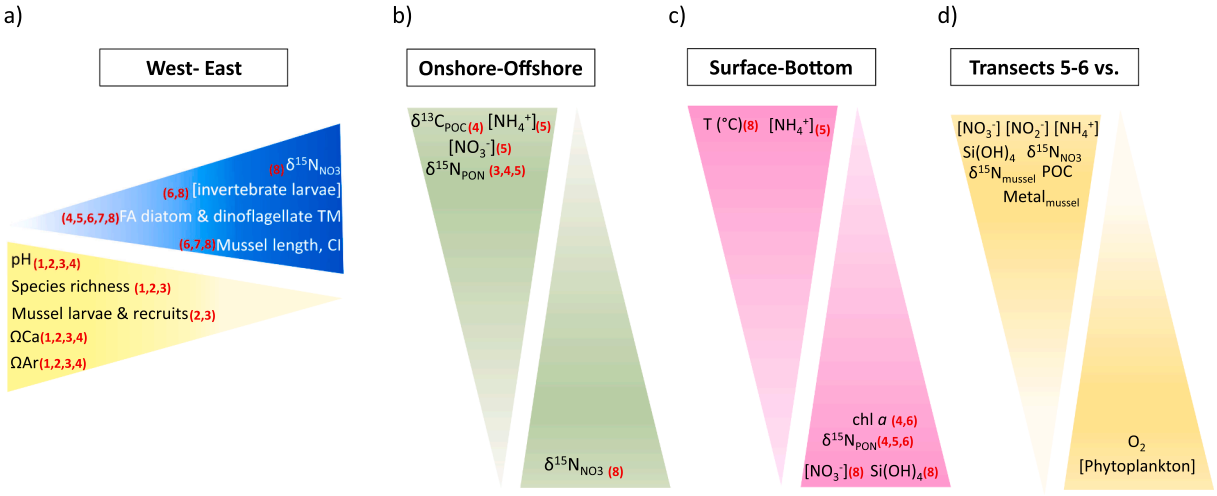

Fig. 8. Summary of the major patterns of variability observed in False Bay in May 2018, which followed a) west-east, b) onshore-offshore, and/or c) surface-depth gradients. Also shown are d) parameters that were significantly different at sites/transects 5 and 6 compared to the other sites/transects. The colour gradient of the triangles indicates the direction of variation (dark colour = highest value, lighter colour = lowest value). The red bold numbers indicate the site or transect at which the maximum value for a specific parameter was observed. (For interpretation of the references to colour in this figure legend, the reader is referred to the web version of this article.)

act to lower the $\delta^{15}N_{PON}$ in False Bay and as such, would not yield high-$\delta^{15}N_{PON}$. Similarly, marine sources of NH_4^+ are generally low in $\delta^{15}N$ (~-5 to 0‰; Checkley and Miller, 1989; Montoya et al., 2002; Lehmann et al., 2003). Additionally, the isotope effect associated with NH_4^+ assimilation is ~3-5‰ at an NH_4^+ concentration of ~5 μM (as observed at the inshore stations of transects 5 and 6) (Liu et al., 2013). The incomplete assimilation of marine NH_4^+ would thus act to lower the $\delta^{15}N_{PON}$, in contrast to our observations. This scenario may be complicated if nitrification occurs coincident with NH_4^+ assimilation (i.e., coupled nitrification-NH_4^+ assimilation). In this case, the nitrifying microorganisms preferentially utilise ^{14}N-NH_4^+, leaving ^{15}N-NH_4^+ to be consumed by phytoplankton, which would in net raise $\delta^{15}N_{PON}$ (Mariotti et al., 1984; Waser et al., 1998; Sigman and Fripiat, 2019). While the nitrification rates were highest at the inshore stations of transects 5 and 6, they were insignificant compared to ρNH_4^+ (e.g., $V_{NO_2^-}$ of 0.6 μM/h vs. ρNH_4^+ of 200 μM/h at station 5A; Table 2). Thus, coupled nitrification-NH_4^+ assimilation also cannot explain the elevated $\delta^{15}N_{PON}$.

A more likely explanation for the high-$\delta^{15}N_{PON}$ is that the dominant source of the NH_4^+ to False Bay at the time of our sampling was anthropogenic rather than marine. The $\delta^{15}N$ of sewage NH_4^+ can range from 10 to 30‰ (Nikolenko et al., 2018), while the $\delta^{15}N$ of manure NH_4^+ used in agriculture is typically ~10‰ (Maeda et al., 2016; Nikolenko et al., 2018). The $\delta^{15}N_{PON}$ produced from the assimilation of NH_4^+ with a $\delta^{15}N$ of 10-20‰ would be ~5-20‰, depending on the degree of its consumption. Assimilation of anthropogenically-derived, high-$\delta^{15}N_{NH4}$ can thus explain the high-$\delta^{15}N_{PON}$ measured in False Bay.

As expected, the dynamics described above were reflected in the $\delta^{15}N_{mussel}$ at site 6, which averaged 8.7 ± 0.1‰, ~2.3‰ higher than their PON food source (McCutchan et al., 2003). This pattern is consistent with previous studies that have reported high-$\delta^{15}N$ primary

consumers living near anthropogenic N sources (Abreu et al., 2006; Lake et al., 2001; Puccinelli et al., 2016b). N-nutrient loading was particularly evident at transects 5 and 6 due to these sites being directly anthropogenically impacted, coupled with the retentive circulation of Gordon's Bay. Nonetheless, a similar relationship between $\delta^{15}N_{NO3}$ and $\delta^{15}N_{PON}$ was evident at the other sites, suggesting that their ecosystems were also supported by a mixture of anthropogenic and marine N, consistent with expectations for coastal environments under anthropogenic pressure (Howard et al., 2014).

The influence of anthropogenic N was also apparent in the high $\delta^{15}N_{mussel}$ measured at site 3 (Muizenberg, 9.1 ± 0.2‰). Here, the $\delta^{15}N_{PON}$ was also elevated (6.6‰) while $\delta^{15}N_{NO3}$ was consistent with the source SAMW and STW (6.8‰). Site 3 is situated in an embayment on the west side of False Bay, considered an upwelling shadow where water originating from the east side of the bay can be retained due to a combination of onshore wind stress and shallow water-column stratification (Largier, 2020). The implication is that, given the right meteorological conditions, pollution inputs to the east side of the bay could be transported and retained in the west. An alternative explanation for the high-$\delta^{15}N_{PON}$ and $\delta^{15}N_{mussel}$ measured at Muizenberg could be outflow of high-$\delta^{15}N$ N from storm water drains, groundwater, or the Zandvlei River. This river experiences eutrophication and poor water quality (van Niekerk et al., 2015, 2013), although its mouth is only intermittently open (generally in winter/spring) (City of Cape Town, 2018) and was closed prior to our sampling. Another source of anthropogenic nutrients to site 3 may be groundwater, as Muizenberg Beach receives a higher groundwater nutrient flux than any other beach along the South African coast because of its proximity to the polluted Cape Flats Aquifer (Engelbrecht, and Tredoux, 1989). High terrestrial nutrient inputs can favour blooms of the diatom *Anaulus australis*, a species that is non-toxic and non-harmful to humans and that proliferates in the surf zone of sandy beaches with elevated wave action (City of Cape Town, 2020). This species dominates the phytoplankton community once present, outcompeting species known to cause harmful algal blooms (Campbell and Bate, 1996). However, *A. australis* was not present during our sampling (Fig. 4), which took place at the end of the Cape Town drought (2015 to mid-2018; Cole et al., 2021) when groundwater inputs to False Bay were likely reduced.

Another possible anthropogenic N source to the bay is atmospheric deposition. The NO_3^-, NH_4^+, and non-sea-salt (nss)-sulfate concentrations in the aerosols collected during this study are typical for mixed coastal and anthropogenic aerosols (Brunke et al., 2004) and the ^{222}Rn data support this provenance (Chambers et al., 2018). Aerosols generated near the coast are usually primarily sea salt. Sodium chloride ions made up ~80% of the total coarse mode and ~60% of the fine mode aerosol concentrations in our samples, with NO_3^- and nss-sulfate as the next-highest-concentration species. In polluted air masses, NO_3^- is typically present as fine mode ammonium nitrate, but in coastal aerosols with large amounts of sea salt, chloride displacement causes NO_3^- to shift into the coarse mode as polluted air mixes with sea spray aerosols (Spokes et al., 2000). Additionally, the concentrations of all species decrease following dilution with relatively clean marine air, causing fine mode NO_3^- and NH_4^+ aerosols to dissociate back to gaseous ammonia and nitric acid (Allen et al., 1989), with the dissociated nitric acid subsequently forming coarse mode sodium nitrate (Spokes et al., 2000). This aerosol size transition influences coastal ecosystems insofar as coarse mode aerosols have much higher deposition velocities than fine mode aerosols. The rate of NO_3^- aerosol dry deposition estimated in our study is consistent with a moderately polluted system (Hastings et al., 2003; Gobel et al., 2013), whereas NH_4^+ deposition was relatively low and more representative of a marine environment (Altieri et al., 2014). The $\delta^{15}N$ of the aerosol NO_3^- (average of 4.8‰) is higher than would be expected for clean marine air (Altieri et al., 2021a) and is instead consistent with anthropogenic N oxide sources, while its $\delta^{18}O$ (average of 71.4‰) indicates a significant contribution of ozone to NO_3^- formation, as expected for polluted regions (Altieri et al., 2016).

Our seawater NO_3^- isotope data suggest that atmospheric NO_3^- deposition may have been significant near Simons Town and Muizenberg. When NO_3^- is assimilated by phytoplankton, its $\delta^{15}N$ and $\delta^{18}O$ rise in a ratio of ~1:1 (Granger et al., 2004; 2010). Such a relationship was observed at all sites/transects except 2 and 3, which were characterized by anomalously high $\delta^{18}O_{NO3}$ for their $\delta^{15}N_{NO3}$ (Fig S.4). This trend is best explained by atmospheric NO_3^- deposition – since aerosol NO_3^- $\delta^{18}O$ is so high compared to that of seawater (while aerosol NO_3^- $\delta^{15}N$ is similar), a fairly modest deposition rate can feasibly influence the surface seawater $\delta^{18}O_{NO3}$ (Hastings et al. 2003).

5.1.2. Metal pollution

Possible anthropogenic effects were further evident, especially at site 6 (Bikini Beach), in the elevated metal concentrations measured in the mussels and sediments, in some cases exceeding permissible levels for shellfish consumption (e.g., Cd and Pb; DOH, 1994, 2004). The high metal concentrations could have resulted from urban-industrial discharge and/or from boat construction and/or repair in the Gordon's Bay Marina located adjacent to site 6. The latter is likely the case for Ba, Cu, Pb, Sn, and Zn, which are commonly found in antifouling paints (Turner, 2010; Ytreberg et al., 2010), although Sn-based paints are banned in South Africa. Our observations require that Sn-containing paint is flaking off old crafts or that Sn-based paints are still in use.

Metals can also enter the coastal environment via aerosol deposition and rainfall (Gao et al., 2003; Mikulic et al., 2004), upwelling events (Johnson et al., 1999), or freshwater inputs (Hydes and Liss, 1977; Stallard and Edmond, 1983). The fact that the highest metal concentrations in both the mussels and sediment occurred at site 6 near the Gordon's Bay Marina and Lourens River outflow implicates a land-based – and thus, anthropogenic – source. The combination of a metal pollution point-source and the anticyclonic circulation of Gordon's Bay may facilitate metal bioaccumulation in the mussels, as well as in the sediments.

Higher than average concentrations of Cd were observed in mussels at sites 1 (Millers Point), 7 (Kogel Bay), and 8 (Rooi-Els), in addition to at site 6. Cd occurs naturally in rocks and soil and is also found in phosphate fertilizers, which are commonly used in the catchment areas near the northern False Bay coast (Thornton, 1992; Mdzeke, 2004; Chiarelli et al., 2019). Cd can also enter aquatic environments via storm water canals during times of drought (Meerkotter, 2012) as its concentration increases in soils, crops, and aquifers in the absence of the diluting effect of rain. Our sampling occurred at the end of the Cape Town drought, which lasted from 2015 to mid-2018 (Cole et al., 2021). Additionally, several storm water outflows are present around False Bay (Taljaard et al., 2000a, 2000b), providing a conduit between land and the coastal environment. This mechanism of supply could explain the high concentrations of Cd found in mussels at sites 1, 7, and 8, which are far from direct anthropogenic inputs. Alternately, the high Cd concentrations at sites 7 and 8 could be due to upwelling events, which occur on the east side of False Bay (Largier, 2020). However, given the low Cd concentrations in oceanic waters (e.g., <400 pM in SAMW, the ultimate source water to the bay; Cloete et al., 2021), it is unlikely that the natural supply of Cd alone can explain the elevated Cd levels measured in the mussels and sediments.

The high metal concentrations in the mussels, in most cases several orders of magnitude higher than in the sediment, indicate that *M. galloprovincialis* can remove these contaminants from the marine environment, thus mitigating anthropogenic inputs. However, metal bioaccumulation, even at low levels, can cause negative effects on mussels, including inhibiting growth (Calabrese et al., 1984) and adversely affecting reproduction (Beiras and Albentosa, 2004; Fitzpatrick et al., 2008) and lipid metabolism (Vlahogianni and Valavanidis, 2007). Moreover, metal bioaccumulation has implications for the ecosystem services that mussels provide, such as being a major food source for humans (Stankovic et al., 2012).

5.1.3. Mussel bed biodiversity

One of our main hypotheses was that we would detect low species diversity associated with mussel beds at sites proximate to anthropogenic inputs, such as site 6 (Bikini Beach). However, this was not the case. Shannon Diversity and Pielou's Evenness Indexes were the lowest at sites 1 (Millers Point) and 8 (Rooi-Els), and highest at site 7 (Kogel Bay), indicating no direct link between diversity and the anthropogenic contaminants identified in our study. In fact, site 1 is located near the Table Mountain National Park marine protected area and site 8 is situated near the mouth of False Bay where open ocean waters frequently intrude (Dufois and Rouault, 2012); both sites are thus distant from the identified hotspots of anthropogenic inputs (sites 5 (Strand) and 6). Studies have shown that high species richness is often associated with pristine marine areas dominated by mussels as these bioengineers provide habitats for numerous other species (López Gappa et al., 1990; Vallarino et al., 2002). In our study, species richness varied considerably, with the highest number of species associated with the mussel beds at sites 1 and 2 (Simons Town), and the lowest at sites 4 (Monwabisi) and 7. Our results suggest that species richness associated with the mussel beds in False Bay is not directly influenced by the pollution sources investigated here.

There are other factors than can influence the communities associated with mussel beds, however. For instance, the low species richness at sites 4 and 7 could be due to the physical characteristics of the sites. The rocky shore of site 4 is exposed to high wave action and is surrounded by sandy beaches that extend for 10–15 km in both directions. In contrast, the other sites are characterised by extended rocky shores, some of which are associated with large kelp forests. The pressure of wave action can inhibit the success of marine species, including *M. galloprovincialis* (Bustamante and Branch, 1996; Blanchette, 1997; Zardi et al., 2008), whereas rocky shores adjacent to kelp forests have been shown to support high species diversity (Blamey and Branch, 2009; Teagle et al., 2017). This is because kelp acts as a nursery area and offers habitat and food for many adult marine species (Graham, et al., 2008; Smale et al., 2013; von Biela et al., 2016) while also acting as a natural barrier, protecting coastal sites from wave action and erosion (Elwany et al., 1995; Løvås and Tørum, 2001; Morris et al., 2020). The absence of kelp may explain the low species richness at site 4; however, the same explanation does not apply to site 7, which is surrounded by kelp. The interactions of bottom-up and top-down processes (e.g., predation, competition, food availability) can also influence the species associated with mussel beds, making it difficult to disentangle the influence of individual factors (Menge, 2000). We also note that our data were collected during one month only, and while mussels integrate chemical signals over a few months (i.e., SI and FA; Hill and McQuaid, 2009; Pirini et al., 2007), the biodiversity associated with mussel beds may change more rapidly due to, for example, the reproductive- or life cycles of the mussel-bed species (Lathlean and McQuaid, 2017). The spatial differences that we observed are nonetheless robust We conclude that mussel-bed biodiversity is either not directly influenced by anthropogenic pressures in False Bay, or that other factors such as water circulation and/or kelp mitigate these anthropogenic inputs, weakening their effect (s) on mussel-bed biodiversity.

5.2. West-east patterns

We observed a clear west-east trend, with several biological components decreasing/increasing from west to east, separating transects 1, 2, 3, and 4 in the west from 5, 6, 7, and 8 in the east. This zonal trend was evident in the number of species associated with the mussel beds, the number of recruits, pH, Ω_{Ca}, and Ω_{Ar}, all of which decreased from west to east. Additionally, the eastern side of the bay hosted mussels that were longer and characterized by diatom and dinoflagellate FA trophic markers, a higher $\delta^{13}C$, and a higher condition index than those on the western side, as well as a higher abundance of benthic invertebrate larvae.

The observations from the east may be linked to topography-wind driven upwelling events (Largier, 2020), which are generally associated with the south-easterly winds that are typical of summer (November-March) (Dufois and Rouault, 2012). Despite our sampling taking place in autumn, the low temperatures recorded at transect 8 (Rooi-Els, minimum of 13.5 °C) and the high NO_3^-, $Si(OH)_4$, and chlorophyll *a* concentrations observed at depth at station 8B, as well as the low pH measured on the eastern side of the bay, may indicate the early stage of an upwelling event.

Upwelling supplies high concentrations of nutrients that typically promote a phytoplankton bloom, initially dominated by diatoms that are succeeded by dinoflagellates when nutrients become depleted (Brink, 1983; Hutchins and Bruland, 1998; Tilstone et al., 2000; Allan et al., 2010). These two phytoplankton taxa are the main producers of poly-unsaturated FA (PUFA) in marine systems, which are critical compounds for the correct functioning of primary consumers and higher trophic levels (Dalsgaard et al., 2003; Parrish et al., 2000), with high levels of PUFA indicating good food quality (Brett and Müller-Navarra, 1997; Ruess and Müller-Navarra, 2019). As such, upwelling events play an important role in providing high-quality food for consumers. Our hypothesis of a role for upwelling in controlling the biological and biogeochemical trends observed in eastern False Bay is supported by the mussel FA results, with specimens collected from the east characterised by diatom and dinoflagellate FA trophic markers, as opposed to those from the west that were characterized by BAME, 20:2NMI, 20:4n-6, 22:4n-6, and 22:5n-3, which together do not indicate the dominance of a specific phytoplankton group. Similarly, mussel condition index and length were higher to the east, indicating a favourable growth environment. Indeed, larger mussels are common in upwelling systems due to the enhanced food supply that supports faster growth rates (Figueiras et al., 2002; Xavier et al., 2007; Smith et al., 2009). A role for upwelling to the east is also supported by the high abundance of phytoplankton at stations 6C (Bikini Beach) and 8B. Combined, analyses indicative of short temporal variability (days) such as nutrient concentrations and phytoplankton abundance, as well as parameters that integrate upwelling signals over longer period (weeks to months) such as FA and condition index, indicate that mussels living on the east side of False Bay were in good condition as a result of high-quality food. That said, the high metal content of some of these east-side mussels (e.g., at site 6) may ultimately be detrimental to higher consumers even though the identified pollutants appear to have had no overt effects on the health of the mussels.

Upwelling on the east side of the bay was not reflected in the $\delta^{13}C_{mussel}$, however, which was instead typical of non-upwelling conditions (-14.5 ± 0.5‰). The $\delta^{13}C$ of consumers is set by the $\delta^{13}C$ of their food source (plus a trophic enrichment factor of ~1‰; McCutchan et al., 2003), which, in the case of mussels, is the suspended material in the water. In coastal areas, the main food source to mussels includes a mix of phytoplankton, macroalgae, and organic and inorganic debris (Bustamante and Branch, 1996; Vizzini et al., 2002) with a combined $\delta^{13}C$ of approximately −15‰ (Hill et al., 2006). By contrast, the $\delta^{13}C_{mussel}$ in upwelling regions reflects a combination of nearshore and pelagic food sources (Puccinelli et al., 2016c, 2019), and is typically 3-4‰ lower than for mussels not influenced by upwelling. Since the abductor muscle in mussels integrates the $\delta^{13}C$ of their food source over approximately nine months (Hill and McQuaid, 2009), which in our case means from before the upwelling season, this tracer may not robustly capture stochastic upwelling events, in contrast to FA that provide information on shorter time scales (approximately one month; Dalsgaard et al., 2003; Pirini et al., 2007).

Although mussel condition index was higher on the east side of the bay, the pattern reversed for the number of species associated with mussel beds, with increased adult and recruit abundance observed in the west. Macrofaunal abundance has been shown to be negatively correlated with mussel size in a bed of *M. galloprovincialis*, indicating that smaller mussels facilitate higher associated species richness by

providing space and food (McQuaid and Lindsay, 2007; Cole and McQuaid, 2010). This dynamic could explain the higher species richness observed on the west side of False Bay. A similar trend was observed for the recruitment of propagules on the rocky shore, a process tightly related to adult mussel abundance, with the highest number of recruits observed at sites 2 (Simons Town) and 3 (Muizenberg). Successful recruitment of benthic propagules depends mainly on two processes: larval supply and post settlement survival. High larval supply is linked to high larval production and/or retention (Porri et al., 2008), yet larval abundance was very low on the west side of the bay and high to the east. The contrasting pattern observed between recruits and larvae could be due to small-scale circulation features such as eddies or onshore transport, resulting in propagules originating in the east being delivered to the west, into what is considered a strong retention zone near sites 2 and 3 (Largier, 2020). Post-settlement processes such as low mortality (Pineda et al., 2010) due to limited competition or elevated habitat availability (von der Meden et al., 2012) could also have enhanced recruitment in the west.

The west-east patterns in pH, Ω_{Ca}, and Ω_{Ar} are consistent with a role for upwelling to the east insofar as the deep cold waters coming to the surface will contain elevated DIC concentrations, resulting in a lower pH, and thus Ω_{Ca} and Ω_{Ar}, than under non-upwelling conditions (Feely et al., 2010). Mussel shell production is tightly linked to Ω_{Ca} and Ω_{Ar} since calcite and aragonite are the main constituents of the outer and inner shell, respectively (Fitzer et al., 2015). Several studies have shown that a decrease in CO_3^{2-} (and thus Ω_{Ca} and Ω_{Ar}) can limit the ability of mussels to produce shells (Doney et al., 2009; Waldbusser et al., 2015) and reduce mussel performance (i.e., growth, survival, recruitment; Talmage and Gobler, 2009; Barton et al., 2012). Since aragonite is more soluble than calcite, Ω_{Ar} will be lower than Ω_{Ca} for a given set of conditions, making it a more sensitive indicator of ocean acidification. While neither Ω_{Ar} nor Ω_{Ca} were <1 at any site (i.e., indicative of undersaturation;Riebesell, et al., 2010)), the values of Ω_{Ar} estimated for the east side of False Bay (1.1 –1.9) were below current mean oceanic values (2 – 2.5; Riebesell, et al., 2010). These results indicate that a continued decline in pH could rapidly become detrimental to mussels in False Bay, and highlight the need for monitoring of carbonate system parameters to assess acidification effects on the filter feeder populations, as well as on the ecosystem services they provide.

5.3. Onshore-offshore gradient

A third observed pattern of variation was an onshore-offshore decrease in $\delta^{13}C_{POC}$ and increase in larval abundance. $\delta^{13}C_{POC}$ decreased from -11.8 ± 0.4‰ at the rocky shore sites to -18.3 ± 0.9‰ at the most offshore stations. Such a decline in $\delta^{13}C_{POC}$ with distance from the coast is commonly observed in marine systems due to a shift from a POC pool comprised of a mix of phytoplankton and macroalgae detritus (~-15‰, Bustamante and Branch, 1996; Vizzini et al., 2002; Hill et al., 2006) to a pelagic POC pool dominated by oceanic phytoplankton (~-20‰, Fry and Sherr, 1989; Hill et al., 2006). The average $\delta^{13}C_{POC}$ recorded at the rocky shore sites (-11.7 ± 2.8‰) was higher than in the coastal waters, suggesting a large contribution of macroalgae detritus.

The onshore-offshore increase in larval abundance can be linked to two processes: propagule supply and circulation. Benthic invertebrate larvae are usually abundant inshore during their early life stage (i.e., eggs just fertilised) or when they are ready to settle on the rocky shore as competent larvae (Porri et al., 2006; Pineda et al., 2010). In our study, the larvae of *M. galloprovincialis* were at an advanced developmental stage, such that we expected their numbers to be highest inshore. Our offshore stations were located within 1.7 km of the coast, however, which can be considered near to the shore if the larvae are competent. The dynamic circulation of the bay could have quickly transported gametes off the coast and promoted larvae fertilisation at our offshore stations (Porri et al., 2008; Weidberg et al., 2015), thus explaining the observed onshore-offshore trend.

5.4. Socio-economic implications

False Bay is an important socio-economical hotspot for South Africa. The bay not only hosts a large residential community, but also supports several small- and medium-scale fisheries (including subsistence fishers) and is a major tourist destination in South Africa, thus contributing to both local communities and the national economy. The tourism value of the bay has been estimated to be approximately US$ 63 million per annum (Pfaff et al., 2019), while the recreational and commercial fisheries of South Africa's west coast (including False Bay) are worth approximately US$ 22 million per annum (Ward et al., 2018). An improved understanding of the potential sources of pollution to False Bay, as well as the processes that may mitigate or exacerbate them, is thus of high importance for the protection and maintenance of the valuable ecosystem services provided by the bay.

Among the recreational areas on the shores of False Bay, the beaches at sites 3 (Muizenberg) and 6 (Bikini Beach) are the most popular and were awarded Blue Flag status in 2019, 2020, and 2021 (The City of Cape Town, 2019, 2020, 2021). This status is awarded on the basis of water quality during the summer months (November-March), which needs to reach a grade of "excellent" in term of the abundance of *Escherichia coli* and enterococci in the water (i.e., water quality is evaluated using a bacterial index only). However, Bikini Beach is the site where we inferred inputs of anthropogenic N and measured the highest metal concentrations (in some cases exceeding the (inter)national thresholds) in both the mussels and sediments. Our results suggest that additional parameters should be considered when evaluating water quality and Blue Flag status. This recommendation is of particular relevance for fishers (particularly subsistence fishers) who may assume that seafood collected from Blue Flag beaches will be safe for human consumption.

In this study, we highlight several potential sources of pollution to False Bay and find that they are largely attenuated by the broad-scale bay circulation (i.e., dilution), as well as by the presence of mussels that act as a sink for some pollutants. In some regions of the bay, however, the local (i.e., small-scale) circulation may retain and/or concentrate certain pollutants such as inorganic N derived from anthropogenic sources, with implications for algal blooms and seawater oxygen concentrations (Dawood, 1990). A higher resolution temporal dataset is required to evaluate the persistence of these pollutants and the severity of their consequences. In addition, while bivalves have been used as model species for environmental assessments and are considered good bioindicators (Ostapczuk et al., 1997; Chandurvelan et al., 2015), under anthropogenic stress, some metabolic features of mussels may be weakened. This may compromise their role as ecosystem services provider, with knock-on consequences for the associated fauna, ecosystem functioning, and ultimately, services.

Our study extends the current knowledge of nearshore False Bay waters, which have been subjected to habitat degradation and overexploitation over the last few decades (Reimers et al., 2014; Ward et al., 2018; Pfaff et al., 2019). While anthropogenic inputs are certainly influencing this region, our results highlight the role that key species and environments play in mitigating such effects. Similar dynamics may apply to any other coastal systems under anthropogenic stress, underscoring the need for such knowledge to be considered in management decisions and used by national and international stakeholders to develop appropriate polices and monitoring strategies for marine ecosystem management.

CRediT authorship contribution statement

Eleonora Puccinelli: Conceptualization, Data curation, Methodology, Investigation, Formal analysis, Project administration, Visualization, Writing – original draft. **Francesca Porri:** Conceptualization, Data

curation, Methodology, Investigation, Resources, Writing – original draft. **Katye Altieri:** Data curation, Methodology, Formal analysis, Resources, Visualization, Writing – original draft. **Raquel Flynn:** Data curation, Methodology, Investigation, Formal analysis, Visualization, Writing – original draft. **Hazel Little:** Investigation, Writing – original draft. **Tayla Louw:** Investigation, Data curation, Formal analysis. **Paula Pattrick:** Investigation, Visualization, Writing – original draft. **Conrad Sparks:** Resources, Writing – original draft. **Mutshutshu Tsanwani:** Data curation, Formal analysis, Writing – original draft. **Sonya de Waardt:** Data curation, Formal analysis, Writing – original draft. **David Walker:** Resources, Writing – original draft. **Sarah Fawcett:** Conceptualization, Methodology, Funding acquisition, Resources, Writing – original draft.

Declaration of Competing Interest

The authors declare that they have no known competing financial interests or personal relationships that could have appeared to influence the work reported in this paper.

Acknowledgements

We acknowledge the Marine Biogeochemistry Lab and the Stable Isotope Laboratory at UCT, the Granger Lab at the University of Connecticut, the LIPIDOCEN at the Institut Universitaire Européen de la Mer, the Central Analytical Facility at Stellenbosch University, and the UC Davis Stable Isotope Facility, as well as the South African Department of Science and Innovation's Biogeochemistry Research Infrastructure Platform (BIOGRIP) and the Aquatic Ecophysiology Research Platform at the South African Institute for Aquatic Biodiversity (SAIAB). We are grateful to Mathieu Rouault for his support of this work, and to Pieter Truter and the Research Dive Unit at UCT for their assistance at sea. Finally, we thank the Altieri, Fawcett, Porri, and Walker research groups for their help with sample collection.

Funding

This work was supported by funding from the South African National Research Foundation (105895, 115335, 116142, 129320), the Claude Leon Foundation, the Swiss Polar Institute through the Antarctic Circumnavigation Expedition (ACE) Project 12, the University of Cape Town (UCT) Research Committee, and a Royal Society/African Academy of Sciences Future Leaders Africa Independent Researcher (FLAIR) fellowship to SF and the ISblue project, Interdisciplinary graduate school for the blue planet (ANR-17-EURE-0015), co-funded by the French government under the program "Investissements d'Avenir" and SAD programme fellowship to EP.

Appendix A. Supplementary data

Supplementary data to this article can be found online at https://doi.org/10.1016/j.ecolind.2022.108899.

References

Abiodun, B.J., Ojumu, A.M., Jenner, S., Ojumu, T.V., 2014. The transport of atmospheric NOx and HNO_3 over Cape Town. Atmos. Chem. Phy. 14, 559–575. https://doi.org/10.5194/acp-14-559-2014.

Abreu, P.C., Costa, C.S.B., Bemvenuti, C., Odebrecht, C., Graneli, W., Anesio, A.M., 2006. Eutrophication processes and trophic interactions in a shallow estuary: preliminary results based on stable isotope analysis ($\delta^{13}C$ and $\delta^{15}N$). Estuaries and Coasts: J. ERF 29, 277–285. https://doi.org/10.1007/BF02781996.

Aguilera, M.A., Tapia, J., Gallardo, C., Núñez, P., Varas-Belemmi, K., 2020. Loss of coastal ecosystem spatial connectivity and services by urbanization: Natural-to-urban integration for bay management. J. Environ. Manage. 276, 111297 https://doi.org/10.1016/j.jenvman.2020.111297.

Ali, E.M., Khairy, H.M., 2016. Environmental assessment of drainage water impacts on water quality and eutrophication level of Lake Idku, Egypt. Environ. Pollut. 216, 437–449. https://doi.org/10.1016/j.envpol.2016.05.064.

Allan, E.L., Ambrose, S.T., Richoux, N.B., Froneman, P.W., 2010. Determining spatial changes in the diet of nearshore suspension-feeders along the South African coastline: Stable isotope and fatty acid signatures. Estuar. Coast. Shelf Sci. 87, 463–471. https://doi.org/10.1016/j.ecss.2010.02.004.

Allen, A.G., Harrison, R.M., Erisman, J.-W., 1989. Field measurements of the dissociation of ammonium nitrate and ammonium chloride aerosols. Atmos. Environ. 1967 (23), 1591–1599. https://doi.org/10.1016/0004-6981(89)90418-6.

Altabet, M.A., 1988. Variations in nitrogen isotopic composition between sinking and suspended particles: implications for nitrogen cycling and particle transformation in the open ocean. Deep Sea Research Part A. Oceanographic Research Papers 35, 535–554. https://doi.org/10.1016/0198-0149(88)90130-6.

Altabet, M.A., Francois, R., 2001. Nitrogen isotope biogeochemistry of the Antarctic polar frontal zone at 170W. Deep Sea Res. Part II 48 (19-20), 4247–4273.

Altieri, K.E., Fawcett, S.E., Hastings, M.G., 2021a. Reactive Nitrogen Cycling in the Atmosphere and Ocean. Annu. Rev. Earth Planet. Sci. 49 (1), 523–550.

Altieri, K.E., Fawcett, S.E., Peters, A.J., Sigman, D.M., Hastings, M.G., 2016. Marine biogenic source of atmospheric organic nitrogen in the subtropical North Atlantic. PNAS 113, 925–930. https://doi.org/10.1073/pnas.1516847113.

Altieri, K.E., Hastings, M.G., Gobel, A.R., Peters, A.J., Sigman, D.M., 2013. Isotopic composition of rainwater nitrate at Bermuda: the influence of air mass source and chemistry in the marine boundary layer. J. Geophys. Res. Atmos. 118 (19), 11,304–16.

Altieri, K.E., Hastings, M.G., Peters, A.J., Oleynik, S., Sigman, D.M., 2014. Isotopic evidence for a marine ammonium source in rainwater at Bermuda. Global Biogeochem. Cycles 28 (10), 1066–1080.

Altieri, K.E., Spence, K.A.M., Smith, S., 2021b. Air-sea ammonia fluxes calculated from high-resolution summertime observations across the Atlantic Southern Ocean. Geophysical Research Letters 48, e2020GL091963. doi: 10.1029/2020GL091963.

Anderson, M., Braak, C.T., 2003. Permutation tests for multi-factorial analysis of variance. J. Stat. Comput. Simul. 73, 85–113. https://doi.org/10.1080/00949650215733.

Anderson, M., Gorley, R., Clarke, K., 2008. PERMANOVA + for PRIMER: guide to software and statistical methods. PRIMER-E.

Anderson, M.J., 2001. A new method for non-parametric multivariate analysis of variance. Austral. Ecol. 26, 32–46. https://doi.org/10.1111/j.1442-9993.2001.01070. pp. x.

Arellano, B., Rivas, D., 2019. Coastal upwelling will intensify along the Baja California coast under climate change by mid-21st century: Insights from a GCM-nested physical-NPZD coupled numerical ocean model. J. Mar. Syst. 199, 103207 https://doi.org/10.1016/j.jmarsys.2019.103207.

Arts, M.T., Ackman, R.G., Holub, B.J., 2001. "Essential fatty acids" in aquatic ecosystems: a crucial link between diet and human health and evolution. Can. J. Fisheries Aquatic Sci. 58, 122–137. https://doi.org/10.1139/f00-224.

Atkins, G.R., 1970. Winds and current patterns in False Bay. Trans. Royal Soc. South Africa 39, 139–148. https://doi.org/10.1080/00359197009519109.

Awad, A.A., Griffiths, C.L., Turpie, J.K., 2002. Distribution of South African marine benthic invertebrates applied to the selection of priority conservation areas. Divers. Distrib. 8, 129–145. https://doi.org/10.1046/j.1472-4642.2002.00132.x.

Bakun, A., 1990. Global climate change and intensification of coastal ocean upwelling. Science 247, 198–201. https://doi.org/10.1126/science.247.4939.198.

Balk, D., Montgomery, M.R., McGranahan, G., Kim, D., Mara, V., Todd, M., 2009. Mapping urban settlements and the risks of climate change in Africa, Asia and South America. In: Guzmán, J.M., Martine, G., McGranahan, G., Schensul, D., Tacoli, C. (Eds.), Population Dynamics and Climate Change. United Nations Population Fund (UNFPA), International Institute for Environment and Development (IIED), New York, London, pp. 80–103.

Balvanera, P., Pfisterer, A.B., Buchmann, N., He, J.-S., Nakashizuka, T., Raffaelli, D., Schmid, B., 2006. Quantifying the evidence for biodiversity effects on ecosystem functioning and services. Ecol. Lett. 9, 1146–1156. https://doi.org/10.1111/j.1461-0248.2006.00963.x.

Barbier, E.B., 2019. Chapter 27 - The Value of Coastal Wetland Ecosystem Services, in: Perillo, G.M.E., Wolanski, E., Cahoon, D.R., Hopkinson, C.S. (Eds.), Coastal Wetlands (Second Edition). Elsevier, pp. 947–964. doi: 10.1016/B978-0-444-63893-9.00027-7.

Barton, A., Hales, B., Waldbusser, G.G., Langdon, C., Feely, R.A., 2012. The Pacific oyster, *Crassostrea gigas,* shows negative correlation to naturally elevated carbon dioxide levels: Implications for near-term ocean acidification effects. Limnol. Oceanogr. 57, 698–710. https://doi.org/10.4319/lo.2012.57.3.0698.

Beiras, R., Albentosa, M., 2004. Inhibition of embryo development of the commercial bivalves *Ruditapes decussatus* and *Mytilus galloprovincialis* by trace metals; implications for the implementation of seawater quality criteria. Aquaculture 230, 205–213. https://doi.org/10.1016/S0044-8486(03)00432-0.

Bendschneider, K., Robinson, R.J., 1952. A new spectrophotometric method for the determination of nitrite in sea water (No. Technical Report No.8). University of Washington.

Benedetti-Cecchi, L., Bertocci, I., Vaselli, S., Maggi, E., 2006. Temporal variance reverses the impact of high mean intensity of stress in climate change experiments. Ecology 87 (10), 2489–2499.

Binning, K., Baird, D., 2001. Survey of heavy metals in the sediments of the Swartkops River Estuary, Port Elizabeth South Africa. Water SA 27, 461–466.

Blamey, L.K., Branch, G.M., 2009. Habitat diversity relative to wave action on rocky shores: implications for the selection of marine protected areas. Aquat. Conserv. Mar. Freshwater Ecosyst. 19, 645–657. https://doi.org/10.1002/aqc.1014.

Blanchette, C.A., 1997. Size and survival of intertidal plants in response to wave action: a case study with *Fucus gardneri.* Ecology 78, 1563–1578. https://doi.org/10.1890/0012-9658(1997)078.

Blumenshine, S.C., Vadeboncoeur, Y., Lodge, D.M., Cottingham, K.L., Knight, S.E., 1997. Benthic-pelagic links: responses of benthos to water-column nutrient enrichment. J. North Am. Benthological Society 16 (3), 466–479.
Böhlke, J.K., Gwinn, C.J., Coplen, T.B., 1993. New reference materials for nitrogen-isotope-ratio measurements. Geostandards Newsletter 17, 159–164. https://doi.org/10.1111/j.1751-908X.1993.tb00131.x.
Böhlke, J.K., Mroczkowski, S.J., Coplen, T.B., 2003. Oxygen isotopes in nitrate: new reference materials for 18O:17O:16O measurements and observations on nitrate-water equilibration. Rapid Commun. Mass Spectrom. 17, 1835–1846. https://doi.org/10.1002/rcm.1123.
Boudjema, K., Badis, A., Moulai-Mostefa, N., 2022. Study of heavy metal bioaccumulation in *Mytilus galloprovincialis* (Lamark 1819) from heavy metal mixture using the CCF design. Environ. Technol. Innovation 25, 102202. https://doi.org/10.1016/j.eti.2021.102202.
Bradl, H.B., 2005. Chapter 1 Sources and origins of heavy metals, in: Bradl, H.B. (Ed.), Interface science and technology, heavy metals in the environment: Origin, interaction and remediation. Elsevier, pp. 1–27. doi: 10.1016/S1573-4285(05)80020-1.
Brett, M., Müller-Navarra, D., 1997. The role of highly unsaturated fatty acids in aquatic foodweb processes. Freshw. Biol. 38, 483–499. https://doi.org/10.1046/j.1365-2427.1997.00220.x.
Brink, K.H., 1983. The near-surface dynamics of coastal upwelling. Prog. Oceanogr. 12, 223–257. https://doi.org/10.1016/0079-6611(83)90009-5.
Brunke, E.-G., Labuschagne, C., Parker, B., Scheel, H.E., Whittlestone, S., 2004. Baseline air mass selection at Cape Point, South Africa: application of 222Rn and other filter criteria to CO_2. Atmos. Environ. 38, 5693–5702. https://doi.org/10.1016/j.atmosenv.2004.04.024.
Bulleri, F., Chapman, M.G., 2010. The introduction of coastal infrastructure as a driver of change in marine environments. J. Appl. Ecol. 47, 26–35. https://doi.org/10.1111/j.1365-2664.2009.01751.x.
Burkholder, J.M., Tomasko, D.A., Touchette, B.W., 2007. Seagrasses and eutrophication. J. Exp. Mar. Biol. Ecol. 350, 46–72. https://doi.org/10.1016/j.jembe.2007.06.024.
Bustamante, R.H., Branch, G.M., 1996. The dependence of intertidal consumers on kelp-derived organic matter on the west coast of South Africa. J. Exp. Mar. Biol. Ecol. 196, 1–28. https://doi.org/10.1016/0022-0981(95)00093-3.
Calabrese, A., MacInnes, J.R., Nelson, D.A., Greig, R.A., Yevich, P.P., 1984. Effects of long-term exposure to silver or copper on growth, bioaccumulation and histopathology in the blue mussel *Mytilus edulis*. Marine Environmental Research 11, 253–274. https://doi.org/10.1016/0141-1136(84)90038-2.
Campbell, E.E., Bate, G.C., 1996. Groundwater as a possible controller of surf diatom biomass. Rev. Chil. Hist. Nat. 69, 503–510.
Casas, S., Bacher, C., 2006. Modelling trace metal (Hg and Pb) bioaccumulation in the Mediterranean mussel, *Mytilus galloprovincialis*, applied to environmental monitoring. J. Sea Res., Dyn. Energy Budgets in Bivalves 56, 168–181. https://doi.org/10.1016/j.seares.2006.03.006.
Casciotti, K.L., Sigman, D.M., Hastings, M.G., Böhlke, J.K., Hilkert, A., 2002. Measurement of the oxygen isotopic composition of nitrate in seawater and freshwater using the denitrifier method. Anal. Chem. 74 (19), 4905–4912.
Castro, P., Valiela, I., Freitas, H., 2007. Eutrophication in Portuguese estuaries evidenced by $\delta^{15}N$ of macrophytes. Mar. Ecol. Prog. Ser. 351, 43–51. https://doi.org/10.3354/meps07173.
Chambers, S.D., Preunkert, S., Weller, R., Hong, S.-B., Humphries, R.S., Tositti, L., Angot, H., Legrand, M., Williams, A.G., Griffiths, A.D., Crawford, J., Simmons, J., Choi, T.J., Krummel, P.B., Molloy, S., Loh, Z., Galbally, I., Wilson, S., Magand, O., Sprovieri, F., Pirrone, N., Dommergue, A., 2018. Characterizing atmospheric transport pathways to Antarctica and the remote Southern Ocean using Radon-222. Front. Earth Sci. 190 https://doi.org/10.3389/feart.2018.00190.
Chandurvelan, R., Marsden, I.D., Glover, C.N., Gaw, S., 2015. Assessment of a mussel as a metal bioindicator of coastal contamination: relationships between metal bioaccumulation and multiple biomarker responses. Sci. Total Environ. 511, 663–675. https://doi.org/10.1016/j.scitotenv.2014.12.064.
Checkley, D.M., Miller, C.A., 1989. Nitrogen isotope fractionation by oceanic zooplankton. Deep Sea Research Part A. Oceanographic Research Papers 36 (10), 1449–1456.
Chen, H.-Y., Chen, L.-D., Chiang, Z.-Y., Hung, C.-C., Lin, F.-J., Chou, W.-C., Gong, G.-C., Wen, L.-S., 2010. Size fractionation and molecular composition of water-soluble inorganic and organic nitrogen in aerosols of a coastal environment. J. Geophys. Res.: Atmos. 115 https://doi.org/10.1029/2010JD014157.
Chiarelli, R., Martino, C., Roccheri, M.C., 2019. Cadmium stress effects indicating marine pollution in different species of sea urchin employed as environmental bioindicators. Cell Stress Chaperones 24, 675–687. https://doi.org/10.1007/s12192-019-01010-1.
City of Cape Town, 2020. Know your coast. Key findings from over 10 000 sample bacterial tests at 99 sites along 307 km of coastline. https://resource.capetown.gov.za/documentcentre/Documents/City%20research%20reports%20and%20review/Know_Your_Coast_2020.pdf.
City of Cape Town Zandvlei Estuarine Management Plan 2018 https://www.westerncape.gov.za/eadp/files/atoms/files/Zandvlei%20EMP_V6_Sept%202018.pdf.
Clarke, K.R., Gorley, R.N., 2006. Primer V6: User Manual - Tutorial. Plymouth Marine Laboratory.
Cloern, J.E., Foster, S.Q., Kleckner, A.E., 2014. Phytoplankton primary production in the world's estuarine-coastal ecosystems. Biogeosciences 11 (9), 2477–2501.
Cloete, R., Loock, J.C., van Horsten, N.R., Menzel Barraqueta, J.-L., Fietz, S., Mtshali, T. N., Planquette, H., García-Ibáñez, M.I., Roychoudhury, A.N., 2021. Winter dissolved and particulate zinc in the Indian Sector of the Southern Ocean: Distribution and relation to major nutrients (GEOTRACES GIpr07 transect). Mar. Chem. 236, 104031 https://doi.org/10.1016/j.marchem.2021.104031.
Cole, H.D., Cole, M.J., Simpson, K.J., Simpson, N.P., Ziervogel, G., New, M.G., 2021. Managing city-scale slow-onset disasters: Learning from Cape Town's 2015–2018 drought disaster planning. Int. J. Disaster Risk Reduct. 63, 102459 https://doi.org/10.1016/j.ijdrr.2021.102459.
Cole, V.J., McQuaid, C.D., 2010. Bioengineers and their associated fauna respond differently to the effects of biogeography and upwelling. Ecology 91, 3549–3562. https://doi.org/10.1890/09-2152.1.
Dallinger, R., Prosi, F., Segner, H., Back, H., 1987. Contaminated food and uptake of heavy metals by fish: a review and a proposal for further research. Oecologia 73, 91–98. https://doi.org/10.1007/BF00376982.
Dalsgaard, J., St. John, M., Kattner, G., Müller-Navarra, D., Hagen, W., 2003. Fatty acid trophic markers in the pelagic marine environment, in: Advances in Marine Biology. Academic Press, pp. 225–340.
Davenport, J., Chen, X., 1987. A comparison of methods for the assessment of condition in the mussel (*Mytilus edulis* L.). J. Molluscan Stud. 53, 293–297. https://doi.org/10.1016/S0065-2881(03)46005-7.
Dawood, A., 1990. A scanning electron and light microscopy study of the red tide dinoflagellate Gymnodinium sp. from False Bay, South Africa.
De Vos, M., 2014. The inshore circulation at Fish Hoek and potential impacts on the Shark Exclusion Net. University of Cape Town, Cape Town, South Africa. MSc Thesis.
DeNiro, M.J., Epstein, S., 1981. Influence of diet on the distribution of nitrogen isotopes in animals. Geochim. Cosmochim. Acta 45, 341–351. https://doi.org/10.1016/0016-7037(81)90244-1.
DeNiro, M.J., Epstein, S., 1978. Influence of diet on the distribution of carbon isotopes in animals. Geochim. Cosmochim. Acta 42, 495–506. https://doi.org/10.1016/0016-7037(78)90199-0.
Diamond, D., 1994. QuikChem Method 10–114-21-1-B: Silicate byflow injection analysis. Lachat Instruments.
Dickson, A.G., 1990. Thermodynamics of the dissociation of boric acid in synthetic seawater from 273.15 to 318.15 K. Deep Sea Research Part A. Oceanographic Research Papers 37, 755–766. https://doi.org/10.1016/0198-0149(90)90004-F.
DOH, 2004. Regulations relating to maximum levels for metals in foodstuffs (No. R.500 30 April 2004). Foodstuffs, Cosmetics and Disinfectants Act, 1972 (Act 54 of 1972). Department of Health, South Africa. https://members.wto.org/crnattachments/2016/SPS/ZAF/16_3892_00_e.pdf.
DOH, 1994. Regulations relating to metals in foodstuffs (No. R.1518 9 September 1994). Foodstuffs, Cosmetics and Disinfectants Act, 1972 (Act 54 of 1972). Department of Health, South Africa.
Doney, S.C., Fabry, V.J., Feely, R.A., Kleypas, J.A., 2009. Ocean acidification: the other CO_2 problem. Annu. Rev. Marine Sci. 1, 169–192. https://doi.org/10.1146/annurev.marine.010908.163834.
Doney, S.C., Ruckelshaus, M., Duffy, J.E., Barry, J.P., Chan, F., English, C.A., Galindo, H. M., Grebmeier, J.M., Hollowed, A.B., Knowlton, N., Polovina, J., Rabalais, N.N., Sydeman, W.J., Talley, L.D., 2012. Climate change impacts on marine ecosystems. Annu. Rev. Marine Sci. 4, 11–37. https://doi.org/10.1146/annurev-marine-041911-111611.
Drimie, S., McLachlan, M., 2013. Food security in South Africa—first steps toward a transdisciplinary approach. Food Security 5, 217–226. https://doi.org/10.1007/s12571-013-0241-4.
Duce, R.A., Liss, P.S., Merrill, J.T., Atlas, E.L., Buat-Menard, P., Hicks, B.B., Miller, J.M., Prospero, J.M., Arimoto, R., Church, T.M., Ellis, W., Galloway, J.N., Hansen, L., Jickells, T.D., Knap, A.H., Reinhardt, K.H., Schneider, B., Soudine, A., Tokos, J.J., Tsunogai, S., Wollast, R., Zhou, M., 1991. The atmospheric input of trace species to the world ocean. Global Biogeochem. Cycles 5, 193–259. https://doi.org/10.1029/91GB01778.
Duffy, J.E., Godwin, C.M., Cardinale, B.J., 2017. Biodiversity effects in the wild are common and as strong as key drivers of productivity. Nature 549, 261–264. https://doi.org/10.1038/nature23886.
Dufois, F., Rouault, M., 2012. Sea surface temperature in False Bay (South Africa): towards a better understanding of its seasonal and inter-annual variability. Cont. Shelf Res. 43, 24–35. https://doi.org/10.1016/j.csr.2012.04.009.
Dugdale, R.C., Wilkerson, F.P., 1986. The use of ^{15}N to measure nitrogen uptake in eutrophic oceans; experimental considerations. Limnol. Oceanogr. 31, 673–689. https://doi.org/10.4319/lo.1986.31.4.0673.
Dumbauld, B.R., Ruesink, J.L., Rumrill, S.S., 2009. The ecological role of bivalve shellfish aquaculture in the estuarine environment: a review with application to oyster and clam culture in West Coast (USA) estuaries. Aquaculture 290, 196–223. https://doi.org/10.1016/j.aquaculture.2009.02.033.
El-Sammak, A.A., Aboul-Kassim, T.A., 1999. Metal pollution in the sediments of Alexandria region, Southeastern Mediterranean. Egypt. Bull. Environ. Contam. Toxicol. 63, 263–270. https://doi.org/10.1007/s001289900975.
Elwany, M.H.S., Oreilly, W.C., Guza, R.T., Flick, R.E., 1995. Effects of Southern California Kelp Beds on Waves. Effects of Southern California kelp beds on waves 121, 143–150. doi: 10.1061/(asce)0733-950x(1995)121:2(143).
Emanuel, B.P., Bustamante, R.H., Branch, G.M., Eekhout, S., Odendaal, F.J., 1992. A zoogeographic and functional approach to the selection of marine reserves on the west coast of South Africa. S. Afr. J. Mar. Sci. 12 (1), 341–354.
J.F.P. Engelbrecht G. Tredoux Preliminary investigation into the occurrence of brown water in False Bay. Report for the Groundwater Programme, Division of Water Technology No. CWAT 73 1989 Cape Town City Council, Cape Town, South Africa.
Fawcett, S.E., Lomas, M.W., Casey, J.R., Ward, B.B., Sigman, D.M., 2011. Assimilation of upwelled nitrate by small eukaryotes in the Sargasso Sea. Nature Geosci 4, 717–722. https://doi.org/10.1038/ngeo1265.

Feely, R.A., Alin, S.R., Newton, J., Sabine, C.L., Warner, M., Devol, A., Krembs, C., Maloy, C., 2010. The combined effects of ocean acidification, mixing, and respiration on pH and carbonate saturation in an urbanized estuary. Estuar. Coast. Shelf Sci. 88, 442–449. https://doi.org/10.1016/j.ecss.2010.05.004.

Figueiras, F.G., Labarta, U., Reiriz, M.J.F., 2002. Coastal upwelling, primary production and mussel growth in the Rías Baixas of Galicia. Hydrobiologia 484, 121–131. https://doi.org/10.1023/A:1021309222459.

Fitzer, S.C., Zhu, W., Tanner, K.E., Phoenix, V.R., Kamenos, N.A., Cusack, M., 2015. Ocean acidification alters the material properties of *Mytilus edulis* shells. J. R. Soc. Interface 12, 20141227. https://doi.org/10.1098/rsif.2014.1227.

Fitzpatrick, J.L., Nadella, S., Bucking, C., Balshine, S., Wood, C.M., 2008. The relative sensitivity of sperm, eggs and embryos to copper in the blue mussel (*Mytilus trossulus*). Comp. Biochem. Physiol. C: Toxicol. Pharmacol. 147, 441–449. https://doi.org/10.1016/j.cbpc.2008.01.012.

Flipse, W.J., Bonner, F.T., 1985. Nitrogen-Isotope ratios of nitrate in ground water under fertilized fields, Long Island, New York. Groundwater 23, 59–67. https://doi.org/10.1111/j.1745-6584.1985.tb02780.x.

Flynn, R.F., Granger, J., Veitch, J.A., Siedlecki, S., Burger, J.M., Pillay, K., Fawcett, S.E., 2020. On-shelf nutrient trapping enhances the fertility of the Southern Benguela Upwelling System. Journal of Geophysical Research: Oceans 125, e2019JC015948. doi: 10.1029/2019JC015948.

Folch, J., Lees, M., Stanley, G.H.S., 1957. A simple method for the isolation and purification of total lipides from animal tissues. J. Biol. Chem. 226 (1), 497–509.

Fripiat, F., Martínez-García, A., Fawcett, S.E., Kemeny, P.C., Studer, A.S., Smart, S.M., Rubach, F., Oleynik, S., Sigman, D.M., Haug, G.H., 2019. The isotope effect of nitrate assimilation in the Antarctic Zone: Improved estimates and paleoceanographic implications. Geochim. Cosmochim. Acta 247, 261–279. https://doi.org/10.1016/j.gca.2018.12.003.

Fry, B., Sherr, E.B., 1989. $\delta^{13}C$ measurements as indicators of carbon flow in marine and freshwater ecosystems. In: Rundel, P.W., Ehleringer, J.R., Nagy, K.A. (Eds.), Stable Isotopes in Ecological Research. Springer, New York, pp. 196–229.

Gao, Y., Fan, S.-M., Sarmiento, J.L., 2003. Aeolian iron input to the ocean through precipitation scavenging: A modeling perspective and its implication for natural iron fertilization in the ocean. J. Geophys. Res.: Atmos. 108 https://doi.org/10.1029/2002JD002420.

Giljam, R., 2002. The effect of the Cape Flats Aquifer on the water quality of False Bay. (MSc Thesis) University of Cape Town, South Africa. https://open.uct.ac.za/handle/11427/6476.

Gobel, A.R., Altieri, K.E., Peters, A.J., Hastings, M.G., Sigman, D.M., 2013. Insights into anthropogenic nitrogen deposition to the North Atlantic investigated using the isotopic composition of aerosol and rainwater nitrate. Geophys. Res. Lett. 40, 5977–5982. https://doi.org/10.1002/2013GL058167.

Gonfiantini, R., Stichler, W., Rozanski, K., 1995. Standards and intercomparison materials distributed by the International Atomic Energy Agency for stable isotope measurements. No. IAEA-TECDOC–825.

Gorman, D., Russell, B.D., Connell, S.D., 2009. Land-to-sea connectivity: linking human-derived terrestrial subsidies to subtidal habitat change on open rocky coasts. Ecol. Appl. 19, 1114–1126. https://doi.org/10.1890/08-0831.1.

Graham, M.H., Halpern, B.S., Carr, M.H., 2008. Diversity and dynamics of Californian subtidal kelp forests, in: Food Webs and the Dynamics of Marine Reefs. Oxford University Press, pp. 103–134.

Granger, J., Sigman, D.M., 2009. Removal of nitrite with sulfamic acid for nitrate N and O isotope analysis with the denitrifier method. Rapid Communication on Mass Spectrometry 23, 3753–3762. https://doi.org/10.1002/rcm.4307.

Granger, J., Sigman, D.M., Needoba, J.A., Harrison, P.J., 2004. Coupled nitrogen and oxygen isotope fractionation of nitrate during assimilation by cultures of marine phytoplankton. Limnol. Oceanogr. 49, 1763–1773. https://doi.org/10.4319/lo.2004.49.5.1763.

Grasshoff, K., 1976. Methods of Seawater Analysis. Verlag Chemie, Weinheim, New York.

Griffiths, C.L., Robinson, T.B., Lange, L., Mead, A., Gratwicke, B., 2010. Marine biodiversity in south africa: an evaluation of current states of knowledge. PLoS ONE 5 (8), e12008.

Grundlingh, M.L., Hunter, I.T., Potgieter, E., 1989. Bottom currents at the entrance to False Bay, South Africa. Cont. Shelf Res. 9, 1029–1048. https://doi.org/10.1016/0278-4343(89)90056-3.

Grundlingh, M.L., Largier, J.L., 1991. Physical oceanography of False Bay – a review. In: Jackson, WPU (ed.), False Bay 21 years on – an environmental assessment. Proceedings of the Symposium. Royal Society of South Africa 47(4–5), 387–400.

Halpern, B.S., Walbridge, S., Selkoe, K.A., Kappel, C.V., Micheli, F., D'Agrosa, C., Bruno, J.F., Casey, K.S., Ebert, C., Fox, H.E., Fujita, R., Heinemann, D., Lenihan, H.S., Madin, E.M.P., Perry, M.T., Selig, E.R., Spalding, M., Steneck, R., Watson, R., 2008. A global map of human impact on marine ecosystems. Science 319, 948–952. https://doi.org/10.1126/science.1149345.

Hansson, S., Hobbie, J.E., Elmgren, R., Larsson, U., Fry, B., Johansson, S., 1997. The stable nitrogen isotope ratio as a marker of food-web interactions and fish migration. Ecology 78, 2249–2257. https://doi.org/10.1890/0012-9658.

Harley, C.D.G., Randall Hughes, A., Hultgren, K.M., Miner, B.G., Sorte, C.J.B., Thornber, C.S., Rodriguez, L.F., Tomanek, L., Williams, S.L., 2006. The impacts of climate change in coastal marine systems. Ecol. Lett. 9, 228–241. https://doi.org/10.1111/j.1461-0248.2005.00871.x.

Hastings, M.G., Sigman, D.M., Lipschultz, F., 2003. Isotopic evidence for source changes of nitrate in rain at Bermuda. J. Geophys. Res.: Atmos. 108 (D24), n/a–n/a.

Hautier, Y., Tilman, D., Isbell, F., Seabloom, E.W., Borer, E.T., Reich, P.B., 2015. Anthropogenic environmental changes affect ecosystem stability via biodiversity. Science 348, 336–340. https://doi.org/10.1126/science.aaa1788.

Hendriks, I.E., Duarte, C.M., Heip, C.H.R., 2006. Biodiversity research still grounded. Science 312, 1715–1715. doi: 10.1126/science.1128548.

Higgins, C.B., Stephenson, K., Brown, B.L., 2011. Nutrient bioassimilation capacity of aquacultured oysters: quantification of an ecosystem service. J. Environ. Qual. 40, 271–277. https://doi.org/10.2134/jeq2010.0203.

Hill, J.M., McQuaid, C.D., 2009. Effects of food quality on tissue-specific isotope ratios in the mussel *Perna perna*. Hydrobiologia 635, 81–94. https://doi.org/10.1007/s10750-009-9865-y.

Hill, J.M., Mcquaid, C.D., Kaehler, S., 2006. Biogeographic and nearshore-offshore trends in isotope ratios of intertidal mussels and their food sources around the coast of southern Africa. Mar. Ecol. Prog. Ser. 318, 63–73.

Holliday, N.P., Bersch, M., Berx, B., Chafik, L., Cunningham, S., Florindo-López, C., Hátún, H., Johns, W., Josey, S.A., Larsen, K.M.H., Mulet, S., Oltmanns, M., Reverdin, G., Rossby, T., Thierry, V., Valdimarsson, H., Yashayaev, I., 2020. Ocean circulation causes the largest freshening event for 120 years in eastern subpolar North Atlantic. Nature Commun. 11, 585. https://doi.org/10.1038/s41467-020-14474-y.

Holmes, R.M., Aminot, A., Kérouel, R., Hooker, B.A., Peterson, B.J., 1999. A simple and precise method for measuring ammonium in marine and freshwater ecosystems. Can. J. Fisheries Aquatic Sci. 56, 1801–1808. https://doi.org/10.1139/f99-128.

Howard, M.D.A., Sutula, M., Caron, D.A., Chao, Y., Farrara, J.D., Frenzel, H., Jones, B., Robertson, G., McLaughlin, K., Sengupta, A., 2014. Anthropogenic nutrient sources rival natural sources on small scales in the coastal waters of the Southern California Bight. Limnol. Oceanogr. 59, 285–297. https://doi.org/10.4319/lo.2014.59.1.0285.

Howarth, R.W., 1988. Nutrient limitation of net primary production in marine ecosystems. Annu. Rev. Ecol. Syst. 19, 89–110. https://doi.org/10.1146/annurev.es.19.110188.000513.

Huijbers, C.M., Schlacher, T.A., Schoeman, D.S., Weston, M.A., Connolly, R.M., 2013. Urbanisation alters processing of marine carrion on sandy beaches. Landscape Urban Plann. 119, 1–8. https://doi.org/10.1016/j.landurbplan.2013.06.004.

Hutchins, D.A., Bruland, K.W., 1998. Iron-limited diatom growth and Si: N uptake ratios in a coastal upwelling regime. Nature 393, 561–564. https://doi.org/10.1038/31203.

Hydes, D.J., Liss, P.S., 1977. The behaviour of dissolved aluminium in estuarine and coastal waters. Estuar. Coast. Mar. Sci. 5, 755–769. https://doi.org/10.1016/0302-3524(77)90047-0.

Idso, S.B., Gilbert, R.G., 1974. On the universality of the poole and Atkins secchi disk-Light Extinction Equation. J. Appl. Ecol. 11, 399–401. https://doi.org/10.2307/2402029.

Iverson, S.J., Frost, K.J., Lowry, L.F., 1997. Fatty acid signatures reveal fine scale structure of foraging distribution of harbour seals and their prey in Prince William Sound, Alaska. Mar. Ecol. Prog. Ser. 151, 255–271. https://doi.org/10.3354/meps151255.

Jacobson, M., 2014. The influence of a spatially varying wind field on the circulation and thermal structure of False Bay during summer: a numerical modelling study. University of Cape Town, Cape Town, South Africa. MSc Thesis.

Jaishankar, M., Tseten, T., Anbalagan, N., Mathew, B.B., Beeregowda, K.N., 2014. Toxicity, mechanism and health effects of some heavy metals. Interdisciplinary Toxicology 7, 60–72. https://doi.org/10.2478/intox-2014-0009.

Janout, M.A., Hölemann, J., Laukert, G., Smirnov, A., Krumpen, T., Bauch, D., Timokhov, L., 2020. On the Variability of Stratification in the Freshwater-Influenced Laptev Sea Region. Frontiers in Marine Science 7.

Johnson, K.S., Chavez, F.P., Friederich, G.E., 1999. Continental-shelf sediment as a primary source of iron for coastal phytoplankton. Nature 398, 697–700. https://doi.org/10.1038/19511.

Johnston, E.L., Mayer-Pinto, M., Crowe, T.P., 2016. Chemical contaminant effects on marine ecosystem functioning. J. Ecol. 140–149 https://doi.org/10.1111/1365-2664.12355@10.1111.

Kelly, J.R., Scheibling, R.E., 2012. Fatty acids as dietary tracers in benthic food webs. Mar. Ecol. Prog. Ser. 446, 1–22. https://doi.org/10.3354/meps09559.

Kemp, W.M., Boynton, W.R., Adolf, J.E., Boesch, D.F., Boicourt, W.C., Brush, G., Cornwell, J.C., Fisher, T.R., Glibert, P.M., Hagy, J.D., Harding, L.W., Houde, E.D., Kimmel, D.G., Miller, W.D., Newell, R.I.E., Roman, M.R., Smith, E.M., Stevenson, J. C., 2005. Eutrophication of Chesapeake Bay: historical trends and ecological interactions. Mar. Ecol. Prog. Ser. 303, 1–29. https://doi.org/10.3354/meps303001.

Kendall, C., Aravena, R., 2000. Nitrate isotopes in groundwater systems. In: Cook, P.G., Herczeg, A.L. (Eds.), Environmental Tracers in Subsurface Hydrology. Springer, US, Boston, MA, pp. 261–297. https://doi.org/10.1007/978-1-4615-4557-6_9.

Kohata, K., Hiwatari, T., Hagiwara, T., 2003. Natural water-purification system observed in a shallow coastal lagoon: Matsukawa-ura, Japan. Marine Pollution Bulletin, Environmental Management of Enclosed Coastal Seas 47, 148–154. doi: 10.1016/S0025-326X(03)00055-9.

La Peyre, M.K., Humphries, A.T., Casas, S.M., La Peyre, J.F., 2014. Temporal variation in development of ecosystem services from oyster reef restoration. Ecol. Eng. 63, 34–44. https://doi.org/10.1016/j.ecoleng.2013.12.001.

Lai, S., Loke, L.H.L., Hilton, M.J., Bouma, T.J., Todd, P.A., 2015. The effects of urbanisation on coastal habitats and the potential for ecological engineering: a Singapore case study. Ocean Coast. Manag. 103, 78–85. https://doi.org/10.1016/j.ocecoaman.2014.11.006.

Lake, J.L., McKinney, R.A., Osterman, F.A., Pruell, R.J., Kiddon, J., Ryba, S.A., Libby, A. D., 2001. Stable nitrogen isotopes as indicators of anthropogenic activities in small freshwater systems. Can. J. Fish. Aquat. Sci. 58, 870–878. https://doi.org/10.1139/f01-038.

Lapointe, B.E., Herren, L.W., Paule, A.L., 2017. Septic systems contribute to nutrient pollution and harmful algal blooms in the St. Lucie Estuary, Southeast Florida, USA. Harmful Algae 70, 1–22. https://doi.org/10.1016/j.hal.2017.09.005.

Largier, J.L., 2020. Upwelling bays: How coastal upwelling controls circulation, habitat, and productivity in bays. Annu. Rev. Marine Sci. 12, 415–447. https://doi.org/10.1146/annurev-marine-010419-011020.

Lathlean, J.A., McQuaid, C.D., 2017. Biogeographic variability in the value of mussel beds as ecosystem engineers on South African rocky shores. Ecosystems 20, 568–582. https://doi.org/10.1007/s10021-016-0041-8.

Lau, S., Mohamed, M., Tan Chi Yen, A., Su'ut, S., 1998. Accumulation of heavy metals in freshwater molluscs. Science of The Total Environment 214, 113–121. doi: 10.1016/S0048-9697(98)00058-8.

Le Pape, O., Del Amo, Y., Menesguen, A., Aminot, A., Quequiner, B., Treguer, P., 1996. Resistance of a coastal ecosystem to increasing eutrophic conditions: the Bay of Brest (France), a semi-enclosed zone of Western Europe. Cont. Shelf Res. 16, 1885–1907. https://doi.org/10.1016/0278-4343(95)00068-2.

Lee, K., Kim, T.-W., Byrne, R.H., Millero, F.J., Feely, R.A., Liu, Y.-M., 2010. The universal ratio of boron to chlorinity for the North Pacific and North Atlantic oceans. Geochim. Cosmochim. Acta 74, 1801–1811. https://doi.org/10.1016/j.gca.2009.12.027.

Lehmann, M.F., Reichert, P., Bernasconi, S.M., Barbieri, A., McKenzie, J.A., 2003. Modelling nitrogen and oxygen isotope fractionation during denitrification in a lacustrine redox-transition zone. Geochim. Cosmochim. Acta 67, 2529–2542. https://doi.org/10.1016/S0016-7037(03)00085-1.

Lewis, E., Wallace, D., 1998. Program developed for CO $_2$ system calculations (No. ORNL/CDIAC-105). Brookhaven National Lab., Dept. of Applied Science, Upton, NY (United States); Oak Ridge National Lab., Carbon Dioxide Information Analysis Center, TN (United States). https://doi.org/10.2172/639712.

Liu, K.-K., Kao, S.-J., Chiang, K.-P., Gong, G.-C., Chang, J., Cheng, J.-S., Lan, C.-Y., 2013. Concentration dependent nitrogen isotope fractionation during ammonium uptake by phytoplankton under an algal bloom condition in the Danshuei estuary, northern Taiwan. Mar. Chem. 157, 242–252. https://doi.org/10.1016/j.marchem.2013.10.005.

J.J. López Gappa A. Tablado N.H. Magaldi Influence of sewage pollution on a rocky intertidal community dominated by the mytilid Brachidontes rodriguezi Marine Ecology Progress Series. 63 1990 163 175 https://doi.org/63:163-175.

Lorey, D.E., 2002. Global environmental challenges of the twenty-first century: resources, consumption, and sustainable solutions. Rowman & Littlefield Publishers.

Løvås, S.M., Tørum, A., 2001. Effect of the kelp *Laminaria hyperborea* upon sand dune erosion and water particle velocities. Coast. Eng. 44, 37–63. https://doi.org/10.1016/S0378-3839(01)00021-7.

Lu, Y., Yuan, J., Lu, X., Su, C., Zhang, Y., Wang, C., Cao, X., Li, Q., Su, J., Ittekkot, V., Garbutt, R.A., Bush, S., Fletcher, S., Wagey, T., Kachur, A., Sweijd, N., 2018. Major threats of pollution and climate change to global coastal ecosystems and enhanced management for sustainability. Environ. Pollut. 239, 670–680. https://doi.org/10.1016/j.envpol.2018.04.016.

Lueker, T.J., Dickson, A.G., Keeling, C.D., 2000. Ocean pCO_2 calculated from dissolved inorganic carbon, alkalinity, and equations for K1 and K2: validation based on laboratory measurements of CO_2 in gas and seawater at equilibrium. Mar. Chem. 70, 105–119. https://doi.org/10.1016/S0304-4203(00)00022-0.

MacKenzie, L., Adamson, J., 2004. Water column stratification and the spatial and temporal distribution of phytoplankton biomass in Tasman Bay, New Zealand: Implications for aquaculture. N. Z. J. Mar. Freshwater Res. 38, 705–728. https://doi.org/10.1080/00288330.2004.9517271.

MAE, 2005. (Millennium Ecosystem Assessment): Ecosystems and Human Well-being: A Framework for Assessment, 2nd ed. Island Press, Washington, DC.

Maeda, K., Toyoda, S., Yano, M., Hattori, S., Fukasawa, M., Nakajima, K., Yoshida, N., 2016. Isotopically enriched ammonium shows high nitrogen transformation in the pile top zone of dairy manure compost. Biogeosciences 13, 1341–1349. https://doi.org/10.5194/bg-13-1341-2016.

Mangialajo, L., Chiantore, M., CattaneoVietti, R., 2008. Loss of fucoid algae along a gradient of urbanisation, and structure of benthic assemblages. Mar. Ecol. Prog. Ser. 358, 63–74. https://doi.org/10.3354/meps07400.

Mariotti, A., Germon, J.C., Hubert, P., Kaiser, P., Letolle, R., Tardieux, A., Tardieux, P., 1981. Experimental determination of nitrogen kinetic isotope fractionation: Some principles; illustration for the denitrification and nitrification processes. Plant Soil 62, 413–430. https://doi.org/10.1007/BF02374138.

Mariotti, A., Lancelot, C., Billen, G., 1984. Natural isotopic composition of nitrogen as a tracer of origin for suspended organic matter in the Scheldt estuary. Geochim. Cosmochim. Acta 48, 549–555. https://doi.org/10.1016/0016-7037(84)90283-7.

Marzinelli, E.M., Qiu, Z., Dafforn, K.A., Johnston, E.L., Steinberg, P.D., Mayer-Pinto, M., 2018. Coastal urbanisation affects microbial communities on a dominant marine holobiont. Biofilms and Microbiomes 4, 1–7. https://doi.org/10.1038/s41522-017-0044-z.

Mayer, B., Boyer, E.W., Goodale, C., Jaworski, N.A., Van Breemen, N., Howarth, R.W., Seitzinger, S., Billen, G., Lajtha, K., Nadelhoffer, K., Van Dam, D., Hetling, L.J., Nosal, M., Paustian, K., 2002. Sources of nitrate in rivers draining sixteen watersheds in the northeastern U.S.: Isotopic constraints. In: Boyer, E.W., Howarth, R.W. (Eds.), The Nitrogen Cycle at Regional to Global Scales. Springer, Netherlands, Dordrecht, pp. 171–197. https://doi.org/10.1007/978-94-017-3405-9_5.

McAfee, D., Cole, V.J., Bishop, M.J., 2016. Latitudinal gradients in ecosystem engineering by oysters vary across habitats. Ecology 97, 929–939. https://doi.org/10.1890/15-0651.1.

McClelland, J.W., Valiela, I., 1998. Changes in food web structure under the influence of increased anthropogenic nitrogen inputs to estuaries. Mar. Ecol. Prog. Ser. 168, 259–271. https://doi.org/10.3354/meps168259.

McClelland, J.W., Valiela, I., Michener, R.H., 1997. Nitrogen-stable isotope signatures in estuarine food webs: a record of increasing urbanization in coastal watersheds. Limnol. Oceanogr. 42 (5), 930–937.

McCutchan, J.H., Lewis, W.M., Kendall, C., McGrath, C.C., 2003. Variation in trophic shift for stable isotope ratios of carbon, nitrogen, and sulfur. Oikos 102 (2), 378–390.

McQuaid, C.D., Lindsay, T.L., 2007. Wave exposure effects on population structure and recruitment in the mussel *Perna perna* suggest regulation primarily through availability of recruits and food, not space. Mar. Biol. 151, 2123–2131. https://doi.org/10.1007/s00227-007-0645-9.

Mdzeke, N.P., 2004. Contamination levels in and cellular responses of intertidal invertebrates as biomarkers of toxic stress caused by heavy metal contamination in False Bay (PhD Thesis). Stellenbosch : Stellenbosch University, South Africa.

Meerkotter, M., 2012. Sources of heavy metals in vegetables in Cape Town, and possible methods of rehabilitation. (Unpublished PhD thesis.). University of the Western Cape, Cape Town, South Africa.

Menge, 2000. Top-down and bottom-up community regulation in marine rocky intertidal habitats. J. Exp. Mar. Biol. Ecol. 250, 257–289.

Merkens, J.-L., Reimann, L., Hinkel, J., Vafeidis, A.T., 2016. Gridded population projections for the coastal zone under the Shared Socioeconomic Pathways. Global Planet. Change 145, 57–66. https://doi.org/10.1016/j.gloplacha.2016.08.009.

Mikulic, N., Orescanin, V., Legovic, T., Zugaj, R., 2004. Estimation of heavy metals (Cu, Zn, Pb) input into Punat Bay. Env Geol 46, 62–70. https://doi.org/10.1007/s00254-004-1015-2.

Montoya, J.P., Carpenter, E.J., Capone, D.G., 2002. Nitrogen fixation and nitrogen isotope abundances in zooplankton of the oligotrophic North Atlantic. Limnol. Oceanogr. 47, 1617–1628. https://doi.org/10.4319/lo.2002.47.6.1617.

Morais, S., Costa, F.G. e, Pereira, M. de L., 2012. Heavy Metals and Human Health. Environmental Health – Emerging Issues and Practice. doi: 10.5772/29869.

Morris, R.L., Graham, T.D.J., Kelvin, J., Ghisalberti, M., Swearer, S.E., 2020. Kelp beds as coastal protection: wave attenuation of *Ecklonia radiata* in a shallow coastal bay. Ann. Bot. 125, 235–246. https://doi.org/10.1093/aob/mcz127.

Nagelkerken, I., Connell, S.D., 2015. Global alteration of ocean ecosystem functioning due to increasing human CO_2 emissions. PNAS 112, 13272–13277. https://doi.org/10.1073/pnas.1510856112.

Nakamura, Y., Kerciku, F., 2000. Effects of filter-feeding bivalves on the distribution of water quality and nutrient cycling in a eutrophic coastal lagoon. J. Mar. Syst. 26, 209–221. https://doi.org/10.1016/S0924-7963(00)00055-5.

Nestler, A., Berglund, M., Accoe, F., Duta, S., Xue, D., Boeckx, P., Taylor, P., 2011. Isotopes for improved management of nitrate pollution in aqueous resources: review of surface water field studies. Environ. Sci. Pollut. Res. 18, 519–533. https://doi.org/10.1007/s11356-010-0422-z.

Neumann, B., Vafeidis, A.T., Zimmermann, J., Nicholls, R.J., Kumar, L., 2015. Future coastal population growth and exposure to sea-level rise and coastal flooding – a global assessment. PLoS ONE 10 (3), e0118571.

Nikolenko, O., Jurado, A., Borges, A.V., Knöller, K., Brouyere, S., 2018. Isotopic composition of nitrogen species in groundwater under agricultural areas: a review. Sci. Total Environ. 621, 1415–1432. https://doi.org/10.1016/j.scitotenv.2017.10.086.

O'Callaghan, M., 1990. The ecology of the False Bay estuarine environments, Cape, South Africa. 1. The coastal vegetation. Bothalia 20, 105–111. https://doi.org/10.4102/abc.v20i1.903.

O'Neil, J.M., Davis, T.W., Burford, M.A., Gobler, C.J., 2012. The rise of harmful cyanobacteria blooms: The potential roles of eutrophication and climate change. Harmful Algae, Harmful Algae. The requirement for species-specific information 14, 313–334. doi: 10.1016/j.hal.2011.10.027.

Ostapczuk, P., Burow, M., May, K., Mohl, C., Froning, M., Süßenbach, B., Waidmann, E., Emons, H., 1997. Mussels and algae as bioindicators for long-term tendencies of element pollution in marine ecosystems. Chemosphere, Biological Environmental Specimen Banking 34, 2049–2058. https://doi.org/10.1016/S0045-6535(97)00067-2.

Paerl, H.W., 2006. Assessing and managing nutrient-enhanced eutrophication in estuarine and coastal waters: Interactive effects of human and climatic perturbations. Ecological Engineering, Advances in coastal habitat restoration in the northern Gulf of Mexico 26, 40–54. doi: 10.1016/j.ecoleng.2005.09.006.

Paerl, H.W., 1997. Coastal eutrophication and harmful algal blooms: importance of atmospheric deposition and groundwater as "new" nitrogen and other nutrient sources. Limnol. Oceanogr. 42 (5part2), 1154–1165.

Parrish, C.C., 2013. Lipids in marine ecosystems. International Scholarly Research Notices 2013 (604045), 16. https://doi.org/10.5402/2013/604045.

Parrish, C.C., Abrajano, T.A., Budge, S.M., Helleur, R.J., Hudson, E.D., Pulchan, K., Ramos, C., 2000. Lipid and phenolic biomarkers in marine ecosystems: analysis and applications, in: Wangersky, P.J. (Ed.), Marine Chemistry. Springer Berlin Heidelberg, pp. 193–223.

Parsons, T.R., Maita, Y., Lalli, C.M., 1984. A manual of chemical & biological methods for seawater analysis. Elsevier. https://doi.org/10.1016/C2009-0-07774-5.

Peng, L., Ni, B.-J., Ye, L., Yuan, Z., 2015. The combined effect of dissolved oxygen and nitrite on N_2O production by ammonia oxidizing bacteria in an enriched nitrifying sludge. Water Res. 73, 29–36. https://doi.org/10.1016/j.watres.2015.01.021.

Pereira, R.R.C., Scanes, E., Parker, L.M., Byrne, M., Cole, V.J., Ross, P.M., 2019. Restoring the flat oyster *Ostrea angasi* in the face of a changing climate. Mar. Ecol. Prog. Ser. 625, 27–39. https://doi.org/10.3354/meps13047.

Peterson, B.J., Fry, B., 1987. Stable isotopes in ecosystem studies. Annu. Rev. Ecol. Syst. 18, 293–320. https://doi.org/10.1146/annurev.es.18.110187.001453.

Pfaff, M.C., Logston, R.C., Raemaekers, S.J.P.N., Hermes, J.C., Blamey, L.K., Cawthra, H. C., Colenbrander, D.R., Crawford, R.J.M., Day, E., du Plessis, N., Elwen, S.H., Fawcett, S.E., Jury, M.R., Karenyi, N., Kerwath, S.E., Kock, A.A., Krug, M., Lamberth, S.J., Omardien, A., Pitcher, G.C., Rautenbach, C., Robinson, T.B., Rouault, M., Ryan, P.G., Shillington, F.A., Sowman, M., Sparks, C.C., Turpie, J.K., van Niekerk, L., Waldron, H.N., Yeld, E.M., Kirkman, S.P., 2019. A synthesis of three

decades of socio-ecological change in False Bay, South Africa: setting the scene for multidisciplinary research and management. Elem. Sci. Anth. 7, 32. https://doi.org/10.1525/elementa.367.
Pineda, J., Porri, F., Starczak, V., Blythe, J., 2010. Causes of decoupling between larval supply and settlement and consequences for understanding recruitment and population connectivity. Journal of Experimental Marine Biology and Ecology, The Biology of Barnacles' in honour of Margaret Barnes 392, 9–21. https://doi.org/10.1016/j.jembe.2010.04.008.
Pirini, M., Manuzzi, M.P., Pagliarani, A., Trombetti, F., Borgatti, A.R., Ventrella, V., 2007. Changes in fatty acid composition of *Mytilus galloprovincialis* (Lamark) fed on microalgal and wheat germ diets. Comp. Biochem. Physiol. B: Biochem. Mol. Biol. 147, 616–626. https://doi.org/10.1016/j.cbpb.2007.04.003.
Porri, F., McQuaid, C., Radloff, S., 2006. Spatio-temporal variability of larval abundance and settlement of *Perna perna*: differential delivery of mussels. Mar. Ecol. Prog. Ser. 315, 141–150. https://doi.org/10.3354/meps315141.
Porri, F., McQuaid, C.D., Lawrie, S.M., Antrobus, S.J., 2008. Fine-scale spatial and temporal variation in settlement of the intertidal mussel *Perna perna* indicates differential hydrodynamic delivery of larvae to the shore. J. Exp. Mar. Biol. Ecol. 367, 213–218. https://doi.org/10.1016/j.jembe.2008.09.026.
Puccinelli, E., McQuaid, C.D., Dobretsov, S., Christofoletti, R.A., 2019. Coastal upwelling affects filter-feeder stable isotope composition across three continents. Mar. Environ. Res. 147, 13–23. https://doi.org/10.1016/j.marenvres.2019.03.015.
Puccinelli, E., McQuaid, C.D., Noyon, M., Melzner, F., 2016a. Spatio-temporal variation in effects of upwelling on the fatty acid composition of benthic filter feeders in the Southern Benguela Ecosystem: not all upwelling Is equal. PLoS ONE 11 (8), e0161919.
Puccinelli, E., Noyon, M., McQuaid, C.D., 2017. Trophic signatures of co-existing invasive and indigenous mussels: selective feeding or different metabolic pathways? Hydrobiologia 784, 187–199. https://doi.org/10.1007/s10750-016-2873-9.
Puccinelli, E., Noyon, M., McQuaid, C.D., 2016b. Does proximity to urban centres affect the dietary regime of marine benthic filter feeders? Estuar. Coast. Shelf Sci. 169, 147–157. https://doi.org/10.1016/j.ecss.2015.12.017.
Puccinelli, E., Noyon, M., McQuaid, C.D., 2016c. Hierarchical effects of biogeography and upwelling shape the dietary signatures of benthic filter feeders. Mar. Ecol. Prog. Ser. 543, 37–54.
Qin, Y., Zhang, D., Wang, F., 2019. Using nitrogen and oxygen isotopes to access sources and transformations of nitrogen in the Qinhe Basin, North China. Environ. Sci. Pollut. Res. 26, 738–748. https://doi.org/10.1007/s11356-018-3660-0.
Reimers, B., Griffiths, C.L., Hoffman, M.T., 2014. Repeat photography as a tool for detecting and monitoring historical changes in South African coastal habitats. Afr. J. Mar. Sci. 36, 387–398. https://doi.org/10.2989/1814232X.2014.954618.
Revilla, M., Alexander, J., Glibert, P.M., 2005. Urea analysis in coastal waters: comparison of enzymatic and direct methods. Limnol. Oceanogr. Methods 3, 290–299. https://doi.org/10.4319/lom.2005.3.290.
Richardson, K., Jørgensen, B.B., 1996. Eutrophication: definition, history and effects. In: Jørgensen, B.B., Richardson, K. (Eds.), Eutrophication in Coastal Marine Ecosystems. American Geophysical Union, pp. 1–19.
Riebesell, U., Fabry, V.J., Hansson, L., Gattuso, J.P.E., 2010. EPOCA guide to best practices for ocean acidification research and data reporting. Publications Office of the European Union, Luxembourg, p. 260.
Robinson, T., Griffiths, C., McQuaid, C., Rius, M., 2005. Marine alien species of South Africa — status and impacts. Afr. J. Mar. Sci. 27, 297–306. https://doi.org/10.2989/18142320509504088.
Romero, E., Garnier, J., Lassaletta, L., Billen, G., Le Gendre, R., Riou, P., Cugier, P., 2013. Large-scale patterns of river inputs in southwestern Europe: seasonal and interannual variations and potential eutrophication effects at the coastal zone. Biogeochemistry 113, 481–505. https://doi.org/10.1007/s10533-012-9778-0.
Rosenberg, R., Loo, L.-O., 1988. Marine eutrophication induced oxygen deficiency: effects on soft bottom fauna, Western Sweden. Ophelia 29, 213–225. https://doi.org/10.1080/00785326.1988.10430830.
Ruess, L., Müller-Navarra, D.C., 2019. Essential biomolecules in food webs. Front. Ecol. Evolution 7. https://doi.org/10.3389/fevo.2019.00269.
Santoro, A.E., Sakamoto, C.M., Smith, J.M., Plant, J.N., Gehman, A.L., Worden, A.Z., Johnson, K.S., Francis, C.A., Casciotti, K.L., 2013. Measurements of nitrite production in and around the primary nitrite maximum in the central California Current. Biogeosciences 10, 7395–7410. https://doi.org/10.5194/bg-10-7395-2013.
Saxberg, B.E.H., Kowalski, B.R., 1979. Generalized standard addition method. Anal. Chem. 51 (7), 1031–1038.
Shannon, L.V., Chapman, P., 1983. Suggested mechanism for the chronic pollution by oil of beaches east of Cape Agulhas, South Africa. S. Afr. J. Mar. Sci. 1, 231–244. https://doi.org/10.2989/025776183784447520.
Sigman, D.M., Altabet, M.A., McCorkle, D.C., Francois, R., Fischer, G., 1999. The $\delta^{15}N$ of nitrate in the southern ocean: Consumption of nitrate in surface waters. Global Biogeochem. Cycles 13, 1149–1166. https://doi.org/10.1029/1999GB900038.
Sigman, D.M., Casciotti, K.L., Andreani, M., Barford, C., Galanter, M., Böhlke, J.K., 2001. A bacterial method for the nitrogen isotopic analysis of nitrate in seawater and freshwater. Anal. Chem. 73, 4145–4153. https://doi.org/10.1021/ac010088e.
Sigman, D.M., Fripiat, F., 2019. Nitrogen Isotopes in the Ocean. In: Cochran, J.K., Bokuniewicz, H.J., Yager, P.L. (Eds.), Encyclopedia of Ocean Sciences (Third Edition). Academic Press, Oxford, pp. 263–278. https://doi.org/10.1016/B978-0-12-409548-9.11605-7.
Smale, D.A., Burrows, M.T., Moore, P., O'Connor, N., Hawkins, S.J., 2013. Threats and knowledge gaps for ecosystem services provided by kelp forests: a northeast Atlantic perspective. Ecol. Evol. 3, 4016–4038. https://doi.org/10.1002/ece3.774.
Smith, J.R., Fong, P., Ambrose, R.F., 2009. Spatial patterns in recruitment and growth of the mussel *Mytilus californianus* (Conrad) in southern and northern California, USA, two regions with differing oceanographic conditions. J. Sea Res. 61, 165–173. https://doi.org/10.1016/j.seares.2008.10.009.
Smith, K., 2011. We are seven billion. Nat. Clim. Change 1, 331–335. https://doi.org/10.1038/nclimate1235.
Spada, L., Annicchiarico, C., Cardellicchio, N., Giandomenico, S., Leo, A.D., 2013. Heavy metals monitoring in mussels *Mytilus galloprovincialis* from the Apulian coasts (Southern Italy). Mediterranean Marine Science 14, 99–108. https://doi.org/10.12681/mms.323.
Spokes, L.J., Yeatman, S.G., Cornell, S.E., Jickells, T.D., 2000. Nitrogen deposition to the eastern Atlantic Ocean. the importance of south-easterly flow. Tellus B: Chemical and Physical Meteorology 52, 37–49. https://doi.org/10.3402/tellusb.v52i1.16080.
Stachowicz, J.J., Bruno, J.F., Duffy, J.E., 2007. Understanding the effects of marine biodiversity on communities and ecosystems. Annu. Rev. Ecol. Evol. Syst. 38, 739–766. https://doi.org/10.1146/annurev.ecolsys.38.091206.095659.
Stallard, R.F., Edmond, J.M., 1983. Geochemistry of the Amazon: 2. The influence of geology and weathering environment on the dissolved load. J. Geophys. Res. Oceans 88, 9671–9688. https://doi.org/10.1029/JC088iC14p09671.
Stankovic, S., Jovic, M., 2012. Health risks of heavy metals in the mediterranean mussels as seafood. Environ. Chem. Lett. 10, 119–130. https://doi.org/10.1007/s10311-011-0343-1.
Stankovic, S., Jovic, M., Stankovic, A.R., Katsikas, L., 2012. Heavy metals in seafood mussels. Risks for human health. In: Lichtfouse, E., Schwarzbauer, J., Robert, D. (Eds.), Environmental Chemistry for a Sustainable World: Volume 1: Nanotechnology and Health Risk, Environmental Chemistry for a Sustainable World. Springer, Netherlands, Dordrecht, pp. 311–373. https://doi.org/10.1007/978-94-007-2442-6_9.
Strickland, J.D.H., Parsons, T.R., 1968. A practical handbook of seawater analysis. Bulletin: Fisheries Research Board of Canada 167, 311. https://epic.awi.de/id/eprint/39262/1/Strickland-Parsons_1972.pdf.
Taljaard, S., 2006. Baseline assessment of sources and management of land- based marine pollution in the BCLME region (Project BEHP/LBMP/03/01). (No. CSIR/NRE/ECO/ER/2006/0010/C). Stellenbosch, South Africa.
Taljaard, S., van Ballegooyen, R.C., Moran, P.D., 2000a. False Bay water quality review. Volume 2: Specialist assessments and inventories of available literature and data. (Report to the False Bay Water Quality Advisory Committee, CSIR Report ENV-S-C2000-086/2). Stellenbosch, South Africa.
Taljaard, S., Van Ballegooyen, R.C., Morant, P.D., 2000b. False Bay water quality review. Volume 1: Executive summary. (Report to the False Bay Water Quality Advisory Committee, CSIR Report ENV-S-C 2000-086/1). Stellenbosch, South Africa.
Talmage, S.C., Gobler, C.J., 2009. The effects of elevated carbon dioxide concentrations on the metamorphosis, size, and survival of larval hard clams (*Mercenaria mercenaria)*, bay scallops (*Argopecten irradians*), and Eastern oysters (*Crassostrea virginica*). Limnol. Oceanogr. 54, 2072–2080. https://doi.org/10.4319/lo.2009.54.6.2072.
Teagle, H., Hawkins, S.J., Moore, P.J., Smale, D.A., 2017. The role of kelp species as biogenic habitat formers in coastal marine ecosystems. J. Exp. Mar. Biol. Ecol. Ecological responses to environmental change in marine systems 492, 81–98. https://doi.org/10.1016/j.jembe.2017.01.017.
Teixeira, H., Lillebø, A.I., Culhane, F., Robinson, L., Trauner, D., Borgwardt, F., Kuemmerlen, M., Barbosa, A., McDonald, H., Funk, A., O'Higgins, T., Van der Wal, J. T., Piet, G., Hein, T., Arévalo-Torres, J., Iglesias-Campos, A., Barbière, J., Nogueira, A.J.A., 2019. Linking biodiversity to ecosystem services supply: Patterns across aquatic ecosystems. Sci. Total Environ. 657, 517–534. https://doi.org/10.1016/j.scitotenv.2018.11.440.
The City of Cape Town, 2019. Know your coast. Cape Town, South Africa. https://resource.capetown.gov.za/documentcentre/Documents/City%20research%20reports%20and%20review/Know_Your_Coast_2020.pdf.
The City of Cape Town, 2020. Cape Town, South Africa. https://wessa.org.za/wp-content/uploads/2020/11/Blue-Flag-Sites-2020.pdf.
The City of Cape Town, 2021. Cape Town, South Africa. https://wessa.org.za/wp-content/uploads/2021/10/WESSA-Blue-Flag-sites_2021_22.pdf.
Thornton, I., 1992. Sources and pathways of cadmium in the environment. IARC Sci. Publ. 149–162.
Tilman, D., Isbell, F., Cowles, J.M., 2014. Biodiversity and Ecosystem Functioning. Annu. Rev. Ecol. Evol. Syst. 45, 471–493. https://doi.org/10.1146/annurev-ecolsys-120213-091917.
Tilstone, G., Míguez, B., Figueiras, F., Fermín, E., 2000. Diatom dynamics in a coastal ecosystem affected by upwelling: coupling between species succession, circulation and biogeochemical processes. Mar. Ecol. Prog. Ser. 205, 23–41. https://doi.org/10.3354/meps205023.
Townsend, M., Davies, K., Hanley, N., Hewitt, J.E., Lundquist, C.J., Lohrer, A.M., 2018. The challenge of implementing the marine ecosystem service concept. Front. Mar. Sci. https://doi.org/10.3389/fmars.2018.00359.
Tsikoti, C., Genitsaris, S., 2021. Review of harmful algal blooms in the coastal Mediterranean Sea, with a focus on Greek waters. Diversity 13, 396. https://doi.org/10.3390/d13080396.
Turner, A., 2010. Marine pollution from antifouling paint particles. Mar. Pollut. Bull. 60, 159–171. https://doi.org/10.1016/j.marpolbul.2009.12.004.
Utermöhl, H., 1958. Zur Vervollkommnung der quantitativen Phytoplankton-Methodik. Schweizerbart, Stuttgart, Germany.
Vallarino, E.A., Rivero, M.S., Gravina, M.C., Elías, R., 2002. The community-level response to sewage impact in intertidal mytilid beds of the Southwestern Atlantic, and the use of the Shannon index to assess pollution. Revista de biología marina y oceanografía 37, 25–33. https://doi.org/10.4067/S0718-19572002000100005.
van Niekerk, L., Adams, J.B., Bate, G.C., Forbes, A.T., Forbes, N.T., Huizinga, P., Lamberth, S.J., MacKay, C.F., Petersen, C., Taljaard, S., Weerts, S.P., Whitfield, A.K.,

Wooldridge, T.H., 2013. Country-wide assessment of estuary health: an approach for integrating pressures and ecosystem response in a data limited environment. Estuarine, Coastal and Shelf Science, Pressures, Stresses, Shocks and Trends in Estuarine Ecosystems 130, 239–251. https://doi.org/10.1016/j.ecss.2013.05.006.

van Niekerk, L., Taljaard, S., Adams, J., Fundisi, D., Huizinga, P., Lamberth, S., Mallory, S., Snow, G., Turpie, J.K., Whitfield, A.K., 2015. Desktop provisional EcoClassification of the temperate estuaries of South Africa. (Water Research Commission Report No. (2187/1): 15.).

Vanni, M.J., 2021. Invasive mussels regulate nutrient cycling in the largest freshwater ecosystem on Earth. Proceedings of the National Academy of Sciences 118, e2100275118. doi: 10.1073/pnas.2100275118.

Vaquer-Sunyer, R., Duarte, C.M., 2008. Thresholds of hypoxia for marine biodiversity. Proc. Natl. Acad. Sci. U.S.A. 105 (40), 15452–15457.

Vizzini, S., Sarà, G., Michener, R.H., Mazzola, A., 2002. The role and contribution of the seagrass Posidonia oceanica (L.) Delile organic matter for secondary consumers as revealed by carbon and nitrogen stable isotope analysis. Acta Oecologica 23, 277–285. https://doi.org/10.1016/S1146-609X(02)01156-6.

Vlahogianni, T.H., Valavanidis, A., 2007. Heavy-metal effects on lipid peroxidation and antioxidant defence enzymes in mussels Mytilus galloprovincialis. Chem. Ecol. 23, 361–371. https://doi.org/10.1080/02757540701653285.

von Biela, V.R., Newsome, S.D., Bodkin, J.L., Kruse, G.H., Zimmerman, C.E., 2016. Widespread kelp-derived carbon in pelagic and benthic nearshore fishes suggested by stable isotope analysis. Estuar. Coast. Shelf Sci. 181, 364–374. https://doi.org/10.1016/j.ecss.2016.08.039.

Von der Meden, C.E.O., Porri, F., Radloff, S., McQuaid, C.D., 2012. Settlement intensification and coastline topography: understanding the role of habitat availability in the pelagic–benthic transition. Mar. Ecol. Prog. Ser. 459, 63–71. https://doi.org/10.3354/meps09762.

Wada, E., 1980. Nitrogen isotope fractionation and its significance in biogeochemical processes occurring in marine environments. Isotope Marine Chemistry 375–398.

Waldbusser, G.G., Hales, B., Langdon, C.J., Haley, B.A., Schrader, P., Brunner, E.L., Gray, M.W., Miller, C.A., Gimenez, I., Hutchinson, G., Ross, P., 2015. Ocean acidification has multiple modes of action on bivalve larvae. PLoS ONE 10 (6), e0128376.

Wang, P.F., Martin, J., Morrison, G., 1999. Water quality and eutrophication in Tampa Bay, Florida. Estuar. Coast. Shelf Sci. 49, 1–20. https://doi.org/10.1006/ecss.1999.0490.

Ward, M., Possingham, H., Rhodes, J.R., Mumby, P., 2018. Food, money and lobsters: Valuing ecosystem services to align environmental management with Sustainable Development Goals. Ecosyst. Serv. 29, 56–69. https://doi.org/10.1016/j.ecoser.2017.10.023.

Waser, N.A., Yin, K., Yu, Z., Tada, K., Harrison, P.J., Turpin, D.H., Calvert, S.E., 1998. Nitrogen isotope fractionation during nitrate, ammonium and urea uptake by marine diatoms and coccolithophores under various conditions of N availability. Mar. Ecol. Prog. Ser. 169, 29–41. https://doi.org/10.3354/meps169029.

Weidberg, N., Porri, F., Von der Meden, C.E.O., Jackson, J.M., Goschen, W., McQuaid, C. D., 2015. Mechanisms of nearshore retention and offshore export of mussel larvae over the Agulhas Bank. J. Mar. Syst. 144, 70–80. https://doi.org/10.1016/j.jmarsys.2014.11.012.

Weigand, M.A., Foriel, J., Barnett, B., Oleynik, S., Sigman, D.M., 2016. Updates to instrumentation and protocols for isotopic analysis of nitrate by the denitrifier method. Rapid Commun. Mass Spectrom. 30, 1365–1383. https://doi.org/10.1002/rcm.7570.

Welschmeyer, N.A., 1994. Fluorometric analysis of chlorophyll a in the presence of chlorophyll b and pheopigments. Limnol. Oceanogr. 39, 1985–1992. https://doi.org/10.4319/lo.1994.39.8.1985.

Winton, M., Griffies, S.M., Samuels, B.L., Sarmiento, J.L., Frölicher, T.L., 2012. Connecting changing ocean circulation with changing climate. J. Clim. 26, 2268–2278. https://doi.org/10.1175/JCLI-D-12-00296.1.

Worm, B., Barbier, E.B., Beaumont, N., Duffy, J.E., Folke, C., Halpern, B.S., Jackson, J.B. C., Lotze, H.K., Micheli, F., Palumbi, S.R., Sala, E., Selkoe, K.A., Stachowicz, J.J., Watson, R., 2006. Impacts of biodiversity loss on ocean ecosystem services. Science 314, 787–790. https://doi.org/10.1126/science.1132294.

Worm, B., Sandow, M., Oschlies, A., Lotze, H.K., Myers, R.A., 2005. Global patterns of predator diversity in the open oceans. Science 309, 1365–1369. https://doi.org/10.1126/science.1113399.

Xavier, B.M., Branch, G.M., Wieters, E., 2007. Abundance, growth and recruitment of *Mytilus galloprovincialis* on the west coast of South Africa in relation to upwelling. Mar Ecol Prog Ser 346, 189–201. https://doi.org/10.3354/meps07007.

Yi, Y., Yang, Z., Zhang, S., 2011. Ecological risk assessment of heavy metals in sediment and human health risk assessment of heavy metals in fishes in the middle and lower reaches of the Yangtze River basin. Environmental Pollution, Nitrogen Deposition, Critical Loads and Biodiversity 159, 2575–2585. https://doi.org/10.1016/j.envpol.2011.06.011.

Ytreberg, E., Karlsson, J., Eklund, B., 2010. Comparison of toxicity and release rates of Cu and Zn from anti-fouling paints leached in natural and artificial brackish seawater. Sci. Total Environ. 408, 2459–2466. https://doi.org/10.1016/j.scitotenv.2010.02.036.

Zardi, G.I., Nicastro, K.R., McQuaid, C.D., Erlandsson, J., 2008. Sand and wave induced mortality in invasive (*Mytilus galloprovincialis*) and indigenous (*Perna perna*) mussels. Mar Biol 153, 853–858. https://doi.org/10.1007/s00227-007-0857-z.